



Titre: Emulsifying Properties of Chitosan and Chitosan/Gelatin Complexes
Title:

Auteur: Xiaoyan Wang
Author:

Date: 2016

Type: Mémoire ou thèse / Dissertation or Thesis

Référence: Wang, X. (2016). Emulsifying Properties of Chitosan and Chitosan/Gelatin Complexes [Thèse de doctorat, École Polytechnique de Montréal]. PolyPublie.
Citation: <https://publications.polymtl.ca/2096/>

 **Document en libre accès dans PolyPublie**
Open Access document in PolyPublie

URL de PolyPublie: <https://publications.polymtl.ca/2096/>
PolyPublie URL:

Directeurs de recherche: Marie-Claude Heuzey
Advisors:

Programme: Génie chimique
Program:

UNIVERSITÉ DE MONTRÉAL

EMULSIFYING PROPERTIES OF CHITOSAN AND CHITOSAN/GELATIN COMPLEXES

XIAOYAN WANG

DÉPARTEMENT DE GÉNIE CHIMIQUE
ÉCOLE POLYTECHNIQUE DE MONTRÉAL

THÈSE PRÉSENTÉE EN VUE DE L'OBTENTION
DU DIPLÔME DE PHILOSOPHIAE DOCTOR
(GÉNIE CHIMIQUE)

MARS 2016

© Xiaoyan Wang, 2016.

UNIVERSITÉ DE MONTRÉAL

ÉCOLE POLYTECHNIQUE DE MONTRÉAL

Cette thèse intitulée:

EMULSIFYING PROPERTIES OF CHITOSAN AND CHITOSAN/GELATIN COMPLEXES

présentée par : WANG Xiaoyan

en vue de l'obtention du diplôme de : Philosophiae Doctor

a été dûment acceptée par le jury d'examen constitué de :

M. FRADETTE Louis, Ph. D., président

Mme HEUZEY Marie-Claude, Ph. D., membre et directrice de recherche

M. VIRGILIO Nick, Ph. D., membre

Mme ORSAT Valérie, Ph. D., membre

DEDICATION

To my beloved husband, cheerful son, and my beloved parents and brother

ACKNOWLEDGEMENTS

I wish to take this opportunity to thank all those who have supported me in the completion of this study or helped me in any way during my living in Canada.

First and foremost, I would like to express my deep and sincere gratitude to my supervisor, Professor Marie-Claude Heuzey, who not only provided me with fundamental advices and solid supports to conduct my research, but also lots of knowledge which are very helpful in all aspects of my life. The success of this project would have been impossible without her encouragement, patience and experience, and it was really a pleasure to work with her.

I am so thankful to Dr. Nick Virgilio, not only for reviewing this thesis, but also for his helpful discussions during my project. Besides, I would like to thank the rest of my thesis committee, namely, Prof. Louis Fradette and Prof. Valérie Orsat, for accepting to evaluate my thesis.

I would also like to extend my thanks to my supervisor during my master study, Prof. Chuan-He Tang, who continued to give me support and encouragement during my PhD study. Many thanks also go to Prof. Charles Dubois for giving me the training and access permission to the ultrasonic homogenizer.

A sincere appreciation to our previous research associate, Mrs. Melina Hamdine, for all her technical assistance and revitalizing friendly discussions we had together. I also acknowledge the help and kind cooperation of the other technical and administrative staff of the Chemical Engineering department at Polytechnique Montreal, especially Ms. Évelyne Rousseau, Ms. Martine Lamarche and Mr. Gino Robin.

I am so grateful for the help of my friend Ms. Andrea Arias for translating the abstract of this thesis to French. A special acknowledgement also goes to Mr. Changsheng Wang for his continued support throughout the whole project as well as the many interesting discussions. Many thanks to Marie, Mounia and Nury for their kind help during the project. I would also like to send a heartfelt thanks to my other friends and colleagues for their support and help during my PhD study and also my life, especially Ahmad, Amir, Amirhossein, Davood, Fatemeh, Gill, Helia, Lin, Maryam, Min, Qingkai, Qinghua, Shan and Xiaojie.

I gratefully acknowledge the financial support from CSC (China Scholarship Council).

Finally, with all my heart, I would like to express my deepest gratitude to my beloved parents, my brother, especially my husband, Jun Wang, for their overwhelming support throughout my life. They are the driving forces behind all of my successes, and there will never be a right word to express my feeling of appreciation for their unconditional love.

RÉSUMÉ

Les systèmes de libération à base d'émulsions sont les plus courants pour encapsuler des composants lipophiles bioactifs, tels que les acides gras ω -3 et les vitamines solubles à l'huile; ces derniers sont largement appliqués dans les domaines alimentaire et pharmaceutique. Cependant, en raison de leur faible solubilité à l'eau et leur instabilité physicochimique, ils ont besoin d'être protégés par des techniques d'encapsulation pendant les procédés de fabrication et le stockage. Idéalement, les matériaux sélectionnés pour former la coque d'encapsulation doivent être des biomatériaux naturels pour des raisons de biocompatibilité, biodégradabilité, etc. Étant donné que les propriétés émulsifiantes sont la caractéristique la plus importante pour qu'un matériau polymère devienne un bon candidat pour la coque, la conception d'une structure macromoléculaire avec des propriétés émulsifiantes améliorées s'avère d'une importance capitale. L'objectif général de cette thèse est de développer de nouveaux émulsifiants à base de biopolymères pour des applications alimentaires et pharmaceutiques, en utilisant un polysaccharide biosourcé (chitosane), une protéine (gélatine) et l'huile de maïs comme un système modèle.

Dans ce travail, les propriétés émulsifiantes du chitosane ont été examinées en préparant des émulsions d'huile dans l'eau (O/W) à l'aide de l'homogénéisation par ultrasons à haute intensité (HIU). Les résultats ont montré que le chitosane est un émulsifiant naturel intéressant pour la fabrication des émulsions O/W classiques ainsi que de type Pickering, toutes les deux avec une taille de gouttelettes très fine et une bonne stabilité à long terme. Ceci a été réalisé sans l'addition d'agents tensioactifs ou agents de réticulation, et tout simplement en ajustant les valeurs du pH des solutions de chitosane. Au cours de la préparation de l'émulsion, l'application de l'HIU a donné lieu à une rupture des agglomérats de chitosane et à une diminution de son poids moléculaire, tandis que l'augmentation du pH a provoqué une transition dans la conformation de la chaîne d'étendue à compacte ce qui a promu davantage l'amélioration des propriétés émulsifiantes du chitosane. L'émulsion de type Pickering formée à pH 6.5 a montré une stabilité remarquable induite par la présence des nanoparticules de chitosane à l'interface gouttelettes huile/eau; l'émulsion classique formée à pH 5.5 a également montré une bonne stabilité en raison de l'encombrement stérique et électrostatique. Les conclusions de cette partie du travail ont suggéré que le chitosane lui-même a un grand potentiel pour être utilisé comme un émulsifiant et

stabilisateur à pH contrôlé pour la production d'émulsions O/W, sans l'ajout d'agents tensioactifs.

Considérant que dans les systèmes commerciaux utilisés dans les domaines alimentaire ou pharmaceutique, les protéines et les polysaccharides coexistent très souvent, les interactions du chitosane (CH) avec une protéine de structure linéaire, la gélatine type B (GB), ont été étudiées. On a constaté que la formation de complexes de polyélectrolytes entre le chitosane et la gélatine était grandement affectée par le pH, la force ionique et le temps d'entreposage. Les complexes CH/GB ont été formés seulement dans la région de pH associée à une opposition de charge ($pI_{GB} < pH < 6.5 (pK_{aCH})$), où les solutions aqueuses ont évolué de transparentes à turbides jusqu'à ce que la séparation de phases ait lieu après une semaine de d'entreposage. La force ionique - de faible à modérée - a intensifié la formation du complexe, tandis que l'augmentation au-delà a entraîné une diminution. En favorisant une durée d'entreposage plus longue, la phase séparée s'est transformée d'un système liquide à un gel colloïdal thermoréversible, comme démontré par microscopie confocale à balayage laser ainsi que par les données rhéologiques.

Enfin, le complexe insoluble CH/GB (avant la séparation de phases) a été utilisé pour la première fois pour fabriquer des émulsions et gels d'émulsions de type Pickering, très stables à long terme, en utilisant à nouveau l'HIU. Le pH a montré un effet remarquable sur l'activité de surface des systèmes mixtes CH/GB, et la présence de complexes CH/GB a diminué de manière significative la tension superficielle à l'interface huile/eau. En comparaison avec les émulsions stabilisées par le CH seul, l'adsorption de particules du complexe CH/GB à l'interface huile/eau a bénéficié la formation de gouttelettes d'émulsion de plus petite taille, et a empêché efficacement leur coalescence, fait supporté par l'allongement de la stabilité de l'émulsion à long terme. La formation de réseaux de gouttelettes a été considérablement accélérée par l'augmentation de la fraction volumique de l'huile, ce qui a donné lieu à des gels d'émulsions thermoréversibles avec un comportement de type solide ayant des propriétés viscoélastiques ajustables, qui peuvent conséquemment être des matériaux appropriés pour l'encapsulation et/ou l'enrobage dans des applications alimentaires et pharmaceutiques.

ABSTRACT

Emulsion-based delivery systems are the most common methods to encapsulate lipophilic bioactive components, such as ω -3 fatty acids and oil-soluble vitamins, which are widely applied in food and pharmaceutical areas but need to be protected during processing and storage by encapsulation techniques, due to their low water-solubility, physical or chemical instability. Ideally, the encapsulating shell materials should be selected from natural biomaterials for reasons of biocompatibility, biodegradability, etc. Considering that the most important characteristics for polymeric materials to act as good shell protections are their emulsifying properties, designing a macromolecular structure with improved emulsifying properties turns out to be of key importance. The overall objective of this thesis is to develop novel biopolymer-based emulsifiers for food and pharmaceutical applications, using bio-sourced polysaccharide (chitosan) and protein (gelatin), and using corn oil as a model system.

In this work the emulsifying properties of chitosan itself were investigated first, by fabricating oil-in-water (O/W) emulsions with the assistance of high intensity ultrasonic (HIU) homogenization. The results showed that chitosan is an interesting natural emulsifier for fabricating both conventional and Pickering O/W emulsions with very fine droplet size and long-term stability. This was achieved without the use of any additional surfactant or crosslinking agent, and simply by adjusting the pH values of the chitosan solutions. During the emulsion preparation, the role of HIU resulted in a disassembly of chitosan agglomerates and a decrease of molecular weight, while increasing pH caused a chain conformation transition from extended to compact, which were found beneficial to the improvement of the emulsifying properties of chitosan. The long-term stability of the Pickering emulsion formed at pH 6.5 was remarkable due to the stabilization induced by chitosan nanoparticles at the oil/water interface, and that of the conventional emulsion formed at pH 5.5 was also considerable due to steric and electrostatic hindrance. The findings in this part of the work suggested that chitosan by itself has a great potential to be used as a pH-controlled emulsifier and stabilizer for the production of biodegradable, surfactant-free and even edible O/W emulsions.

Considering that in real food or pharmaceutical systems, proteins and polysaccharides most often coexist, the interactions of chitosan (CH) with a linear structured protein, gelatin type B (GB), were investigated. It was found that the formation of polyelectrolyte complexes between

chitosan and gelatin was greatly affected by pH, ionic strength, and storage time. CH/GB complexes were only formed in the oppositely charged pH region ($5 (pI_{GB}) < pH < 6.5 (pK_{aCH})$), where the aqueous solutions evolved from transparent to turbid until phase separation occurred after one week of storage. Low and moderate ionic strength intensified complex formation, while it decreased it at higher salt content. With increasing storage time, the separated dense phase changed from a liquid-like system to a thermoreversible colloidal gel, as supported by confocal laser scanning microscopy as well as rheological data.

Finally, the corresponding insoluble CH/GB complexes (before phase separation) were used to fabricate, for the first time, long-term stability Pickering emulsions and emulsion gels, using again HIU homogenization. The pH showed a remarkable effect on the surface activity of CH/GB mixed systems, and the presence of CH/GB complexes significantly decreased the surface tension of the oil/water interface. Compared to CH-stabilized emulsions, the adsorption of CH/GB complex particles at the oil/water interface benefited the formation of smaller size emulsion droplets, and effectively hindered droplet coalescence as supported by the increase of the emulsion's long-term stability. The formation of droplet network structures was significantly accelerated by increasing the oil volume fraction, resulting in a more solid-like thermoreversible emulsion gel with tunable viscoelastic properties, which could be adequate candidates for encapsulation and as coating materials in food and pharmaceutical applications.

TABLE OF CONTENTS

DEDICATION	iii
ACKNOWLEDGEMENTS	iv
RÉSUMÉ.....	vi
ABSTRACT	viii
TABLE OF CONTENTS	x
LIST OF TABLES	xiii
LIST OF FIGURES.....	xiv
LIST OF ABBREVIATIONS	xix
CHAPTER 1 INTRODUCTION.....	1
CHAPTER 2 LITERATURE REVIEW.....	3
2.1 Emulsion-based delivery systems	3
2.1.1 Emulsion classification	3
2.1.2 Emulsion preparation	6
2.1.3 Emulsion stability.....	9
2.1.4 Emulsion characterization and stability assessment.....	12
2.2 Protein/polysaccharide complexes	14
2.2.1 Molecular characteristics of proteins and polysaccharides	14
2.2.2 Emulsifying properties of proteins and polysaccharides.....	17
2.2.3 Protein-polysaccharide interactions	18
2.2.4 Emulsifying properties of protein/polysaccharide complexes	24
2.3 Chitosan and gelatin	26
2.3.1 Molecular structures of chitosan	26
2.3.2 Potential of chitosan as an emulsifier.....	28

2.3.3	Molecular structures of gelatin.....	31
2.3.4	Potential of gelatin as an emulsifier	32
2.4	Summary	33
CHAPTER 3 RESEARCH OBJECTIVES AND COHERENCE OF ARTICLES.....		34
3.1	Research objectives	34
3.2	Presentation of articles and coherence with research objectives.....	34
CHAPTER 4 ARTICLE 1: CHITOSAN-BASED CONVENTIONAL AND PICKERING EMULSIONS WITH LONG-TERM STABILITY		36
4.1	Abstract	36
4.2	Introduction	37
4.3	Experimental section	39
4.4	Results and discussion.....	40
4.5	Conclusion.....	50
4.6	Supporting information	56
CHAPTER 5 ARTICLE 2: COMPLEXATION OF CHITOSAN AND GELATIN: FROM SOLUBLE COMPLEXES TO COLLOIDAL GEL		58
5.1	Abstract	58
5.2	Introduction	58
5.3	Experimental	60
5.3.1	Materials.....	60
5.3.2	Preparation of chitosan-gelatin soluble and insoluble complexes	60
5.3.3	Zeta potential and particle size determination.....	61
5.3.4	Turbidity measurements	61
5.3.5	CLSM observation of soluble CH/GB complexes	61
5.3.6	Water content determination	62

5.3.7 Rheological measurements.....	62
5.4 Results and discussion.....	63
5.4.1 Characterization of CH/GB soluble complexes	63
5.4.2 Characterization of insoluble CH/GB complexes	69
5.5 Conclusions	76
CHAPTER 6 ARTICLE 3: PICKERING EMULSION GELS BASED ON INSOLUBLE CHITOSAN/GELATIN ELECTROSTATIC COMPLEXES	79
6.1 Abstract	79
6.2 Introduction	80
6.3 Experimental	81
6.4 Results and discussion.....	84
6.5 Conclusion.....	95
6.6 Supporting information	100
CHAPTER 7 GENERAL DISCUSSION.....	102
CHAPTER 8 CONCLUSION AND RECOMMENDATIONS.....	105
8.1 Conclusion.....	105
8.2 Recommendations	106
BIBLIOGRAPHY	107

LIST OF TABLES

Table 2.1: Thermodynamic and physicochemical properties of different types of emulsions [18].	4
Table 2.2: Molecular characteristics of food-grade proteins [60]	16
Table 2.3: Molecular characteristics of food-grade polysaccharides [7]	17
Table 2.4: Published studies on emulsifying properties of some protein/polysaccharide complexes.	25
Table 4.1: Diffusion rate constants (k_{diff}) and surface pressure at the end of adsorption (900 s; π_{900}) for chitosan molecules at an oil/water interface.	46
Table 6.1: Diffusion rate constants (k_{diff}) and surface pressure at the beginning (0 s; π_0) and end (9000 s; π_{9000}) of adsorption for CH/GB complexes (1 wt %, CH:GB = 1:2, 3 days of age) at an oil/water interface.	89

LIST OF FIGURES

Figure 2.1: Different types of emulsions in accordance with the continuous and disperse phase [17].	3
Figure 2.2: Schematic graphs of an O/W classical (surfactant-based) emulsion and an O/W Pickering emulsion [24].	4
Figure 2.3: Schematic representation of solid particles at an oil/water interface and influence of the contact angle on the type of emulsion.	5
Figure 2.4: A general process of O/W emulsion preparation, at the presence of oil, water and emulsifying agents.....	6
Figure 2.5: Schematic illustration on failures of O/W emulsions.....	9
Figure 2.6: Schematic diagram illustrating depletion (a) and bridging (b) flocculation mechanisms in the presence of a polymer [8].	10
Figure 2.7: Schematic representation of the formation of multilayer emulsions [1].	11
Figure 2.8: The 20 amino acids found in proteins.....	14
Figure 2.9: A protein consists of a polypeptide backbone with attached hydrophobic and hydrophilic side chains.....	15
Figure 2.10: Schematic illustration of protein-polysaccharide interaction [7].....	19
Figure 2.11: Phase contrast micrographs of the different structures that can be formed during the electrostatic complexation of proteins and polysaccharides: (a) coacervates; (b) insoluble complexes; and (c) electrostatic gel. The scale bars is 40 μm [75].....	21
Figure 2.12: Schematic representation of the turbidity evolution over the course of acidification for a hypothetical system containing a globular protein (circles) interacting with a anionic polysaccharide (coils) [76].	22
Figure 2.13: Schematic representation of the structural evolution of a electrostatic gel formed with oppositely charged proteins (circles) and polysaccharides (coils) [78].	23
Figure 2.14: Chemical structure of chitosan, containing <i>N</i> -acetyl-D-glucosamine (left) and D-glucosamine (right) units [89].	26

Figure 2.15: The protonated and deprotonated forms of chitosan [89].....	27
Figure 2.16: Scheme illustrating the potential electrostatic interactions of chitosan at the surface of emulsion droplets [89].	28
Figure 2.17: A scheme representing the assembly of chitosan on the oil/water interface [108]. ..	29
Figure 2.18: The formation of pH-responsive Pickering emulsion using chitosan alone [109]. ...	30
Figure 2.19: The molecular structure of collagen and gelatin, as well as the thermoreversible gelling property of gelatin.	31
Figure 4.1: Zeta (ζ) potential of chitosan solutions (0.1 wt %) as a function of pH and HIU treatment. CH indicates chitosan without HIU; CH-HIU indicates chitosan with 8 min HIU.	41
Figure 4.2: (a) AFM images of chitosan solutions with and without HIU at various pH; the inserts are photographs of chitosan solutions at pH 6.5 without HIU (right top) and with 8 min HIU (right bottom). (b) Volume fraction of chitosan molecular agglomerates size (chitosan concentration, 0.1 wt %) before and after 8 min HIU as a function of pH.	42
Figure 4.3: (a) Effect of HIU treatment on the complex viscosity of 2 wt % chitosan (pH 3.9). (b) Effect of pH on the complex viscosity of 2 wt % chitosan (without HIU treatment).	44
Figure 4.4: Time evolution of surface pressure for the absorption of chitosan molecules at an oil/water interface for different pH values: (a) without HIU treatment; (b) with 8 min HIU. The concentration of chitosan solution is 1 wt %.	46
Figure 4.5: (a) Optical micrographs of chitosan-based emulsions prepared at different pH values (3.5-6.5), after 1 h of preparation. (b) Volume- and number- average diameter as well as size distribution of fresh chitosan-based emulsions droplets. The emulsions were prepared with 1 wt % chitosan and an oil volume fraction of 0.1, using HIU homogenization for 8 min.	47
Figure 4.6: (a) Photographs and (b) creaming index of emulsions prepared with chitosan solution (1 wt %) at different pH values (3.5 to 6.5) and storage time (up to 5 months), with an oil volume fraction of 0.1. (c) Digital photographs of emulsion prepared with 1% (v/v) AcOH, with an oil volume fraction of 0.1.	49
Figure 4.7: The formation of chitosan-based emulsions: the role of pH and ultrasonication.	50

Figure 4.8: Turbidity profile of chitosan solutions (1 wt %) with and without HIU treatment and as a function of pH.	56
Figure 4.9: The effect of sonication time on the complex viscosity (1 rad/s) of a chitosan solution (DDA, 85%; dynamic viscosity, 60 mPa.s; concentration, 2 wt %, pH 3.9).	56
Figure 4.10: (a) Complex viscosity of chitosan solutions (1 wt %) at pH 4 for samples with same DDA (90%) but different molecular weights (dynamic viscosity varies from 60 to 1000 mPa.s). (b) Optical microscopy images of chitosan-based emulsions after 1 h of preparation, at an oil volume fraction of 0.2.	57
Figure 5.1: Zeta-potential of chitosan, gelatin and CH/GB complexes (0 mM NaCl) as a function of pH (a); CH/GB complexes at various pH and NaCl concentrations (b). Region A and Region B represent the same and opposite charge pH ranges, respectively, for chitosan and gelatin-B.	64
Figure 5.2: Photographs of CH/GB mixtures (total polymer concentration = 1 wt %, CH:GB = 1:2) at different pH and storage time.	65
Figure 5.3: Turbidity profile (a) and average radius (b) of CH/GB complexes (total polymer concentration = 1 wt %, CH:GB = 1:2, storage time = 3 days) at various pH and NaCl concentration.	67
Figure 5.4: Schematic diagram and photographs of time evolution of CH/GB complexes (total polymer concentration = 1 wt %, CH:GB = 1:2, pH = 5.5).	68
Figure 5.5: CLSM graph of CH/GB complexes (total polymer concentration = 1 wt %, CH:GB = 1:2, pH = 5.5, storage time = 3 days) with various NaCl concentration (A, 0 mM; B, 10 mM; C, 50 mM; D, 100 mM).....	69
Figure 5.6: Water content of CH/GB insoluble complexes (CH:GB = 1:2, pH 5.5) at various NaCl concentration and for two storage times (day 7 and day 40).	70
Figure 5.7: Time evolution of complex viscosity (a) and moduli (G' and G'') (b) for insoluble CH/GB complexes formed at pH 5.5 without salt.	72

Figure 5.8: Effect of salt concentration and storage time on storage and loss moduli ($\omega = 1$ rad/s) of insoluble CH/GB complexes formed at pH 5.5 (reproducibility was within 5% for all conditions).....	74
Figure 5.9: Temperature sweep (two cycles) of insoluble CH/GB complexes formed at pH 5.5 in the presence of 50 mM NaCl (storage time = 40 days).....	75
Figure 6.1: (A) Zeta potential of CH solutions (0.1 wt %), GB solutions (0.1 wt %) and CH/GB mixtures (0.1 wt %, CH:GB = 1:2) at different storage times, as a function of pH; (B) Comparison of ζ_{CH} , $\zeta_{CH/GB}$, and calculated $\zeta_{CH/GB}$ for freshly prepared samples.....	85
Figure 6.2: (A) Time evolution of turbidity for CH/GB mixtures (1 wt %, CH:GB = 1:2) as a function of pH; (B) CLSM images of CH/GB complexes (1 wt %, CH:GB = 1:2, pH 5.5, 3 days of age); (C) hydrodynamic diameter of CH/GB complexes as functions of pH, storage time and HIU treatment. D1, D3 indicates freshly prepared CH/GB complexes and CH/GB with three days of age, and D3-HIU means CH/GB complexes stored for 3 days and then treated with HIU for 8 min.	87
Figure 6.3: Time evolution of surface pressure for the adsorption of CH/GB complexes (1 wt %, CH:GB = 1:2, 3 days of age) at an oil/water interface for different pH values.	88
Figure 6.4: (A) Optical microscopy images of fresh emulsions prepared with CH/GB mixtures at different pH values (3.5-6.5). (B) Volume- and number-average diameter as well as size distribution of fresh CH/GB-based emulsion droplets. The concentration of CH/GB mixtures is 1 wt %, and the oil volume fraction is 0.1.	90
Figure 6.5: (A) Photographs of vials and (B) creaming index of emulsions prepared with CH/GB mixtures at different pH (3.5 to 6.5) and storage time (up to 5 months), with an oil volume fraction of 0.1.	92
Figure 6.6: Moduli (G' and G'') of fresh emulsions prepared with CH/GB complexes at different pHs (4.5 to 6.5) and oil volume fractions (0.2 to 0.4).	93
Figure 6.7: Temperature sweep (three cycles) of fresh CH/GB-based emulsions prepared at pH 5.5 (A) and 6.5 (B), at an oil volume fraction (ϕ) of 0.4.	94
Figure 6.8: The formation of Pickering emulsion gels stabilized with CH/GB insoluble complexes.....	95

Figure 6.9: Visual observation of CH/GB complexes (1 wt %, CH:GB = 1:2) at various pH values (3.5 to 6.5) and storage times (day 2 and day 3). All the samples are transparent on day 1 except for pH 6.5.....	100
Figure 6.10: Visual observation of high intensity ultrasonication-treated CH/GB complexes (1 wt %, CH:GB = 1:2, storage time: 3 days) at various pH values (3.5 to 6.5).	100
Figure 6.11: Optical microscopy images of fresh emulsions prepared with GB at different pH values (3.5-6.5).	101
Figure 6.12: Creaming index of GB-based emulsions (oil volume fraction = 0.1) prepared at different pH (3.5 to 6.5) and storage time (up to 1 month).	101

LIST OF ABBREVIATIONS

AcOH	Acetic acid
AFM	Atomic force microscopy
CH	Chitosan
CH/GB	Chitosan/gelatin complexes
CH-HIU	Chitosan with HIU treatment
CLSM	Confocal laser scanning microscope
CI	Creaming index
DDA	Degree of deacetylation
FITC	Fluoresceine isothiocyanate
GB	Gelatin type B
HIU	High intensity ultrasonication
HCl	Hydrochloric acid
LBL	Layer-by-layer
Mw	Molecular weight
NaCl	Sodium chloride
NaOH	Sodium hydroxide
O/W	Oil-in-water
O/W/O	Oil-in-water-in-oil

pI	Isoelectric point
SAOS	Small amplitude oscillatory shear
SEM	Scanning electron microscope
SDS	Sodium dodecyl sulphate
TGA	Thermogravimetry analyzer
W/O/W	Water-in-oil-in water

CHAPTER 1 INTRODUCTION

Background and problem identification

Bioactive lipids such as ω -3 fatty acids and oil-soluble vitamins are commonly regarded as health enhancers. However, their wide application in food and pharmaceutical areas have been limited by characteristics such as low water-solubility, poor incorporation to food matrices, physical or chemical instability, undesirable interactions with other compounds, oxidation or even decomposition [1]. Therefore, they need to be protected during processing, storage and maybe also during gastrointestinal transit before they reach the desired body site. To address these problems, microencapsulation technology that is able to protect and improve the stability of lipophilic nutrients has been introduced in food and nutraceutical industries [2, 3].

Microencapsulation is the packaging of tiny particles or droplets within a secondary material, to give small capsules of many useful properties [4]. The most common used method to encapsulate sensitive lipophilic bioactive ingredients is based on emulsion-delivery systems, which can be supplied in liquid, gelled or powered formats, and more importantly, their properties can be well controlled by tailoring the characteristics of shell materials (e.g., charge and interfacial properties) as well as the emulsion microstructures [1, 5, 6].

Ideally, the coating materials used to encapsulate lipophilic nutrients should be selected from a diverse range of natural biomaterials, or food additives that have been granted GRAS (generally regarded as safe) status [3]. In the past few years, encapsulation of lipophilic nutrients based on biopolymers or polymeric interactions has attracted increasing attention, due to the economically viable processing operations of food-grade coating materials [7, 8]. However, in most cases, the robustness of polymeric shell is not strong enough to resist environmental stress and thus physical or chemical cross-linking needs to be carried out to increase the stability of the capsules [9]. Currently, in order to avoid toxicity and cost increment induced by cross-linking, there is a growing number of investigations directed at designing more robust functional encapsulation systems using polymeric materials [10-13]. Since the most important properties for polymeric materials to act as good coating materials are their emulsifying properties and their properties to enhance viscosity or to form a gel-like structure, designing a macromolecular structure with improved emulsifying properties, turn to be of key importance [14, 15].

In this project, two bio-sourced polymers, namely chitosan (polysaccharide) and gelatin (protein), are used to encapsulate an oil ingredient (corn oil as a model oil), via fabricating oil-in-water emulsion systems using high intensity ultrasonic homogenizer. Chitosan alone is first used to prepare emulsions with long-term stability by altering its conformational structure through pH control. Subsequently, the interactions of chitosan and gelatin are investigated and the corresponding chitosan/gelatin complexes are used to produce emulsions. This Ph.D. work is expected to contribute to the development of lipophilic functional foods with improved stability based on natural biopolymers, and may also be useful in the design and formation of delivery systems for the pharmaceutical industry.

Organization of the thesis

This thesis is based on three articles that have been published by or submitted to scientific journals, and consists of the following chapters:

- Chapter 2 provides a literature review considering the related issues.
- Chapter 3 describes the objectives and the coherence of the articles.
- Chapters 4, 5, and 6 present the three articles describing the main achievements obtained in this study.
- Chapter 7 reports a general discussion about the main results.
- Chapter 8 states the conclusions as well as recommendations for future work.

CHAPTER 2 LITERATURE REVIEW

2.1 Emulsion-based delivery systems

2.1.1 Emulsion classification

As an important method of introducing lipophilic components into food or pharmaceutical matrices, emulsification is a process of dispersing two immiscible liquids in the presence of emulsifiers, which are amphiphilic molecules that can decrease the oil/water interfacial tension by adsorbing at the oil/water interface [16]. There are many terms used to describe different emulsion types. Generally, for typical emulsions containing oil and water, in accordance with their continuous and disperse phases, they can be divided conventionally into two types, i.e., oil-in-water (O/W) emulsions and water-in-oil emulsions (W/O), and in some cases, multiple emulsions, i.e., oil-in-water-in-oil (O/W/O) emulsions and water-in-oil-in-water emulsions (W/O/W) can also be formed, as shown in Figure 2.1.

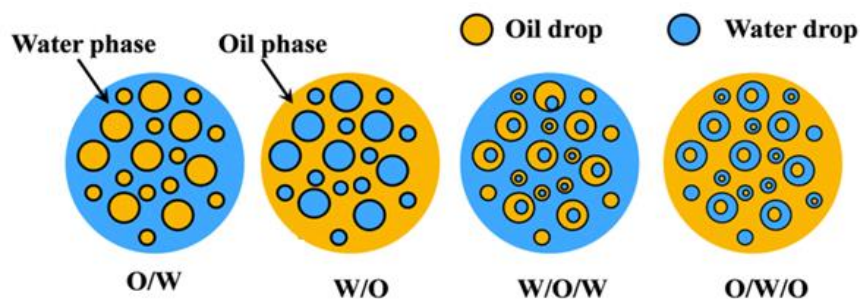


Figure 2.1: Different types of emulsions in accordance with the continuous and disperse phase [17].

Besides, emulsions can be also classified based on droplet size, thermodynamic characteristics and type of emulsifier. The droplet size of emulsions greatly determines their physical and thermodynamic properties, and consequently is one of the most important characteristic of an emulsion [18]. As shown in Table 2.1, based on the droplet size and thermodynamic characteristics, emulsions can be classified as macroemulsions (droplet diameters between 100 nm and 100 μ m), which are turbid or opaque because droplet size is of the same order of dimension as the light wavelength, nanoemulsions (droplet diameters between 10 and 100 nm) and microemulsions (droplet diameters between 2 and 100 nm), which are less turbid

since they spread less light [19]. Compared with macroemulsions, nanoemulsions are more kinetically stable and more resistant to flocculation, coalescence and the Oswald ripening process [20]. However, from a long-term aspect, only microemulsions are thermodynamically stable, while both macroemulsions and nanoemulsions are not, since microemulsions are formed by self-assembly, while macroemulsions and nanoemulsions are formed by mechanical force [21]. Therefore, the main difference between microemulsions and micro-size emulsions arise from thermodynamic characteristics of emulsion rather than droplet size. In the food industry, the most common used emulsion type is macroemulsion, which can be found in many different products, such as milk, beverages, mayonnaise, coatings, desserts, etc. [4].

Table 2.1: Thermodynamic and physicochemical properties of different types of emulsions [18]

<i>Emulsion Type</i>	<i>Droplet Size</i>	<i>Thermodynamic Stability</i>	<i>Optical Properties</i>
Macroemulsion	100 nm-100 μ m	Instable	Opaque/Turbid
Nanoemulsion	10-100 nm	Instable	Lucent/Turbid
Microemulsion	2-100 nm	Stable	Lucent/Turbid

In terms of emulsifying agents, emulsions can be divided into two types: classical emulsions and Pickering emulsions. Classical emulsions are stabilized by surface-active agents like surfactants (small amphiphilic molecules with both hydrophilic groups and hydrophobic groups) and amphiphilic polymers (e.g., proteins and polysaccharides from natural sources, synthetic surface-active polymers) [22, 23], while in case of Pickering emulsions, solid particles absorb at the oil/water interface to stabilize the emulsion droplets [24], as shown in Figure 2.2.

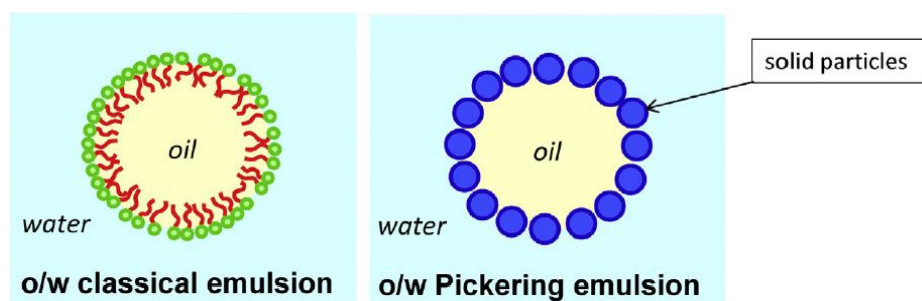


Figure 2.2: Schematic graphs of an O/W classical (surfactant-based) emulsion and an O/W Pickering emulsion [24].

Compared to classical emulsions, the specific property of Pickering emulsions is their high resistance to coalescence [25]. Meanwhile, Pickering emulsions retain the basic characteristics of classical emulsions and can be emulsions of any type, either O/W emulsions, W/O emulsions, or even multiple emulsions, therefore, a Pickering emulsion can be substituted for a classical emulsion in most cases [26]. Different to surfactants, being amphiphilic is not a necessary condition for the adsorption of solid particles at the oil/water interface, and thus the adsorption mechanism of solid particles is very different than from surfactants. Normally, the adsorption of solid particles at the oil/water interface requires the partial or intermediate wetting of the surface of solid particles by water and oil. Consequently, the contact angle (θ) of the oil/water interface with the solid particles turned out to be a very important factor, which determines the emulsion type and stability. As illustrated in Figure 2.3, an optimum stabilization of emulsions is located at $\theta = 90^\circ$, while O/W emulsions are formed preferentially for θ slightly less than 90° and W/O emulsions can be formed for θ slightly larger than 90° . However, no stable emulsions can be obtained if the particles are completely wetted either by the water or by the oil (i.e., they become dispersed in either individual phase, respectively) [24, 27].

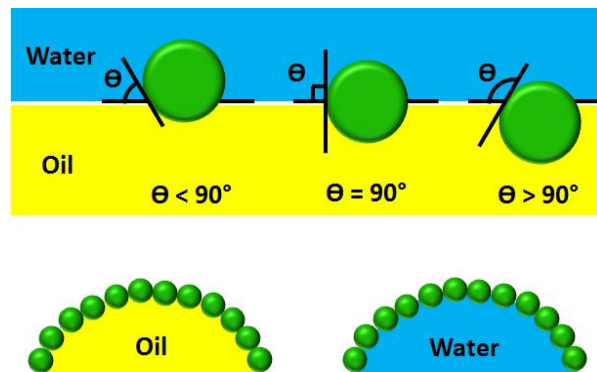


Figure 2.3: Schematic representation of solid particles at an oil/water interface and influence of the contact angle on the type of emulsion.

To stabilize oil droplets, the diameter of solid particles should be smaller than emulsion droplets, e.g., nanometric solid particles are able to stabilize emulsion droplets as small as few micrometers. Considering that the size of solid particles is small enough, so that the gravity effect can be neglected, the energy (E) required in removing a solid particle with a radius r from the oil/water interface turns out to be:

$$\Delta E = \pi r^2 \gamma_{ow} (1 \pm \cos \theta)^2 \quad (1)$$

where γ_{ow} and θ represent the oil/water interfacial tension and contact angle, respectively [28]. Since the energy barrier (E) to remove the solid particle from the oil/water interface is generally multiple orders of magnitude larger than the thermal energy (kT), the adsorption of solid particle can be considered as irreversible once they are attached to the interface [26]. This is different to surfactants which adsorb and desorb on a relatively fast timescale. In addition, the droplet size of Pickering emulsions can be reduced by increasing particle concentration or by decreasing particle size, and is also affected by process conditions such as emulsification times and energy levels [29]. The high stability of Pickering emulsions combined with their surfactant-free character makes them attractive in plenty of fields, especially in food and pharmaceutical applications, when using food-grade or biocompatible particles as Pickering emulsifiers.

2.1.2 Emulsion preparation

Generally, the preparation of emulsion systems requires a continuous phase, a dispersed phase, an emulsifying agent and energy input (homogenization). In the special case of encapsulation of lipophilic components, these should be first dispersed in the oil phase prior to homogenization (Figure 2.4). The selection of emulsifying agents and homogenization techniques is a key issue for emulsion preparation processes, which not only affects the emulsion type and stability, but also affects the final application. In the following sections, emulsifying agents and homogenization techniques used to produce emulsions are discussed.

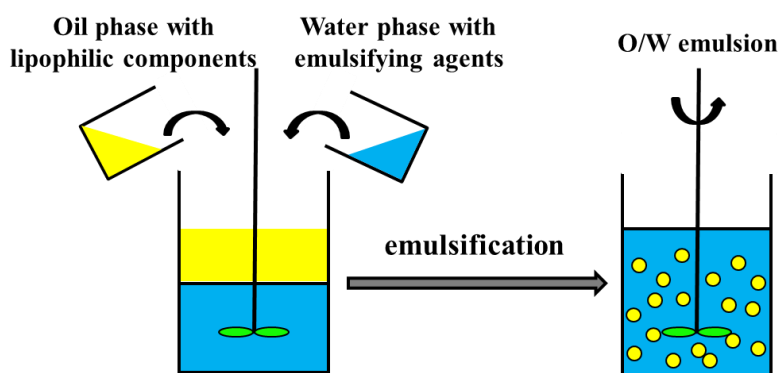


Figure 2.4: A general process of O/W emulsion preparation, at the presence of oil, water and emulsifying agents.

2.1.2.1 Emulsifying agents

Emulsifying agents used for emulsion preparation include surfactants, amphiphilic polymers as well as solid particles, as mentioned above. It should be noted that thickening agents that are used for the stabilization of emulsions are different than emulsifying agents. Thickening agents are typically used to develop emulsion stability by increasing the viscosity in the continuous phase of emulsions and limiting the movements of droplets, but it alone cannot form emulsions and needs the assistance of emulsifying agents [30]. The main functions of emulsifying agents include [5, 31]:

- Reducing the oil/water interfacial tension, and decreasing the requirement for energy input for the degradation of coarse droplets and thus facilitating the formation of smaller droplets;
- Preventing coalescence and separation into two immiscible phases by creating an interfacial protective layer on the surface of droplets, based on steric and/or electrostatic interactions;
- Providing additional functions like interacting with other bioactive components, forming films and controlling the transport of moisture or oxygen.

Surfactants. Surfactant is a class of small surface-active molecules that consist of a hydrophilic head group and lipophilic tail group. Low molecular weight surfactants are very mobile at the interface and the rapid adsorption of surfactants at the freshly created oil/water interface during emulsification can greatly reduce the surface tension of this interface, and thus ensure the formation of smaller emulsion droplets (Figure 2.2, left) [26]. The tail group varies in number, length and degree of saturation, while the head group may vary in physical dimensions and electrical charge. Surfactants can be classified as anionic, cationic and nonionic according to the type of polar group on the head group. The ionic surfactants have good water solubility and are generally used to make O/W emulsions, while the nonionic surfactants can be used to make either type of emulsions. Surfactants are very common ingredients in many application fields, especially in food, pharmaceutical and cosmetic industries. However, the presence of some synthetic surfactants often show adverse effects (e.g., tissue irritation, hemolytic behaviour, etc.), and in some cases, the deposition of surfactant-contained industrial and household waste on land and into water systems is found to be toxic to animals, humans and ecosystems, which somehow

increases environmental contaminants [32]. Therefore, the identification of other surface-active compounds with good surface activity but low toxicity turns out to be of great interest.

Surface-active biopolymers. In food and pharmaceutical applications, the emulsifying agents used to prepare emulsions should be safe accepted substances (generally recognized as safe-GRAS). For lipophilic ingredients encapsulation, it is better to select wall materials from a diverse range of natural biomaterials or food additives that have good surface-active properties. Natural biopolymers, e.g., proteins, polysaccharides, co-polymers (protein/polysaccharide complexes) have been employed to deliver a range of functional ingredients into foods [19, 36]. Compared to synthetic surfactants and polymers, the emulsifying agents obtained from natural polymers are biocompatible, biodegradable, and also have low toxicity, thus attracting more and more attention. Details about the emulsifying properties of proteins, polysaccharides, and protein/polysaccharide complexes will be presented later in Sections 2.2.2 and 2.2.4, respectively.

Pickering emulsifiers. In the case of Pickering emulsions, most of the particles used in the fundamental studies are synthetic or inorganic particles (e.g., silica particles), which greatly limit their applications in food and pharmaceutical industries [33, 34]. Recently, the development of bio-sourced particulate Pickering emulsifiers has received increasing attention. However, Pickering emulsifiers should have intermediate wettability and meanwhile insolubility in both the water and oil phases [35, 36], which makes the development of an effective bio-based Pickering emulsifier a very challenging task. In the past decades, only a few biocompatible materials, including chitin nanocrystal particles [37], starch granules [38], cellulose particles [39], and water-insoluble zein [40] have been shown employable as effective Pickering emulsifiers. Therefore, in order to meet the variable requests for specific applications, the development of more bio-sourced and even edible Pickering emulsifiers is desirable.

2.1.2.2 Homogenization techniques

Emulsions can be prepared by mechanical and non-mechanical methods. During the formation of emulsion droplets, a considerable amount of energy input is required. Currently, the most widely applied method for emulsion preparation is using intense mechanical force to homogenize the mixture of oil and aqueous phase in the presence of emulsifiers [41, 42]. The best-known homogenizers using mechanical force to prepare emulsions are high shear mixers, high pressure homogenizers, ultrasonic homogenizers and membrane homogenizers [43].

Generally, the level of energy input for homogenization increases in the following order: high-shear mixers, ultrasonic homogenizers, and high-pressure homogenizers. The energy input level not only affects the emulsification efficiency (e.g., affecting emulsion droplet size), but also may influence the properties of emulsifiers, e.g., their surface activities or aggregated state could be changed during homogenization because of the intense mechanical force [44]. The determination of homogenization techniques and processing conditions usually depends on the characteristics of the materials being homogenized (e.g., interfacial tension, viscosity) and also the requirements for the final applications (e.g., droplet size and droplet concentration).

2.1.3 Emulsion stability

2.1.3.1 Destabilization mechanism

The most challenging part raised by the use of emulsions is their thermodynamic instability. Emulsions tend to be physically unstable especially when they undergo environmental stress such as heating, freezing, pH and ionic strength changes [31, 45]. After homogenization, the interfacial area between the continuous and the dispersed phases is significantly increased; therefore, the interfacial free energy is considerably augmented. With respect to thermodynamic concepts, emulsions tend to separate into two phases in order to minimize the interfacial area and towards their minimum energy state [46]. Generally, emulsions can fail in four different ways, including flocculation, coalescence, creaming and breaking (as shown in Figure 2.5).

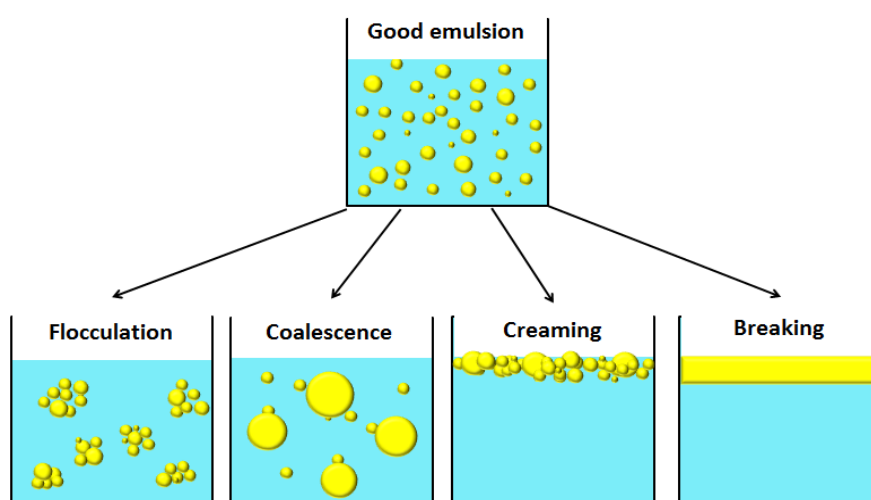


Figure 2.5: Schematic illustration on failures of O/W emulsions.

Flocculation and coalescence are the main destabilization mechanisms. Flocculation occurs when there is not sufficient repulsion to keep droplets away from each other and thus the van der Waals attraction has an opportunity to drive the system. It may occur either by depletion or bridging mechanisms, as shown in Figure 2.6 in the presence of a polymer [8].

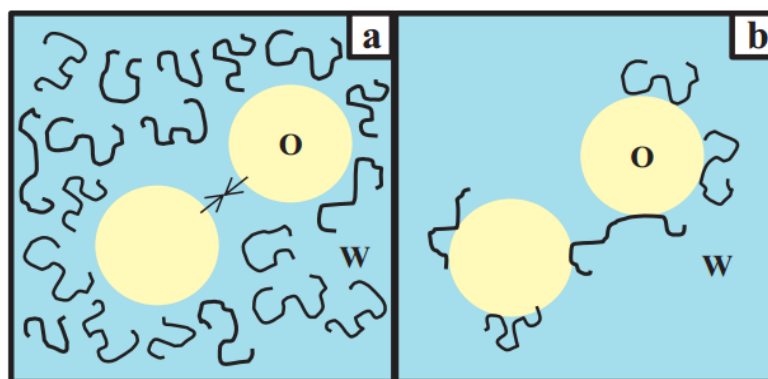


Figure 2.6: Schematic diagram illustrating depletion (a) and bridging (b) flocculation mechanisms in the presence of a polymer [8].

The formed flocs are the first step to coalescence and creaming. In some cases, the flocculation is reversible and can be broken by simple hand shaking or magnetic stirring; while in other cases, it is irreversible and droplets tend to coalesce, and then the droplet size distribution gradually shifts toward larger values. Over time, emulsions may further undergo creaming, which is the migration of oil droplets to the top of the dispersion because of the gravitational force on oil and water phases that differ in density. Ultimately, these can lead to the oiling off where emulsions separate into oil and water phases. For a specific application, it is very important to determine the effect of environmental conditions (e.g., pH, temperature) on emulsion stability, thus to find appropriate conditions to slow down these destabilization mechanisms.

2.1.3.2 Stabilization methods

To kinetically stabilize emulsions, corresponding methods have to be established, such as electrostatic stabilization, steric stabilization, the addition of small particles, surfactants or thickening agents [47, 48]. The traditional method is using monomeric surfactants such as sodium dodecyl sulphate (SDS) to decrease the O/W interfacial tension and increase emulsion stability. However, it can be potentially toxic towards the environment or causing irritation, as discussed in the previous section. The presence of some biopolymers (like proteins and

polysaccharides) can prevent flocculation and coalescence by providing both electrostatic and steric stabilization. In other cases, non-adsorbing thickening polysaccharides and biopolymer gels can reduce emulsion droplets movements and contacts by increasing the viscosity of the continuous phase. Small particles acting as Pickering emulsifiers can also strongly adsorb on the droplet surface and form protective physical barriers, thus preventing coalescence effectively as mentioned before. Here, it should be noted that the efficiency of emulsion stabilization by a biopolymer is determined by several factors, including polymer nature and concentration, solution pH and ionic strength, etc. Therefore, it is of key importance to control these parameters when formulating a biopolymer-stabilized emulsion [8].

The stability of emulsion can also be improved by designing a multilayer interfacial structure [49-51]. The multilayer emulsion is one example of electrostatic and polymeric stabilization. The scheme for multilayer emulsion preparation is shown in Figure 2.7. Compared to conventional emulsions, the continuous layer-by-layer (LBL) adsorption of oppositely charged polyelectrolytes onto primary emulsion droplets improves the physical stability of emulsions, thus enhances the robustness of the interface and protects sensitive active agents against undesirable physical and chemical influences [31].

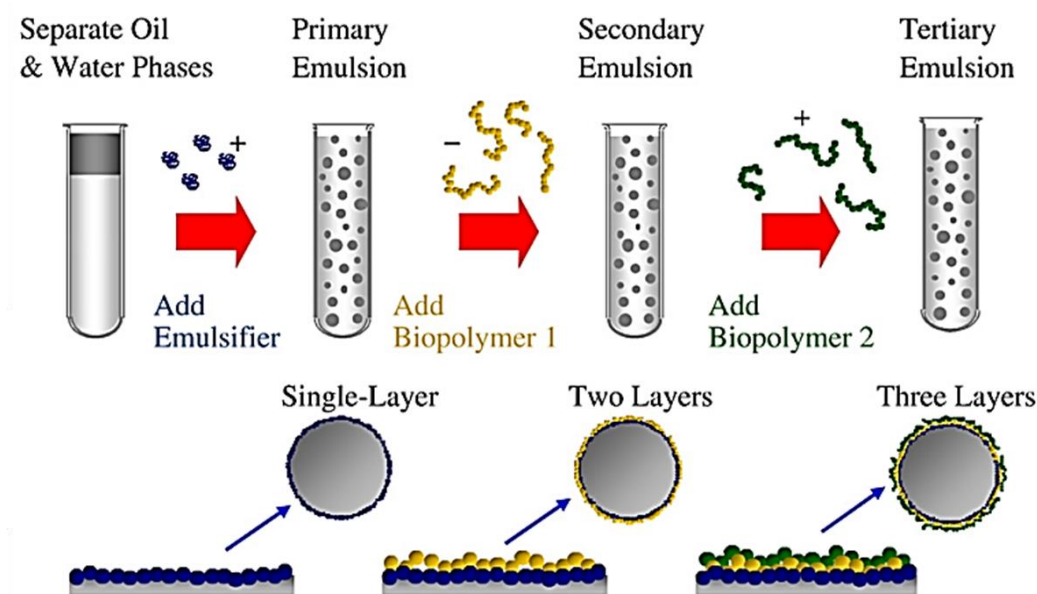


Figure 2.7: Schematic representation of the formation of multilayer emulsions [1].

2.1.4 Emulsion characterization and stability assessment

A general overview of the most common but not exhaustive used techniques for the characterization of emulsion is summarized in this section. All the characterization methods are utilized for the elucidation of the stabilization mechanisms and thus to find a way to control them.

2.1.4.1 Droplet size determination

The measurement of droplet size is one of the most important characterization for emulsion systems, since other properties such as appearance, stability and rheological behavior are significantly affected by droplet size. Droplet size and size distribution can be measured by means of various techniques, such as optical microscopy [52], dynamic light scattering [53] and laser diffraction [54]. For poly-dispersed emulsions, a mean droplet size is often presented rather than the whole distribution. The widely used terms for mean droplet size determination are area-weighted averaged diameter (d_{32}) which is related to the average surface area of droplets exposed to the continuous phase per unit volume of emulsion, and volume-weighted average diameter (d_{43}) which is more sensitive to the presence of large droplets.

2.1.4.2 Zeta potential measurement

Measuring the zeta potential of emulsions can provide valuable information to predict flocculation and coalescence in the case of electrostatically stabilized emulsions [55]. It is worthy to mention that the effective charge of a droplet is different from its actual charge due to the presence of counter-ions in the solution. The counter-ions close to the droplet surface are attached by electrostatic interactions and form the Stern layer, which decreases the actual charge of the droplet. Once applying an electrical field, the adsorbed Stern layer can move together with the droplet. The electrophoretic mobility (μ_{ep}) of the droplet is first measured and then the zeta potential is calculated using Henry's equation:

$$\mu_{ep} = 2\varepsilon\zeta f(ka)/3\eta \quad (2)$$

where ε is the liquid dielectric constant, ζ is the zeta potential, η is the viscosity of the continuous phase and $f(ka)$ is Henry's function constant. Therefore, the calculated zeta potential is actually related to the electronic potential of the Stern layer. In emulsion systems, a lower zeta potential value facilitates droplet contact and flocculation may occur, and conversely, a higher zeta

potential value can effectively avoid droplet flocculation. In addition, the presence of ions in emulsion systems can electrostatically screen the droplet charge and induce flocculation, which can also be detected by zeta potential measurements [56].

2.1.4.3 Emulsion stability

Emulsion stability is one of the most important factors that need to be considered during the development of a novel emulsion system. The physical stability can be evaluated by classical or accelerated aging methods. The classical method monitors the emulsion stability by storing emulsion samples under test conditions and examines the time-evolution of droplet size and appearance (e.g., the height of the creaming layer) at regular periodic intervals. In accelerated aging methods, the conditions that an emulsion could undergo during transportation and storage are mimicked. For example, it allows evaluating emulsion stability at different temperatures and storage times by conducting repeated heating/cooling cycles, or it can speed up the creaming rate by introducing centrifugation [57]. However, when using accelerated methods to map out the emulsion stability, conclusions should be drawn carefully since these methods do not perfectly mimic the natural aging process.

2.1.4.4 Rheological properties

The rheological properties of emulsions are influenced by various parameters, including oil volume fractions, droplet-droplet interactions and the viscosity of the continuous phase [58]. Several analyses are available to investigate emulsion rheological properties, such as steady flow, creep and oscillatory experiments. The most encountered rheological behavior of emulsions is its shear-thinning behavior, i.e., the apparent viscosity decreases as shear rate increases. In small amplitude oscillatory shear (SAOS) measurements, it allows the determination of viscoelastic properties like storage (G') and loss moduli (G''). Based on these rheological parameters it is possible to infer the properties of the emulsions, i.e. its texture. Besides, the conduction of time and temperature sweeps in SAOS tests could also provide valuable data for the evaluation of emulsion stability and droplet interactions.

2.2 Protein/polysaccharide complexes

2.2.1 Molecular characteristics of proteins and polysaccharides

Knowledge on molecular characteristics such as composition, molecular weight, charge density and structural properties is of great importance for protein-polysaccharide interactions. During the selection process of proteins and polysaccharides to form biopolymer complexes, it should not only consider the assembly ability of the biopolymers and the functional requirements for the final applications (e.g., charge, size and stability to environmental conditions), but also put emphasis on cost and composition.

Proteins are biopolymers containing 20 different types of amino acids, each with distinct chemical properties (as shown in Figure 2.8). The amino acids are linked to each other through a covalent peptide bond and then form a long peptide chain, namely, the primary structure of a protein. The side chain of the amino acid can be polar or nonpolar, positive or negative. Each type of protein is different in its amino acid sequence and number, which makes each protein unique.

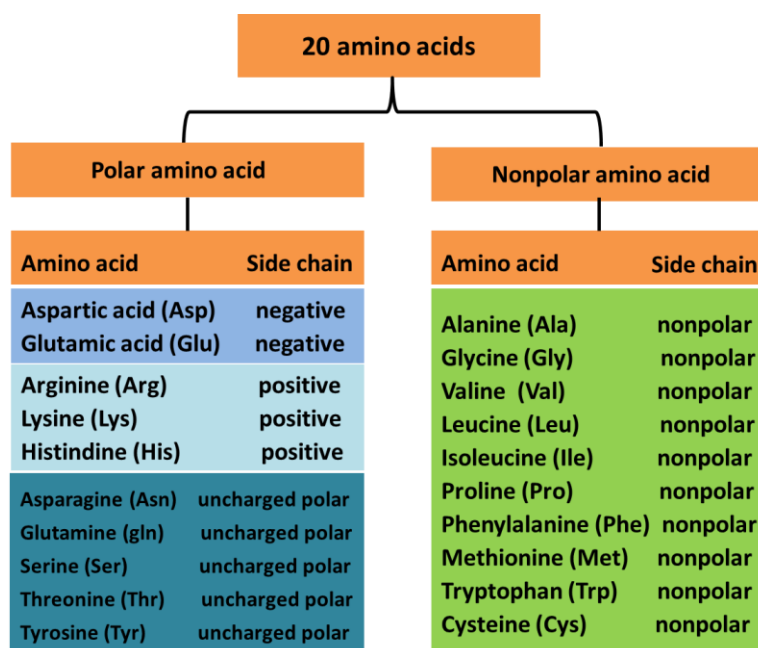


Figure 2.8: The 20 amino acids found in proteins.

Secondary structure of a protein refers to the coiling or folding of a polypeptide chain, which gives the protein a unique shape. It mainly contains two types of structure, namely, alpha helices

and beta sheets, which are secured by hydrogen bonding in the polypeptide chain. In the tertiary structure of proteins, the alpha helixes and beta sheets are folded into a compact globular structure, maintained by several types of bond and forces, including hydrophobic interactions, hydrogen bonding, ionic bonding, disulfide bonds and van der Waals forces. Quaternary structure is the three-dimensional structure of a protein macromolecule formed by the interactions of multiple polypeptide chains; each of them is referred to as a subunit. Similar as the tertiary structure, the quaternary structure is stabilized by the same non-covalent interactions and disulfide bonds.

The 3-D structure of a protein is intrinsically determined by its primary structure, and the sequence of amino acids establishes a protein's structure and specific function. For example, in Figure 2.9, it is clearly illustrated how the conformational structure of a protein is affected by amino acid composition. The hydrophobic side chains (green one) seek to avoid water and position themselves towards the center of the protein, and amino acids with hydrophilic side chains (blue one) tend to expose themselves to the aqueous environment, which finally leads to the formation of a globular structure. While for linear proteins such as collagen and gelatin, the specific amino acid composition and sequence lead to the formation of a triple helical structure or a random coil, instead of a globular structure [59].

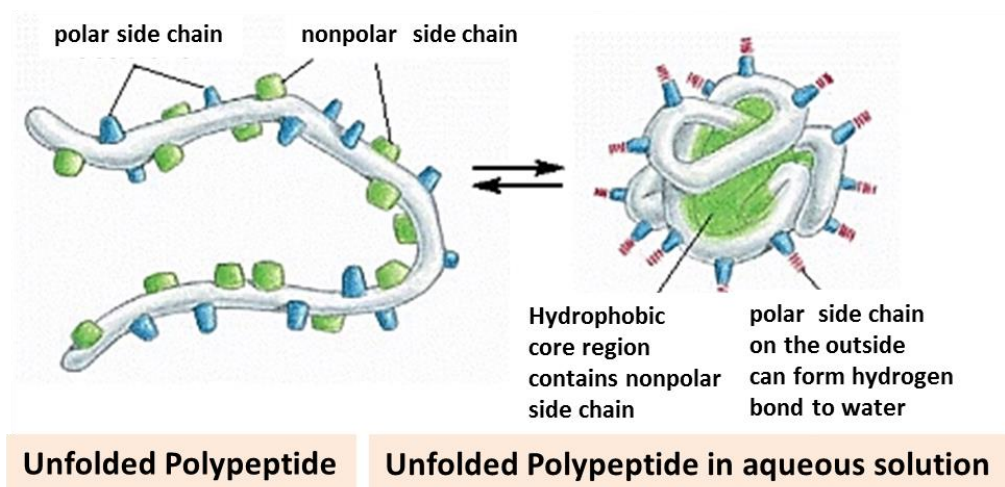


Figure 2.9: A protein consists of a polypeptide backbone with attached hydrophobic and hydrophilic side chains.

From a chemical aspect, proteins are by far the most structurally complex and functionally sophisticated biomolecules. The organization of proteins also greatly depends on various environmental conditions such as temperature, pH, ionic strength and solvent, and as a response, proteins tend to form a structure with minimum free energy in order to reach the most stable state [7]. Among them, pH is the most important factor that determines the conformation and charge density of protein molecules, and the pH where the net charge is equal to zero is called the isoelectric point (pI). The structure and pI of several food-grade proteins including both animal and plant proteins are listed in Table 2.2 [60]. Except for gelatin which is a linear protein, most proteins are globular. Besides, the price of gelatin is lower as compared to most globular proteins.

Table 2.2: Molecular characteristics of food-grade proteins [60]

Name	Source	Structure	pI
Bovine serum albumin	Bovine blood/milk	Globular	4.7
Gelatin	Collagen	Linear	7-9.4 ^a ; 4.8-5.5 ^b
Ovalbumin	Egg white	Globular	4.5-4.7
Soy glycinin	Soybean	Globular	5
β -Lactoglobulin	Whey protein	Globular	4.8-5.1

^a Type A gelatin; ^b Type B gelatin.

Polysaccharides are biopolymers comprised of repeated monosaccharide units that are conjugated by a glycosidic bond. The molecular structure of polysaccharides can range from linear to highly branched, depending on the monomer sequence and environmental conditions. The molecular characteristics of several food-grade polysaccharides are summarized in Table 2.3. The molecular properties of a polysaccharide such as molecular weight, flexibility, branching degree and charge properties can greatly affect its functional properties, and thus should be taken into account. The charge property of polysaccharides depends on the number and character of protonated functional groups, which can be adjusted by varying solution conditions, especially the pH value. A polysaccharide can be positively charged (e.g., chitosan), negatively charged (e.g., gum Arabic and carrageenan) or neutral (e.g., starch and cellulose), according to the pK_a of the charged groups, if present. Cationic polysaccharides tend to be positive at a pH value above their pK_a but neutral below, whereas anionic polysaccharides tend to be negative at a pH value above their pK_a but neutral below.

Table 2.3: Molecular characteristics of food-grade polysaccharides [7]

Name	Main structure type	Major monomer
Chitosan	Linear	2-Amino-2-deoxy- β -D-glucose
Carrageenan	Linear/helical	Sulfated galactan
Gum Arabic	Branched coil domains on protein	Galactose
Pectin	Highly branched coil	Glucuronate (backbone)
Alginate	Linear	β -D-Mannuronic Acid

2.2.2 Emulsifying properties of proteins and polysaccharides

In the food industry, both proteins and polysaccharides have been employed as emulsifiers or stabilizers in the production of food emulsions. Proteins are of particular interest in terms of their emulsifying properties due to their amphiphilic nature and nutritional content. The hydrophobic side chains of proteins can interpenetrate in the lipid phase to various degrees, while the hydrophilic side chains remain in the water phase [61], so protein-stabilized emulsions can provide both types of stabilization, either steric or electrostatic. There are three main stages for the adsorption of proteins at the oil/water interface: diffusion from the bulk to the vicinity of the interface, actual adsorption and reorganization of the adsorbed proteins. Compared to small surfactant molecules, the adsorption rate of protein molecules is relatively slow, but it is faster than for polysaccharides. The intermolecular interactions between protein molecules adsorbed at the oil/water interface can lead to the formation of a viscoelastic film that prevents coalescence [62]. Since each protein has a unique primary structure, different proteins possess various amounts of hydrophobic groups and exhibit different flexibility, and consequently diverse interfacial properties. Many proteins, like whey proteins (ovalbumins, lactoglobulins and lysozymes), bovine serum albumins, gelatin, etc., have been investigated and used as emulsifiers for several decades [63]. The adsorption of proteins at the oil/water interface can effectively stabilize emulsions by preventing droplet aggregation and coalescence. However, once the pH value of the emulsion is close to the isoelectric point of the adsorbed protein, droplet aggregation may occur because of the net zero charge on the protein. This is one of the limitations when using proteins to stabilize emulsions.

The hydrophilic character and high molecular weight of polysaccharides make them well known for their water-holding and thickening properties. For their use in stabilizing emulsion droplets, two categories can be proposed, i.e., adsorbing polysaccharides and non-adsorbing polysaccharides [8]. As their name says, non-adsorbing polysaccharides do not have much of a tendency to adsorb at fluid interfaces and decrease the oil/water interfacial tension, thus they have no or limited surface activity. The non-adsorbing polysaccharides, such as xanthan gum, alginate, carrageenan, etc., improve the emulsion stability mainly by gelling or increasing the viscosity of the continuous phase, which can effectively slow down droplet movements and encounters [64]. Adsorbing polysaccharides, like gum Arabic, cellulose derivatives, acetylated pectin from sugar beet, etc. can adsorb at the oil droplet surface to lower the oil/water interfacial tension, and then stabilize emulsion droplets through electrostatic and/or steric repulsive forces [65]. However, as mentioned in the previous section, the adsorption rate of polysaccharides at the oil/water interface is much slower than that of proteins, which somehow limits their applications in the stabilization of emulsion systems.

The combination of the advantages of polysaccharides (steric repulsion and/or viscosity enhancement) and proteins (fast adsorption) in the same system has shown the potential to create novel emulsions with improved stability and functionality, and thus has been increasingly studied. In Sections 2.2.3 and 2.2.4, the interactions between proteins and polysaccharides as well as the emulsifying properties of protein/polysaccharide complexes will be discussed.

2.2.3 Protein-polysaccharide interactions

The interactions between proteins and polysaccharides depend on the nature of the polymers used, the solution composition and environmental conditions. Phase separation can occur through two different physicochemical mechanisms, namely, associative and segregative separation (Figure 2.10). For an aqueous solution containing a protein and a polysaccharide that have a sufficiently strong attractive force (normally, electrostatic attraction) between them, it can form a homogeneous solution with protein/polysaccharide soluble complexes, or when the soluble complexes further flocculate to reduce the free energy of the system, it will separate into two phases, i.e., a concentrated phase that is rich in biopolymers and a dilute phase that is depleted [66].

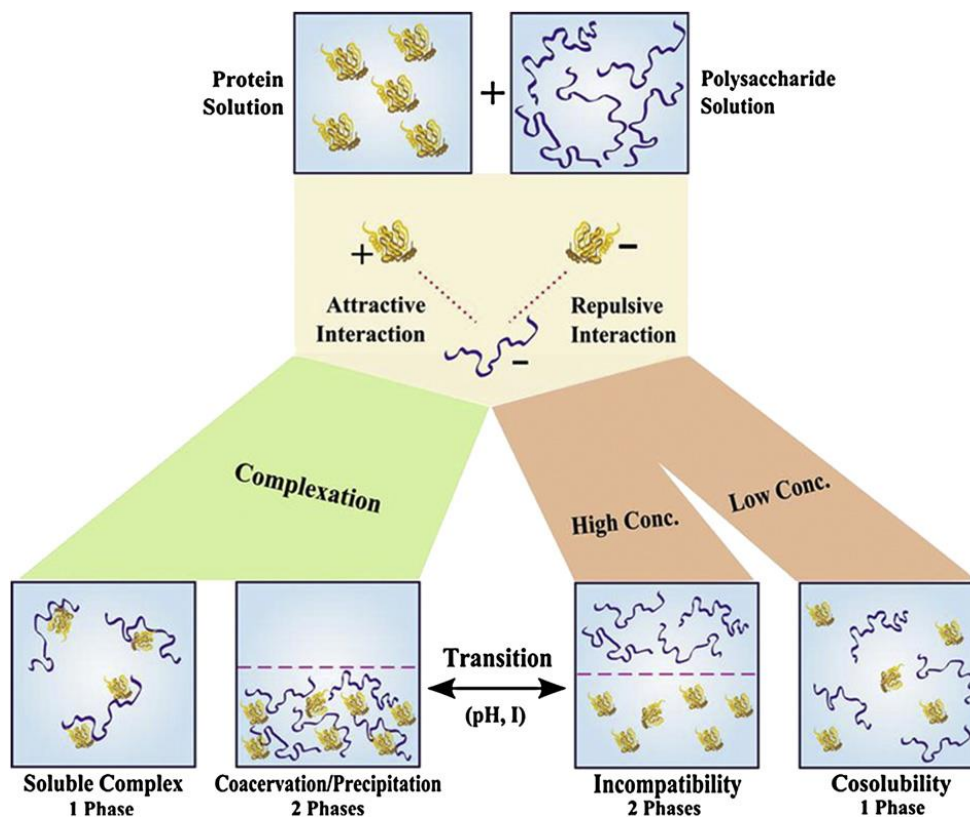


Figure 2.10: Schematic illustration of protein-polysaccharide interaction [7].

2.2.3.1 Driving force

It is generally acknowledged that electrostatic interactions are the most common forces involved in complex formation between charged macromolecules. Therefore, the physicochemical parameters influencing the charge density of proteins and polysaccharides play an important role in the control of the final complexes. Besides, processing conditions affecting charge properties also have a significant influence on the formation of protein/polysaccharide complexes [67, 68]. The most important physicochemical and processing parameters include pH value, ionic strength, temperature, and protein to polysaccharide ratio, total biopolymer concentration, biopolymer molecular weight and chain flexibility. For example, attractive interactions may occur between positively charged proteins ($\text{pH} < \text{pI}$) and anionic polysaccharides at low ionic strength, or between negatively charged proteins ($\text{pH} > \text{pI}$) and cationic polysaccharides. In some cases, complex formation is still possible for proteins and polysaccharides with the same net charge because of the presence of oppositely charged regions on the proteins, usually called “patches” [69].

Other non-Coulombic interactions such as hydrogen bonding and hydrophobic effect may also affect the formation of protein/polysaccharide complexes. Several approaches can be used to determine the effect of hydrogen bonding and hydrophobic interactions on protein/polysaccharide complexation. Altering temperature is one strategy to detect the contribution of hydrogen bonding or hydrophobic interactions, since a lower temperature is favourable to hydrogen bonding, while a higher temperature favors hydrophobic interactions [70]. For example, for the complexation of soybean 11S globulin and carboxymethyl cellulose, a decrease of temperature was found to induce phase separation, indicating the importance of hydrogen bonding in the formation of large-scale complexes [71]. Adding urea (which can disturb hydrogen bonding) and altering the ionic strength are other approaches applied to study non-Coulombic interactions of proteins and polysaccharides [72]. It is also suggested by some authors that the formation of primary soluble complexes of biopolymers could be mainly driven by electrostatic interactions, while the secondary large-scale aggregation would be greatly related to hydrophobic interactions or hydrogen bonding [73]. It should be mentioned that the contribution of non-Coulombic interactions intrinsically depends on the molecular characteristics of both protein and polysaccharide that are used to form the complexes. So, the question remains open, and in order to draw a clear picture, it would be necessary to investigate the molecular interactions of multiple combinations of proteins and polysaccharides in mixed systems.

2.2.3.2 Diverse structures of protein/polysaccharide complexes

During the complexation of proteins and polysaccharides, diverse structures including soluble/insoluble complexes, coacervates and gels are formed (as shown in Figure 2.11). The final structure of the protein/polysaccharide complexes mainly depends on protein/polysaccharide binding affinity, molecular charge density, and molecular conformation (e.g., chain flexibility) [74]. Both insoluble complexes and coacervates are related to phase separation phenomena, so there is some confusion in the scientific literature where sometimes complexes are referred to as “coacervates”. Actually, a coacervate is a liquid phase and always presents a spherical structure within another liquid phase (Figure 2.11 a), whereas insoluble complexes are referred to as “co-precipitates” with irregular microscopic structures (Figure 2.11 b). It is still not completely understood which mechanisms favor the formation of these different structures, but a general trend is that the formation of insoluble complexes and coacervates could be related to the chain

stiffness and charge density of polysaccharides, namely, polysaccharides having moderate charge density and flexible conformation would preferably form coacervates with proteins, whereas the reverse, i.e., polysaccharides with high charge density and/or stiffer structure would favor the formation of insoluble complexes [75]. Here, it should be noted that protein/polysaccharide complexes formed with different protein/polysaccharide couples bear enormous structural differences and functional properties, even if they have a similar structural type.

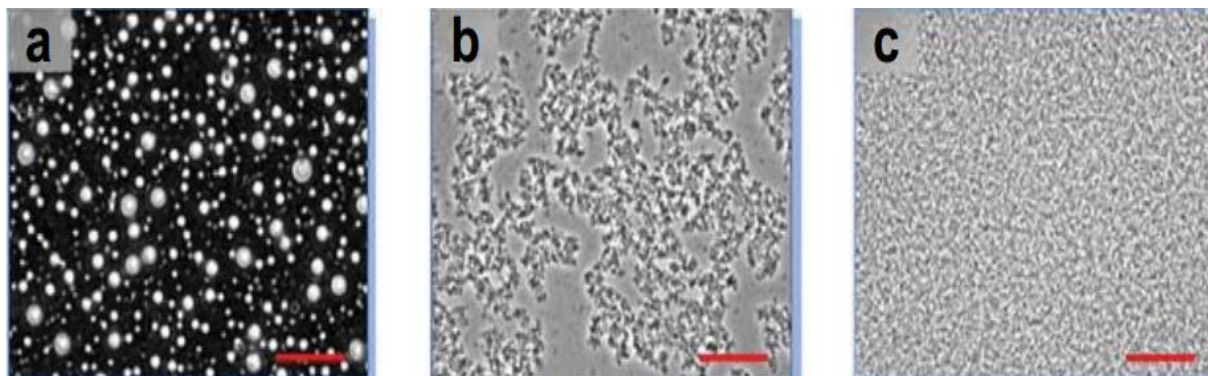


Figure 2.11: Phase contrast micrographs of the different structures that can be formed during the electrostatic complexation of proteins and polysaccharides: (a) coacervates; (b) insoluble complexes; and (c) electrostatic gel. The scale bars is 40 μm [75].

2.2.3.3 Structural evolution of protein/polysaccharide complexes

In the previous section, different final structures of protein/polysaccharide complexes were presented. In fact, for a certain protein/polysaccharide couple, the formation of complexes is a kinetic process affected by pH and storage time, and the structure of complexes can evolve from a soluble to an insoluble state, or to coacervate or gel.

pH-induced structural evolution. As an electrostatic-induced process, the structural transition of protein/polysaccharide complexes is very much influenced by pH. Turbidity measurement is a commonly used method to monitor the structural evolution of protein/polysaccharide complexes. Figure 2.12 shows the pH-controlled turbidity evolution of complexes formed with an anionic polysaccharide ($\text{pK}_a = 2$) and a globular protein ($\text{pI} = 4.5$) [76]. When pH is above the pI of the protein, or below the pK_a of the polysaccharide, no complexes are formed; while when the pH is close to the pI of the protein, the curve begins at a critical pH_c , which is characterized by a slow increase in turbidity and indicates the formation of soluble complexes. As pH continues to

decrease, the increasing charges on the protein molecules favor the interactions with the polysaccharide until pH_ϕ is reached, which is characterized by a sharp increase in turbidity. At this point, the net charge of the primary soluble complexes is quite low and they tend to self-associate to form large-scale insoluble complexes or coacervates. At the point of charge equivalence or stoichiometry, complexes can achieve neutrality, and usually the complex yield is highest at this point. In the literature, similar pH-induced structural evolution has been reported for other protein/polysaccharide couples (e.g., whey protein isolate/acacia gum and β -lactoglobulin/pectin systems) [75, 77].

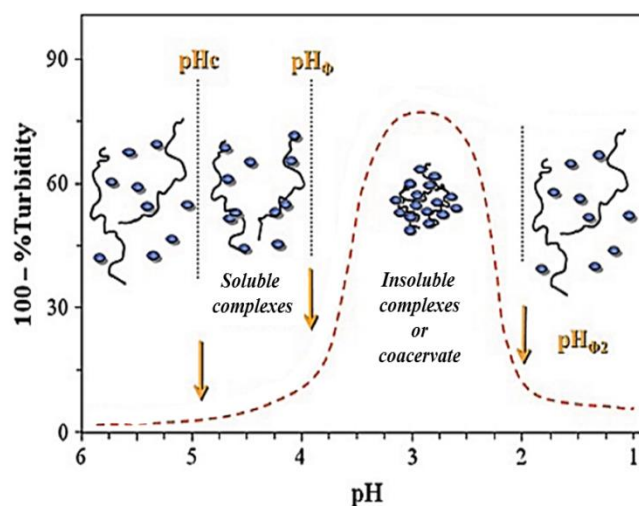


Figure 2.12: Schematic representation of the turbidity evolution over the course of acidification for a hypothetical system containing a globular protein (circles) interacting with an anionic polysaccharide (coils) [76].

Similar as the formation of insoluble complexes and coacervates, the generation of protein/polysaccharide electrostatic gels can also be pH-controlled. In Laneuville's work, where β -lactoglobulin and xanthan gum are used to form electrostatic gels, it shows that the increase of the net opposite charge can finally lead to the formation of electrostatic gels, as shown in Figure 2.13 [78]. The soluble complexes start to be formed based on the interaction between negatively charged xanthan gum and positively charged patches on the β -lactoglobulin protein surface. As the net opposite charge continues to increase, the primary complexes first aggregate into secondary complexes with denser structure, and then cluster-cluster aggregation makes the whole structure freeze-in at the point of gelation.

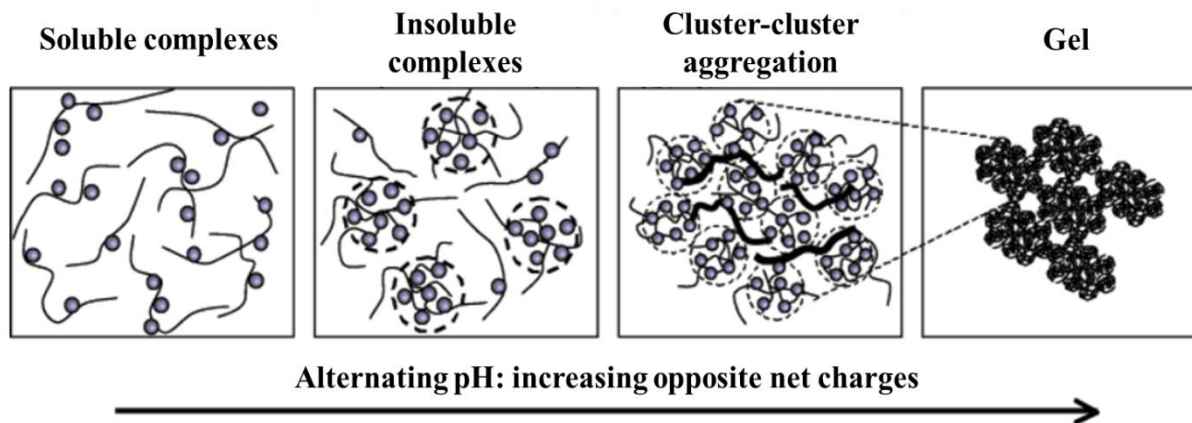


Figure 2.13: Schematic representation of the structural evolution of a electrostatic gel formed with oppositely charged proteins (circles) and polysaccharides (coils) [78].

Time-induced structural evolution. Although many protein/polysaccharide systems macroscopically change (e.g., from being transparent to turbid, or even leading to phase separation) over the course of minutes to days, little attention has been paid to the temporal domain based on the existing literature. Most of the prior studies have focused on the effects of mixing ratio, pH, ionic strength, and other external parameters on the formation of protein/polysaccharide complexes, usually at a fixed point in time [73, 75, 76]. However, the effect of the time-induced structural evolution of protein/polysaccharide systems is expected to be significant for any industrial application, especially with regard to colloidal stability. Very recently, Zhang and his coworkers investigated the colloidal stability and temporal evolution of polyelectrolyte complexes formed with two model polyelectrolytes: an anionic polyelectrolyte (poly (sodium 4-styrenesulfonate, (PSS)) and a cationic polyelectrolyte (poly (diallyldimethylammonium chloride) (PDAC)) [79]. They found that the process of complexation contains two steps: formation of primary polyelectrolyte complexes followed by a growth of secondary polyelectrolyte complex particles due to the aggregation of the primary particles. The altering of salt concentration appeared to strongly affect the time-dependent behavior of the polyelectrolyte complexes. Their results based on the strong polyelectrolyte systems have shed a light on the understanding of the temporal behavior of polyelectrolyte complexes. For the investigation of temporal evolution of protein/polysaccharide systems, which are both weak polyelectrolytes, more studies based on different protein/polysaccharide couples are required.

2.2.4 Emulsifying properties of protein/polysaccharide complexes

The formation of electrostatic complexes between proteins and polysaccharides enable the design of novel microstructures with improved physicochemical properties including gelling, foaming and emulsifying properties, and has been of general interest in various applications such as pharmaceuticals, tissue engineering, food, environmental and cosmetic fields, due to the versatility of materials prepared with this approach, as well as the bio-based source characteristics and unique functional properties of proteins and polysaccharides [80, 81].

There have been extensive studies on the emulsifying properties of protein/polysaccharide complexes, which are able to create novel emulsions with improved stability and functionality because of the combination of the advantages of polysaccharides (steric repulsion or viscosity enhancement) and proteins (fast adsorption compared to polysaccharides). Table 2.4 shows the main studies based on the emulsifying properties of protein/polysaccharide complexes. Specifically, there are two alternative procedures that can be used to prepare emulsions stabilized with protein/polysaccharide complexes. One of them is premixing protein and polysaccharide solutions in appropriate conditions, and then using the corresponding protein/polysaccharide complexes to prepare emulsions [82, 83]. Another procedure is the layer-by-layer (LBL) electrostatic deposition technique, as mentioned in Section 2.1.3. Normally, a protein is first used for the emulsification due to its faster adsorption at the oil/water interface, and then a polysaccharide is added to form a second layer at the protein-stabilized droplet surface through attractive electrostatic interactions. A multilayer protection can be achieved by repeating the last step using oppositely charged biopolymers [52, 55]. Once the physicochemical conditions (e.g., protein/polysaccharide ratio, pH, total biopolymer concentration, ionic strength, etc.) are well-established, the emulsions prepared based on the LBL method can have a better stability to environmental stresses such as pH, heating, freezing and dehydration, than a single interfacial layer, because of the stronger protection. However, it is a time-consuming process for the selection of suitable conditions and materials, and sometimes the presence of extra polysaccharide in the solution bulk can result in depletion flocculation and strongly reduce emulsion stability [84]. Compared to LBL methods, using protein/polysaccharide complexes directly to form emulsions is more attractive for large-scale production, due to the simplicity, fastness, and relative cost-efficiency of this method.

Table 2.4: Published studies on emulsifying properties of some protein/polysaccharide complexes.

	Protein ₁	Polysaccharide ₁	Polysaccharide ₂ or protein ₂	Experimental conditions (pH; incorporation order)	Ref.
Bi-layer or complexes	Whey protein isolated	Chitosan	-	pH 5.5; pr ₁ /ps ₁ premixed	[82]
		Pectin	-	pH 2-8; pr ₁ /ps ₁ premixed	[83]
		Xanthan gum	-	pH 7; pr ₁ then ps ₁	[85]
	β-lactoglobulin	Pectin	-	pH 4-7; pr ₁ then ps ₁	[52]
		Alginate	-	pH 3-7; pr ₁ then ps ₁	[86]
		Gum Arabic	-	pH 4.2; pr ₁ /ps ₁ premixed	[87]
Tri-layer	β-lactoglobulin	Pectin	Chitosan	pH 4; pr ₁ , ps ₁ then ps ₂	[52]
		Chitosan	Pectin	pH 3-7; pr ₁ , ps ₁ then ps ₂	[55]
		Chitosan	Alginate	pH 3-7; pr ₁ , ps ₁ then ps ₂	[55]

The emulsifying properties of protein/polysaccharide complexes intrinsically depend on the characteristics of the raw materials that are used to form the complexes. Plenty of pairs of protein/polysaccharide have been investigated for their ability to stabilize emulsions, e.g., whey protein isolate/pectin complexes [83], β -lactoglobulin/gum Arabic complexes [87], etc. Most of these studies focus on the interactions of globular proteins and anionic polysaccharides, however, the investigations are very limited in terms of the complexation of linear proteins (e.g., gelatin) and cationic polysaccharides (e.g., chitosan) because of the narrow pH range available for complexation, however these systems may be of interest both from a theoretical and practical point of view. On the one hand, the linear structure of proteins may result in complexes with different conformational structures; on the other hand, the cationic character of the polysaccharide may affect the pH range available for complexation, as well as for the emulsion preparation. From a practical point of view, novel complex systems combining the specific properties of linear proteins and cationic polysaccharides may enable the design of new emulsion

systems with targeted properties. In the following section, the molecular characteristics and emulsifying properties of chitosan (the only cationic polysaccharide of natural origin) and linear gelatin are introduced in details, aiming to provide information for the understanding of their complexation and also the emulsifying properties of the corresponding complexes.

2.3 Chitosan and gelatin

2.3.1 Molecular structures of chitosan

Chitosan is a naturally derived polysaccharide, commonly obtained by the alkaline or enzymatic deacetylation of chitin, the second most abundant polysaccharide on earth after cellulose, with a DDA (or degree of deacetylation) greater than 60% [88]. As a linear unbranched polysaccharide, it is composed of randomly distributed deacetylated units (β -(1-4)-linked D-glucosamine) and acetylated units (*N*-acetyl-D-glucosamine). The chemical structure of chitosan is shown in Figure 2.14.

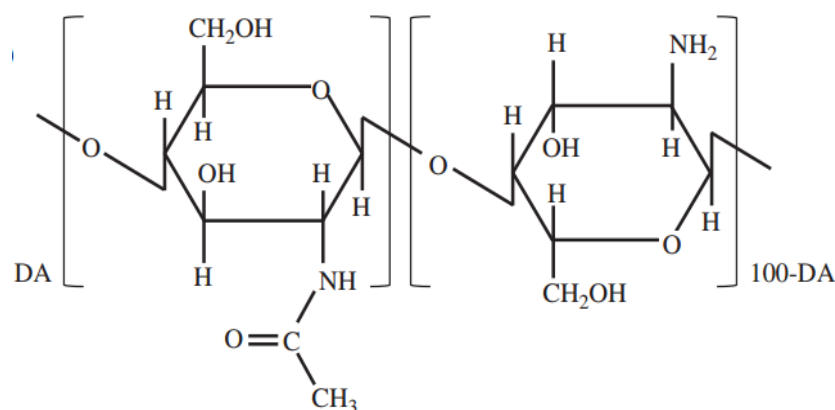


Figure 2.14: Chemical structure of chitosan, containing *N*-acetyl-D-glucosamine (left) and D-glucosamine (right) units [89].

According to its chemical structure, chitosan is a potentially pH-responsive polymer. The protonation of the amino groups makes it soluble and behaves as a cationic polyelectrolyte at a pH below its *pK_a* (6.2~6.5), while it is insoluble at a pH over its *pK_a* [90]. The protonated and deprotonated forms of chitosan are shown in Figure 2.15.

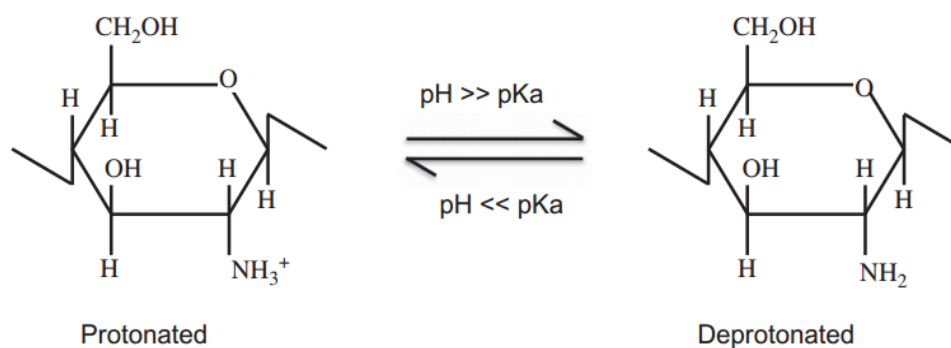


Figure 2.15: The protonated and deprotonated forms of chitosan [89].

The resulting charge density on the chitosan chains, which can be affected by DDA, molecular weight (M_w) and the distribution of acetyl and amino groups along the polymer backbone [91], may influence its conformation and thus the intermolecular forces, including electrostatic interaction, hydrophobic effect and hydrogen bonding [92]. For example, an increase in DDA can directly augment the number of amino ($-NH_2$) groups and thus increase the charge density of chitosan in acidic conditions. Besides, changing the charge density of chitosan chains by means of varying pH, ionic strength or solvent type, it is also an effective way to modify the physicochemical and rheological properties of chitosan solutions [93].

The molecular weight (M_w) of chitosan is another key factor that can influence its physicochemical properties, such as solubility and viscosity. The M_w of commercially available chitosan ranges from 100 to 1200 kDa. As for other polymers, the viscosity of chitosan solution is related to its M_w . Owing to its high molecular weight and linear unbranched structure, chitosan is a good viscosity-enhancing agent in acidic conditions below its pK_a [94].

The good biodegradability and biocompatibility, as well as low toxicity make chitosan attractive in a wide range of applications in food technology, biomedical, and pharmaceutical industries [95-97]. Meanwhile, the cationic properties of chitosan also enable it to strongly interact with oppositely charged polyelectrolytes, or lipids of bio-membranes [8]. Chitosan has been approved as a food additive in Japan and Korea since 1983 and 1995, respectively, and approved as a food thickener in meat products in China since 2007 [89]. In USA, chitosan has been received a GRAS (generally recognised as safe) status for its use in foods in 2001 [98].

2.3.2 Potential of chitosan as an emulsifier

Chitosan has been employed in emulsion stabilization mainly due to its viscosity enhancement, since the addition of chitosan in emulsion systems can increase the viscosity of the continuous phase, thus slowing down the diffusion of droplets and decreasing the creaming rate [99]. In addition, the polyelectrolyte character makes chitosan able to electrostatically interact with oppositely charged surface-active polymers or surfactants that are already adsorbed on the surfaces of oil droplets, to form a protective interfacial layer via electrostatic and steric stabilization, as shown in Figure 2.16. Compared to emulsions containing anionic droplets or those coated with thinner layers, emulsions containing cationic chitosan droplets with relatively thick interfacial layers can provide better stability against lipid oxidation [100, 101] and particle aggregation [102, 103].

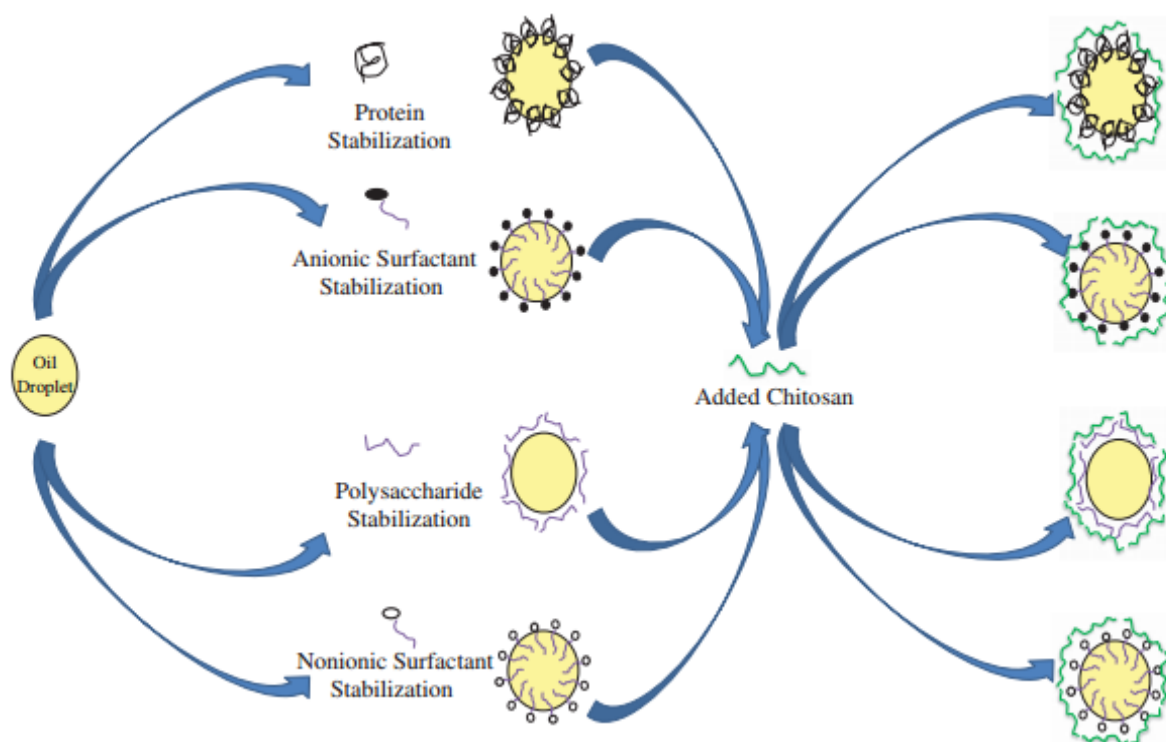


Figure 2.16: Scheme illustrating the potential electrostatic interactions of chitosan at the surface of emulsion droplets [89].

However, the potential of chitosan as an emulsifier is still a matter of debate. That is one of the reasons why chitosan is classified in the non-adsorbing polysaccharide category. Only few papers describe the emulsifying properties of chitosan alone without hydrophobic modification or

without combining it with other surface active agents. In some articles, chitosan is reported for its low surface activity at the oil/water interface, and the increase of chitosan concentration just leads to a small overall decrease of surface tension compared to traditional amphiphilic molecules [89, 104]. With respect to its molecular structure, the lower surface activity of chitosan can be understood. Chitosan has many hydrophilic sites (amine groups), but limited hydrophobic sites (acetyl amine groups), and moreover, the random distribution of the hydrophobic groups may further reduce their capacity to access the oil/water interface because of steric hindrance [105].

In some other cases, chitosan is found able to form O/W emulsions. For example, Schulz *et al.* first reported that chitosan can form a water-in-oil-in-water (W/O/W) multiple emulsion in aqueous acetic acid [106]. Then, they investigated the effect of DDA, M_w and polymer concentration on the emulsifying properties of chitosan under similar acidic conditions, and found that increasing chitosan concentration first augmented its emulsifying properties and then decreased them, while DDA showed a reverse effect. They also concluded that chitosan with lower M_w had better emulsifying activities than those with higher M_w , because low M_w chitosan can adsorb on the surface of oil droplet more easily and compactly [107]. The discrepancies in the emulsifying properties of chitosan may be due to the differences in the characteristics of oil and the chitosan grades used in different studies.

Later, Payet *et al.* reported that as the pH of a chitosan solution increased to 5, a dense polyelectrolytic brush on the water side of the oil/water interface could be produced while the hydrophobic sites adsorb on the oil side (as shown in Figure 2.17), and thus the corresponding O/W emulsion stability can be increased owing to steric and electrostatic hindrance [108].

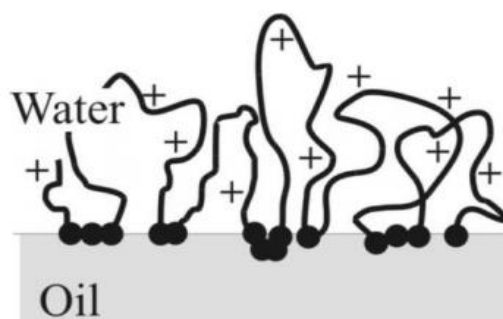


Figure 2.17: A scheme representing the assembly of chitosan on the oil/water interface [108].

Very recently, Liu *et al.* found that a simple, reversible O/W Pickering emulsion can be formed on the basis of chitosan alone at higher pH values ($> pK_{a \text{ chitosan}}$) [109, 110]. When pH value was close or above the pK_a of chitosan, it turned to be insoluble because of the aggregation of chitosan chains induced by the deprotonation of amino groups. When these chitosan aggregates were used to prepare O/W emulsions, they could act as a Pickering emulsifier and adsorb on the surface of oil droplets to form a physical barrier against coalescence and creaming. Interestingly, once the pH was decreased, demulsification happened due to the solubilisation of chitosan. In Figure 2.18, the formation the chitosan-based pH-responsive Pickering emulsion is presented. Although the droplet size and size distribution is still not as good as other commonly used Pickering emulsifiers, the application of chitosan aggregates in the formation of Pickering emulsions opens new possibility for the development of bio-based Pickering emulsifiers. The advantage of self-aggregated chitosan particles as a novel Pickering emulsifier is that they are bio-sourced, biocompatible, relatively inexpensive and even edible, and thus can be promising candidates to replace synthetic or inorganic particles in stabilizing food-grade Pickering emulsions [111, 112].

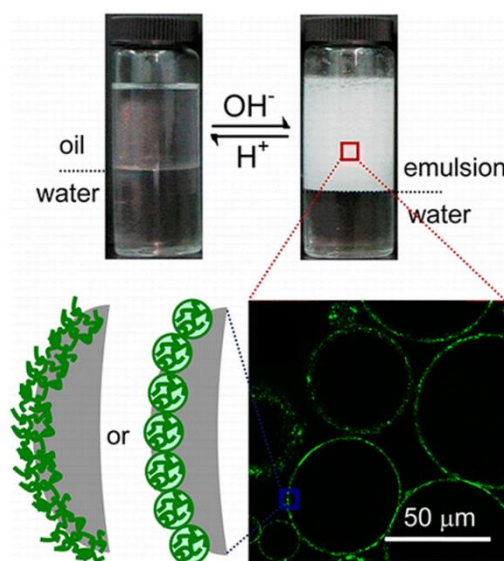


Figure 2.18: The formation of pH-responsive Pickering emulsion using chitosan alone [109].

All the above-mentioned literature suggests the importance of pH on the formation of chitosan-stabilized emulsions; however, there is no systematic study on this topic yet, thus pointing to the necessity of investigating further the role of pH on the emulsifying properties of chitosan. On the other hand, the stability of these chitosan-based emulsions (for both

conventional and Pickering) is still a limiting factor for their industrial applications, and thus needs to be improved in further studies.

2.3.3 Molecular structures of gelatin

Gelatin is a versatile biodegradable polymer derived from animal collagen (e.g., pig, cow or fish), and has been employed in numerous applications in food, pharmaceutical, medical and cosmetic fields [113, 114]. As shown in Figure 2.19, collagen is a protein made up of three polypeptide strands, which are wound together into a right handed triple helix by hydrogen bonds. When collagen is denatured by heating, it undergoes partial hydrolysis and the three amino chains are broken down into random coil globs, which is so called gelatin. Gelatin has a structure of a linear chain with very little ramifications [115]. The thermoreversible gelling property is a unique characteristic of gelatin, which is capable of forming thermally reversible hydrogels. Upon cooling, gelatin random coil globs can rearrange to build up hydrogen bonds, and thus the gelatin solution is then converted into an elastic gel; while upon heating, the hydrogen bonds can be destroyed and the structure of gelatin goes back to random coil globs. The sol-gel transition temperature is between 15-36 °C, depending on the type and source of gelatin. Since the sol-gel transition temperature is below body temperature, it gives gelatin specific organoleptic and flavor release properties [116].

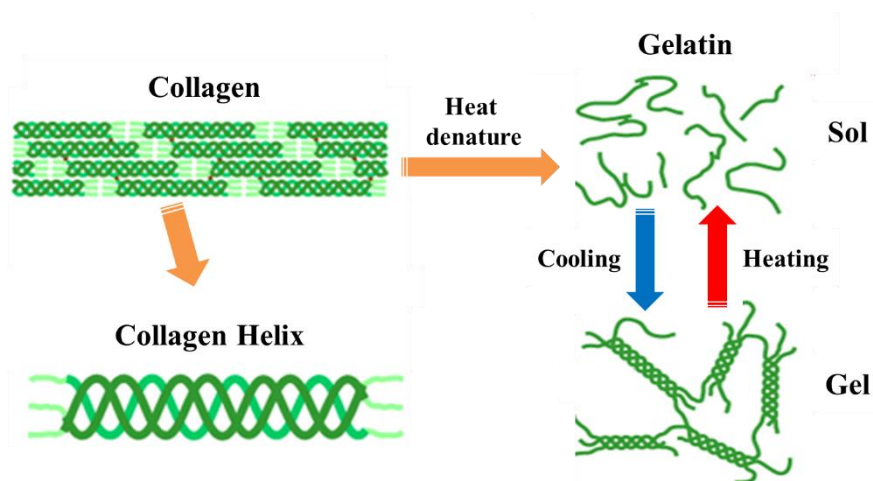
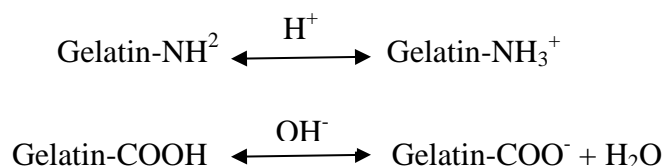


Figure 2.19: The molecular structure of collagen and gelatin, as well as the thermoreversible gelling property of gelatin.

According to the difference in hydrolysis processes, two types of gelatin can be obtained, namely, gelatin type A (acid pre-treatment) with an isoelectric point (pI) of 7-9 and gelatin type B (alkaline pre-treatment) with a pI of 4.7-5.2. Gelatin contains 18-20 amino acids and about one-third to half of the total amino acid residues is glycine or alanine. Alanine is the predominant N-terminal residue of gelatin-A, whereas the proportion of glycine tends to be larger in gelatin-B. The amino and carboxyl groups on the peptide chain make gelatin an amphoteric polyelectrolyte. A variation of pH affects the charge density of gelatin molecules and the net charge of gelatin can evolve from cationic to anionic, as shown below:



2.3.4 Potential of gelatin as an emulsifier

The amphoteric characteristic combined with the hydrophobic sites on the gelatin chain give gelatin surface-active and emulsion-stabilizing properties. Gelatin has been used as an emulsifying, foaming, and wetting agent in food, medical, pharmaceutical, and cosmetic applications [117]. Gelatin is capable of adsorbing at the oil/water interface and forming a continuous viscoelastic film on the surface of oil droplets, thus improving the emulsion stability [118]. However, compared to other surface-active components like globular proteins, gelatin is generally a weak emulsifier, and the emulsion prepared with gelatin alone often shows relatively large droplet sizes [119]. Therefore, hydrophobic modification by the attachment of nonpolar side-groups [120], or conjunction with oppositely charged surface-active substances [84] is usually carried out to improve the emulsifying properties of gelatin. In addition, the emulsifying properties of gelatin also depend on the source and manufacturing process of gelatin. For example, mammalian gelatin shows better emulsifying properties compared to gelatin from marine resources [121]. It should be mentioned that gelatin is chosen in most applications not only for its surface-active properties, but rather due to its unique combination of surface-active, chemical, and gelling properties.

2.4 Summary

As reviewed above, proteins and polysaccharides as emulsifiers are of great interest in the formation of food-grade emulsions because of their versatility and natural source characteristics. There have been extensive studies on the emulsifying properties of commonly used polymeric emulsifiers such as whey protein isolate, β -lactoglobulin, gum Arabic, and pectin, because of their good surface-active properties. However, investigations on other abundant-occurring biopolymers such as chitosan are limited, due to their relatively lower surface activities.

Chitosan is the only naturally-derived cationic polysaccharide, the second most abundant polysaccharides on earth after cellulose. The good biodegradability, biocompatibility, low toxicity, as well as the cationic properties make chitosan attractive in a wide range of applications. However, the potential of chitosan as an emulsifier is still a matter of debate. Several recent studies show that the stability of chitosan-based emulsions can be improved by altering the solution pH, and a Pickering emulsion can even be formed once the pH is close or above the pK_a of chitosan. These findings indicate the importance of pH on the formation of chitosan-stabilized emulsions and point out to the necessity of investigating further the role of pH on the emulsifying properties of chitosan. Meanwhile, the stability of chitosan-based emulsions still needs to be improved further to fulfill the requirements for their use in industrial applications.

Using protein/polysaccharide complexes to stabilize emulsions also attracts more and more attention, because this approach combines the functional and nutritional properties of proteins and polysaccharides and also gives emulsions novel functionalities. The emulsifying properties of protein/polysaccharide complexes greatly depend on the properties of proteins and polysaccharides that are used to form complexes. Plenty of protein/polysaccharide couples have been investigated for their emulsifying properties and most of these studies have focused on the interactions of globular proteins and anionic polysaccharides. However, the potential emulsifying properties of complexes fabricated from linear proteins (e.g., gelatin) and cationic polysaccharides (e.g., chitosan) are rarely studied because of the narrow pH range available for complexation, although they could combine the specific properties of both building blocks and enable the design of more diverse emulsion systems.

CHAPTER 3 RESEARCH OBJECTIVES AND COHERENCE OF ARTICLES

3.1 Research objectives

According to the literature review presented in Chapter 2, the emulsifying properties of chitosan are still a matter of debate, and the electrostatic complexation using a cationic polysaccharide with linear proteins (especially gelatin and the only naturally derived polycation, chitosan) has not been widely investigated, despite the fact that these systems could enable the design of more diverse emulsion systems with novel functionalities. Thus, the main objective of this work is:

“To investigate and also improve the emulsifying properties of chitosan and chitosan/gelatin complexes”

The specific objectives of the current work are:

- 1) To develop long-term stable chitosan-based oil/water emulsions through the control of pH.
- 2) To establish a comprehensive understanding of the electrostatic interactions between chitosan and gelatin type B.
- 3) To develop long-term stable oil/water emulsions using chitosan/gelatin complexes.

3.2 Presentation of articles and coherence with research objectives

The following three chapters comprise the articles containing the main scientific findings of this study and represent the core of the thesis, which is presented in the form of three peer-reviewed journal papers.

Chapter 4 presents the results of the first paper “*Chitosan-based conventional and Pickering emulsions with long-term stability*” that has been published in *Langmuir* (VOL. 32, NO. 4, 929–936, 2016) (impact factor = 4.457). This journal was chosen because it is the leading journal focusing on the fundamental science of systems and materials in which the interface dominates structure and function. This paper was submitted on September 24, 2015 and accepted on January 07, 2016. In this work, a chitosan-stabilized emulsion with considerable long-term stability was developed

with the assistance of ultrasonication. The role of pH and ultrasonication on the molecular characteristics of chitosan was first investigated and a link between the molecular characteristics and emulsifying properties of chitosan was established. Increasing pH of chitosan solution as well as ultrasonication treatment was found beneficial for the improvement of the emulsion stability. The results in this work suggest that chitosan possesses great potential to be used as an effective pH-controlled emulsifier and stabilizer without the need of other additives.

Chapter 5 contains the results of the second article “*Complexation of chitosan and gelatin: from soluble complexes to colloidal gels*” that has been published in *International Journal of Polymeric Materials and Polymeric Biomaterials* (VOL. 65, NO. 2, 96–104, 2016) (impact factor = 3.586). This journal was selected because it addresses innovation needs in the areas of both polymeric biomaterials and biomedical polymers. This article was submitted on April 10, 2015 and accepted on July 16, 2015. In this work, the complexation of chitosan and gelatin was comprehensively studied as function of pH, ionic strength and storage time. As storage time increased, the chitosan/gelatin complexes evolved from soluble to insoluble complexes and finally to a viscoelastic colloidal gel. The insoluble CH/GB complexes and the corresponding colloidal gel developed in this work may find interesting uses in the scope of delivery of sensitive bioactive molecules or nutrients with tailored properties.

Chapter 6 presents the results of the third paper “*Pickering emulsion gels based on insoluble chitosan/gelatin electrostatic complexes*” that was submitted to *RSC Advances* (impact factor = 3.8). This journal was selected because it is one of the most prestigious platforms for publications on the latest progress in chemical science. In this work, insoluble chitosan/gelatin complexes were used to prepare Pickering emulsions and gels. The adsorption of CH/GB particles at the oil/water interface benefited the formation of smaller emulsion droplet size and effectively hindered oil droplets coalescence, as supported by the increase of emulsion long-term stability. The results in this work suggest that CH/GB insoluble complex particles are promising particulate emulsifiers to fabricate surfactant-free Pickering emulsion gels.

CHAPTER 4 ARTICLE 1: CHITOSAN-BASED CONVENTIONAL AND PICKERING EMULSIONS WITH LONG-TERM STABILITY

Xiao-Yan Wang and Marie-Claude Heuzey

Department of Chemical Engineering, CREPEC, Polytechnique Montreal, PO Box 6079, Station Centre-Ville, Montreal, QC Canada H3C 3A7

(This work was published in *Langmuir* on January 07, 2016)

4.1 Abstract

In this work, chitosan-based conventional and Pickering oil-in-water (O/W) emulsions with very fine droplet size (volume average diameter, d_v , as low as $1.7 \mu\text{m}$) and long-term stability (up to 5 months) were ultrasonically generated at different pH values without the addition of any surfactant or crosslinking agent. The ultrasonication treatment was found to break and disperse chitosan agglomerates effectively (particularly at $\text{pH} \geq 4.5$) and also reduce the chitosan molecular weight, benefiting its emulsification properties. The emulsion stability and emulsion type could be controlled by chitosan solution pH. Increasing pH from 3.5 to 5.5 led to the formation of conventional emulsions with decreasing droplet size (d_v from 14 to $2.1 \mu\text{m}$) and increasing emulsion stability (from a few days to 2 months). These results can be explained by the increase of dynamic interfacial pressure, which results from the conformation transition of chitosan molecules from an extended state to a more flexible structure as pH increases. At $\text{pH} = 6.5$ (the acid dissociation constant (pK_a) of chitosan), the chitosan molecules self-assembled into well-dispersed nanoparticles ($d_v = 82.1 \text{ nm}$) with the assistance of ultrasonication, which resulted in a Pickering emulsion with the smallest droplet size ($d_v = 1.7 \mu\text{m}$) and highest long-term stability (up to 5 months) because of the presence of chitosan solid nanoparticles at the oil/water interface. The key originality of this study is the elucidation of the role of pH in the formation of conventional and Pickering chitosan-based O/W emulsions with the assistance of ultrasonication.

Our results suggest that chitosan possesses great potential to be used as an effective pH-controlled emulsifier and stabilizer without the need of other additives.

4.2 Introduction

Chitosan is the only naturally occurring cationic polysaccharide. It is derived from the alkaline deacetylation of chitin, which is the second most abundant biopolymer after cellulose. As a linear polysaccharide, it is composed of randomly distributed deacetylated units (β -(1-4)-linked D-glucosamine) and acetylated units (N-acetyl-D-glucosamine). According to its chemical structure, chitosan is a potential pH-responsive polymer. The protonation of the amino groups makes it soluble and behave as a cationic polyelectrolyte at $\text{pH} < \text{pKa}_{\text{chitosan}}$ (6.5), while it is insoluble at pH over its pKa .¹⁻³ Other molecular characteristics that can affect the physicochemical properties include the degree of deacetylation (DDA), the average molecular weight (M_w) and the distribution of acetyl and amino groups along the polymer backbone.⁴ Owing to its good biodegradability, high biocompatibility, low toxicity, and effective antibacterial activity, chitosan is employed in a wide range of applications in food technology, biomedical, pharmaceutical, etc.⁵⁻⁷

Using chitosan to stabilize or produce emulsions is attracting increasing attention. In most cases, chitosan acts as an emulsion stabilizer through the formation of an interfacial complex with absorbed surface-active agents (e.g., anionic surfactants or proteins), or through viscosity enhancement.⁸⁻¹⁰ The cationic character makes chitosan-stabilized emulsions less prone to destabilization by multivalent cations (e.g., Ca^{2+}),¹¹ and thus lipids in droplets are less susceptible to iron-catalyzed oxidation,¹² resulting in emulsion formulations with a high antimicrobial efficacy.¹³ The positively charged droplets also favor interactions with negative biological membranes, enhancing the capacity for transport and transfer of drugs into cells.¹⁴

Only few papers describe the emulsification properties of chitosan alone without hydrophobic modification or without combining with other surface active agents. Chitosan has many hydrophilic sites (amine groups), but limited hydrophobic sites (acetyl amine groups), and the random distribution of the hydrophobic groups may further reduce their access to the oil/water interface because of steric hindrance.¹⁰ Schulz *et al.* first reported on a water-in-oil-in-water (W/O/W) multiple emulsion system using chitosan in aqueous acetic acid.¹⁵ Then, the effect of

DDA, M_w and chitosan concentration on the emulsifying properties was studied under similar acidic conditions. It was found that increasing chitosan M_w or concentration first increased the emulsifying properties of chitosan and then decreased them, while DDA showed a reverse effect.¹⁶ Later, Payet *et al.* found that increasing pH of chitosan solution to 5 resulted in a dense polyelectrolytic brush on the water side of the oil/water interface, and thus the stability of the corresponding O/W emulsion was increased owing to steric and electrostatic hindrance.¹⁷ Very recently, it was reported that chitosan aggregates formed at high pH value ($> pK_{a \text{ chitosan}}$) could be used as particulate emulsifiers to produce Pickering emulsions.¹⁸⁻²⁰ Pickering emulsions are stabilized by the presence of solid particles instead of surfactants and attract great interest owing to some specific characteristics, including high resistance to coalescence and a surfactant-free character.²¹ The above-mentioned literature suggests the importance of pH on the formation of chitosan-stabilized emulsions, pointing to the necessity of investigating further the role of pH on the emulsification properties of chitosan. In addition, in previous studies, the emulsion droplet sizes were relatively large (typically over tens of microns) and emulsion stability was not satisfying (e.g., creaming happened within one month). Generally, emulsion stability is a kinetic concept (i.e., stability over a period of time), since emulsions are thermodynamically unstable.²² Therefore, to extend the shelf life of commercial products, designing an emulsion with a sufficiently long kinetic stability is of primary importance.²³ According to Stokes law, the creaming rate of emulsions is proportional to the square of the droplet diameter, and thus the emulsion stability can be effectively increased by reducing the droplet size.²⁴

In the current work, a cost-effective method, i.e., high intensity ultrasonication (HIU), is used to produce long-term stability O/W emulsions in the presence of chitosan solely, without using any other surfactant. Compared to previous studies, the droplet size is significantly decreased and therefore, the emulsion stability is greatly improved, which is of high importance for beverage, cosmetic and pharmaceutical applications.²⁵⁻²⁶ The effect of pH and HIU conditions on the physicochemical and emulsification properties of chitosan is investigated thoroughly through zeta potential and interfacial tension measurements, optical microscopy and atomic force microscopy (AFM) observations, as well as rheological testing. This study aims at understanding how chitosan molecular characteristics are affected by pH and HIU, and how these influence its emulsifying properties, thus providing fundamental information for well controlling the stability of chitosan-based emulsions.

4.3 Experimental section

Materials. Commercial chitosan grades (DDA 85%, dynamic viscosity 60 mPa.s; DDA 90 %, dynamic viscosity 60, 200, 1000 mPa.s) were supplied in powder form by BioLog Biotechnologie und Logistik GmbH (Landsberg, Germany). The dynamic viscosity was measured using 1 wt % chitosan dissolved in 1% (v/v) acetic acid at 20 °C. Acetic acid (AcOH, 99.9%, Fisher Scientific, USA) was used to dissolve chitosan. Corn oil was purchased from a local supermarket in Montreal (Canada). All other chemicals used in this work were of analytical grade from Sigma-Aldrich.

Sample Preparation. Chitosan solutions were prepared by dissolving the powder in a 1% (v/v) acetic acid aqueous solution and stirring with a magnetic stirrer at a rate of 300 rpm for 4 h, and then stored overnight to allow complete hydration and dissolution. The pH of chitosan solutions was adjusted from 3.5 to 6.5 by using NaOH or HCl solutions at concentrations of 0.5 to 5 M (the higher concentration was used first to minimize the dilution effect). HIU-treated chitosan solutions were produced using a high intensity ultrasonic processor (UIP1000hd (20 kHz, 1000 W), Hielscher Ultrasonics GmbH, Teltow, Germany) with 90% amplitude for 8 min, using an ice bath to control temperature and avoid overheating. Deionized water was used for all solution preparation and the concentration of chitosan solutions was varied from 0.1 to 2 wt %, depending on the requirement for characterization, and thus to ensure the accuracy of the corresponding measurement. O/W emulsions containing chitosan were prepared by mixing a 1 wt % chitosan solution with corn oil at an oil volume fraction (ϕ) = 0.1 or 0.2, and homogenizing with the high intensity ultrasonic processor at 90% amplitude for 8 min with an ice bath. A control emulsion without chitosan was also prepared for comparison.

Characterization. (a). *Chitosan Solutions.* Zeta (ζ) potential and particle size were measured for three individual samples with a microelectrophoresis and dynamic light scattering instrument (Nano-ZPS, Malvern Instruments, Worcestershire, UK). The turbidity profile was also collected using spectrophotometric measurements in a UV-Vis Varian spectrophotometer (Cary100, Palo Alto, CA, USA), in transmittance mode (% T) at 633 nm. The turbidity index (100 - % T at 633 nm) was plotted against pH. Rheological measurements were carried out using a rotational rheometer (MCR 502, Anton Paar, Graz, Austria) with a coaxial double gap flow geometry (DG26.7) under small amplitude oscillatory shear (SAOS) mode at 25 °C, within the linear

viscoelastic range. Atomic force microscopy (AFM) images were acquired in tapping mode using a Nanoscope MultiMode AFM (Veeco Instrument, Santa Barbara, USA) driven by a Nanoscope III controller. Surface tension (γ) was determined using an optical contact angle measuring system (OCA-20, DataPhysics Instruments GmbH, Germany) and through numerical analysis of the pendant drop shape using the Young-Laplace equation. Surface pressure (π), calculated as $\gamma_s - \gamma_c$, where γ_s and γ_c are the surface tensions of the solvent and the corresponding chitosan solution (at a comparable test time), respectively, was used to interpret the results of surface tension.

(b). *Chitosan Emulsions.* The microstructure of chitosan-based emulsions was observed using a Zeiss Axioskop 40 optical microscope (Carl Zeiss Microscopy GmbH, Jena, Germany). The microscopy images were then used to measure the average emulsion droplet size in terms of volume-average diameter (d_v) and number-average diameter (d_n), using a digitizing table from Wacom and SigmaScan v.5 software. Three images were selected randomly from two parallel experiments and at least 500 droplets were chosen to perform the calculations. The emulsion stability was evaluated by visual observation and calculation of the creaming index, which reveals the information on the extent of droplet aggregation or coalescence in an emulsion.²⁷⁻²⁸ The percentage of creaming index was reported as $(H_s/H_t) \times 100$, where H_s is the height of the serum layer (the sum of the transparent and/or the turbid layers at the bottom of the container) and H_t is the total height of the emulsion.

Unless otherwise specified, all measurements were performed at least in duplicates at room temperature.

4.4 Results and discussion

Molecular Characteristics of Chitosan Affected by pH and HIU. The existing literature related to the emulsification properties of chitosan has shed light on the relationships between chitosan's molecular characteristics and its emulsification properties.^{10, 15-18} However, the evolution of chitosan molecular structure during the emulsifying process is still an issue to be addressed. To further clarify this topic, the physicochemical properties of chitosan solutions that can reflect the molecular characteristics (e.g., molecular weight, conformational structure, charge density, etc.) were examined as a function of pH and HIU. The charge density illustrated by the zeta (ζ) potential is shown in Figure 4.1. Due to the deprotonation of amino groups, there is a

sharp decrease of the ζ potential from 55.9 mV to 29.1 mV when the pH increases from 3.5 to 4.5; further increase of pH to 6.5 results in a moderate decrease of the ζ potential to 16.8 mV. The decrease with pH of the ζ potential gradually induces the self-agglomeration of chitosan molecules, as supported by an increase of turbidity for corresponding chitosan solutions (Supporting Information Figure 4.8). On the other hand, the HIU treatment does not affect the ζ potential in the tested pH range (Figure 4.1), indicating that the number of amino groups in the HIU treated chitosan (CH-HIU) samples is the same as for the original chitosan (CH). It means that the DDA of chitosan is not influenced by HIU treatment, which is in accordance with results from the literature.²⁹

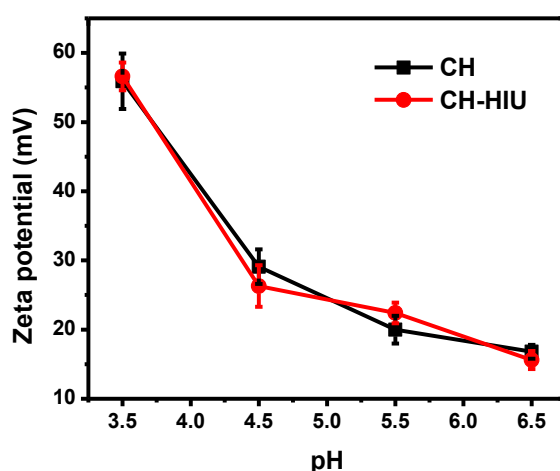


Figure 4.1: Zeta (ζ) potential of chitosan solutions (0.1 wt %) as a function of pH and HIU treatment. CH indicates chitosan without HIU; CH-HIU indicates chitosan with 8 min HIU.

The effect of pH and ultrasonication on the physical properties of chitosan solutions was further confirmed by AFM observations, as shown in Figure 4.2. Without HIU treatment, increasing pH leads to more intra- and inter- attractions in chitosan chains due to lower electrostatic force, thus a more compact chain structure and an increase of agglomerates, and large insoluble ones are even visually observed when the pH is close to the pK_a of chitosan (pH 6.5). Interestingly, after HIU treatment, the agglomerates formed at higher pH values (5.5-6.5) disappear. The insoluble agglomerates at pH 6.5 are broken by HIU and assemble into compacted CH nanoparticles, indicated from visual comparison of inserted vials as well as AFM observations (Figure 4.2a, right top and bottom). The effect of HIU on agglomerate size of

chitosan solutions at lower pH (e.g., pH 3.5) is much less than that of higher pH since CH is more protonated at lower pH and the strong electrostatic repulsion makes the agglomeration of CH negligible, and it is more evident when comparing the turbidity curves of samples CH-HIU and CH (Supporting Information Figure 4.8). Similar information can also be gathered from DLS analysis, as shown in Figure 4.2b. The agglomeration of chitosan chains induced by increasing pH is quantitatively assessed by considering the right-shift of the distribution of volume fraction and the increase of volume average diameter (d_v) from 4.0 to 850.3 nm. In terms of HIU effect, except for pH 3.5, a left-shift on the size distribution curve can be observed for higher pH values (pH 4.5 to 6.5), and especially at pH 6.5, where the peaks representing large CH agglomerates have all disappeared. As a consequence, d_v decreases more at higher pH, e.g., d_v goes from 4.0 to 3.57 nm for pH 3.5, but from 850 to 82.1 nm for pH 6.5. The above results indicate that pH effectively affects the size of chitosan agglomerates, and HIU is an effective approach to disperse CH, especially at higher pH (5.5-6.5).

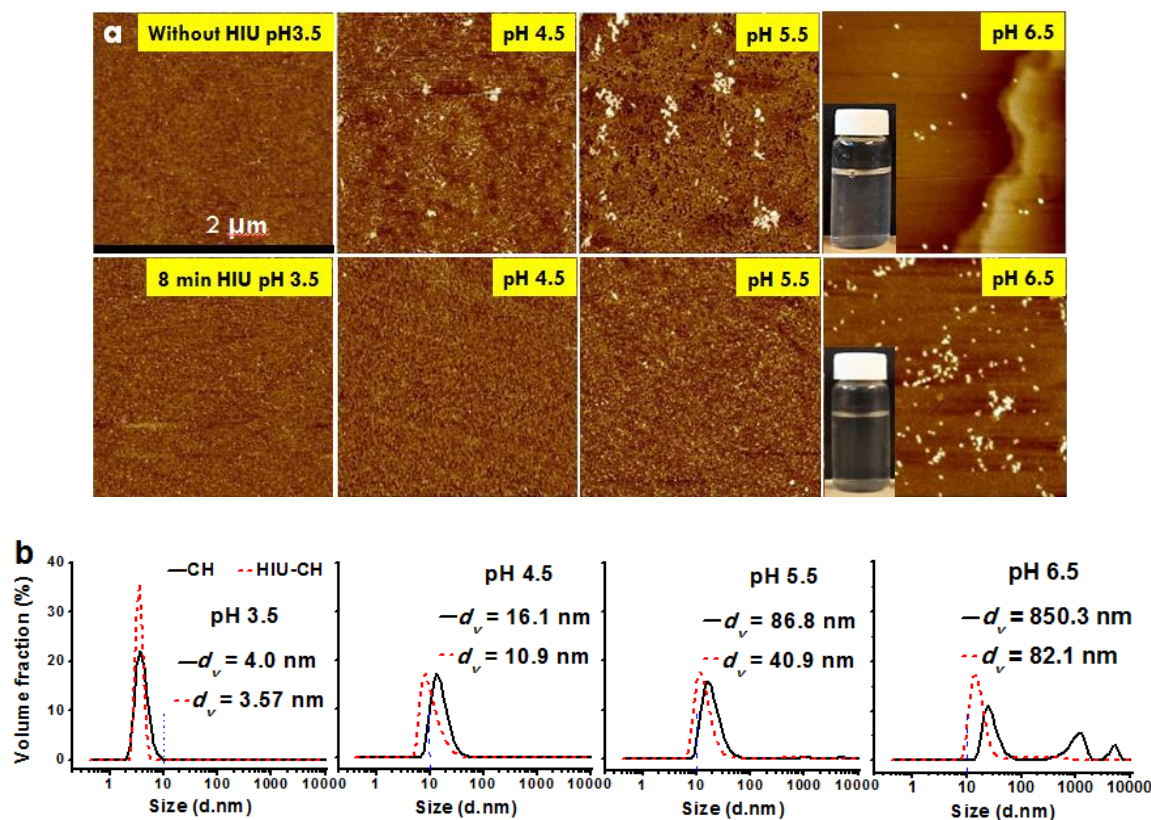


Figure 4.2: (a) AFM images of chitosan solutions with and without HIU at various pH; the inserts are photographs of chitosan solutions at pH 6.5 without HIU (right top) and with 8 min HIU

(right bottom). (b) Volume fraction of chitosan molecular agglomerates size (chitosan concentration, 0.1 wt %) before and after 8 min HIU as a function of pH.

Rheological properties can give information on molecular weight and conformational structure of polymer chains. The complex viscosity (η^*) of chitosan solutions (2 wt %, pH 3.9) with and without HIU treatment is shown in Figure 4.3a. There is a notable decrease of η^* : 4 min HIU leading to a 52.4% drop on η^* , and another 4 min HIU resulting in a decrease of η^* by another 42.6%. Considering that the agglomerate size is not affected significantly by the HIU treatment in the lower pH range ($< \text{pH } 4.5$) (Figure 4.2b), the decrease of η^* at the testing pH is mainly due to the HIU-induced decrease of molecular weight. The decrease rate of molecular weight can be quantitatively assessed using the adapted form of the power law predicted by the theory of reptation ($\eta_0 \propto M_w^3$), where the zero shear viscosity (η_0) is taken as proportional to the power of 3 of the weight average molecular weight (M_w).³⁰⁻³¹ The calculations show that the first 4 min HIU result in a decrease of M_w of about 24%, and the additional 4 min HIU cause a further drop of M_w around 15.8%. Longer HIU treatment (8 to 20 min) also decreases η^* , but much less than the first 8 min, and overall, the η^* is exponentially decreasing with increasing sonication time (Supporting Information Figure 4.9). Similar trend is obtained in terms of M_w following the power law ($\eta_0 \propto M_w^3$), which is in accordance with results from the literature.^{29, 32}

The conformation of chitosan chains in the solid state is coil-like, owing to intramolecular hydrogen bonding. After dissolution in acidic medium, hydrogen bonds formed between water molecules and chitosan monomeric units may replace parts of intramolecular hydrogen bonds, and meanwhile, the protonation of amino groups allows chitosan chains to open up as elongated chains because of electrostatic repulsion.³³ As a key factor that affects the protonation of polyelectrolytes, the pH value therefore influences the chain conformation of chitosan. For example, increasing the pH of a chitosan solution from 3 to 5 results in a decrease of the persistence length of CH chains for several tested DDAs (from 80 to 100%), which indicates a more flexible and compact chain structure.³⁴ The overall tendency agrees with the results of the current work, where rheological properties are examined in the scope of conformation change. As shown in Figure 4.3b, increasing pH from 3.5 to 5.5 (no HIU treatment) leads to a decrease of the complex viscosity and more shear-thinning at high frequency. In general, it is easier for disentangled extended chains to form new entanglements, and thus present less shear-thinning.³⁵

So the rheological results imply a more compact chain conformation at higher pH (pH 5.5), while a more expanded structure at lower pH (pH 3.5).

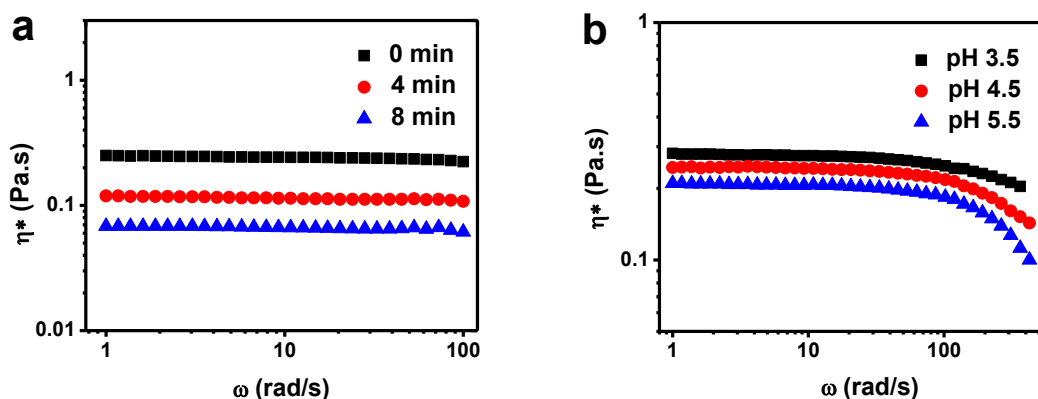


Figure 4.3: (a) Effect of HIU treatment on the complex viscosity of 2 wt % chitosan (pH 3.9). (b) Effect of pH on the complex viscosity of 2 wt % chitosan (without HIU treatment).

Surface Activity of Chitosan: Absorption Kinetics at the Oil-water Interface. Generally, biopolymer emulsifiers can absorb at an oil/water interface and decrease the interfacial tension due to their amphiphilic properties. The production of a fine emulsion requires a rapid absorption of emulsifier molecules on the surface of oil droplets to avoid coalescence. To better elucidate the effect of pH and ultrasonication on the emulsifying properties of chitosan, the absorption kinetics of chitosan was investigated by monitoring the interfacial tension as a function of time. Figure 4.4a shows the time evolution of surface pressure (π) for absorbed chitosan molecules at the oil/water interface, at varying pH values of 3.5-5.5. For chitosan at pH 6.5 without ultrasonication, the data was not reproducible, probably due to the presence of large agglomerates (Figure 4.2a, right top). As a consequence of the absorption of chitosan molecules at the oil/water interface, all the curves in Figure 4.4a show an increase in the π value, especially in the first 200 s. In the initial diffusion-controlled absorption process, a plot of π against $t^{1/2}$ is linear and the slope represents the diffusion rate constant (k_{diff}).³⁶ The increase of pH from 3.5 to 5.5 results in an increase of k_{diff} from 0.08 to 0.25 mN m⁻¹ s^{-0.5} (Table 4.1), suggesting a higher diffusion rate and a faster initial absorption at higher pH values. It is also noted that the π value for pH 5.5 at the beginning of the absorption is above 0, which implies that the very initial absorption rate at this pH is too fast to be detected. The increased chain flexibility is a reasonable interpretation for this rate increase, since it would benefit the accessibility of hydrophobic sites (acetyl groups) to

the oil/water interface and then decrease of the interfacial tension.³⁷ The significant effect of HIU treatment can be seen by comparing the results of Figure 4.4a and 4b. The π value increases for all the tested pH (pH 3.5-5.5) at comparable times, and the k_{diff} value also increases (Table 4.1), indicating a much higher surface activity and a faster absorption at the oil/water interface after HIU treatment, as compared to the related samples at the same pH without HIU treatment. The effect of pH and HIU are also summarized by comparing the π value at the end of the adsorption period (900 s; π_{900}), as shown in Table 4.1. For both CH and CH-HIU, π_{900} is significantly increased as pH increases, and the variation for different pH values is larger than that in initial adsorption (π_0), indicating a lower absorption barrier for chitosan at higher pH values. HIU treatment leads to an increase of π_{900} for all pHs, and it reaches a maximum value (10 mN/m) for CH-HIU at pH 6.5.

In the literature, the surface tension of low molecular weight chitosan is reported to be lower than that of high molecular weight chitosan, due to lower steric hindrance, as well as less entanglements and inter-molecular hydrogen bonding.¹⁵ Therefore, the main reason for the increase of the π value in HIU treated chitosan is expected to be the reduced molecular weight and the disassembly of chitosan agglomerates, triggered by ultrasonication. For HIU-treated chitosan, the effect of increasing pH is similar to that for untreated chitosan, i.e., the higher pH, the larger π and k_{diff} values. At pH 6.5, considering that HIU treatment turns visible agglomerates (Figure 4.2a, right top) into nanoparticles (Figure 4.2b, right bottom), the absorption kinetics is more complicated. Generally, the absorption energy barrier for a sphere particle is determined as:

$$\Delta E = \pi r^2 \gamma_{\text{ow}} (1 \pm \cos \theta)^2 \quad (3)$$

Where r , γ_{ow} and θ represent the particle radius, and the oil/water interfacial tension and contact angle, respectively³⁸. Even though the CH nanoparticles are not exactly spherical, this equation can still be used to estimate the energy barrier. Considering the large π value (i.e., small γ_{ow} value), an intermediate wettability (namely, θ between 50° and 130°) of chitosan nanoparticles is expected, which should result in good emulsifying capacity and emulsion stability.

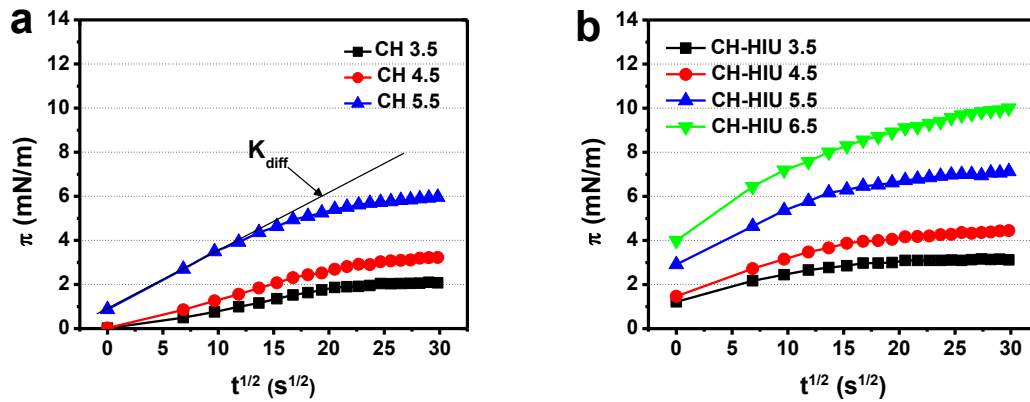


Figure 4.4: Time evolution of surface pressure for the absorption of chitosan molecules at an oil/water interface for different pH values: (a) without HIU treatment; (b) with 8 min HIU. The concentration of chitosan solution is 1 wt %.

Table 4.1: Diffusion rate constants (k_{diff}) and surface pressure at the end of adsorption (900 s; π_{900}) for chitosan molecules at an oil/water interface.

pH	k_{diff} ($\text{mN m}^{-1} \text{s}^{-0.5}$) (LR)		π_{900} (mN m^{-1})	
	Before HIU	After HIU	Before HIU	After HIU
3.5	0.08 (0.970)	0.12 (0.971)	2.07	3.11
4.5	0.13 (0.989)	0.17 (0.978)	3.22	4.44
5.5	0.25 (0.988)	0.27 (0.981)	5.95	7.12
6.5	ND	0.31 (0.966)	ND	10.01

LR = linear regression coefficient (in parenthesis), ND = not determined.

Emulsifying Capacity and Emulsion Stability. Optical microscopy images of chitosan O/W emulsions after 1 h of preparation are shown in Figure 4.5a, and the evolution of average droplet size is summarized in Figure 4.5b. It can be observed that the emulsifying capacity of chitosan greatly depends on pH: the average emulsion droplet size decreases significantly as pH increases from 3.5 to 6.5. At pH 3.5, a multiple emulsion (W/O/W) with large droplet size ($d_v = 14 \mu\text{m}$) and wider distribution (d_v/d_n up to 2.36) can be observed. Considering the fact that the W/O/W emulsion droplets gradually disappear as pH increases, it is believed that the formation of the double emulsion at pH 3.5 is mainly due to the more rigid chain conformation at lower pH.

The chitosan used in this work has a DDA of 85%, which means that the proportion of acetyl amine groups (hydrophobic sites) is only 15%, and in acidic conditions, the stiffer conformation of chitosan molecules makes it even harder for the limited hydrophobic sites to locate themselves in the oil phase and form O/W droplets. Therefore, smaller W/O droplets may be preferably formed first and then larger W/O/W droplets generated subsequently. Further increase of pH to 4.5 and 5.5 significantly decreases d_v to 5.25 μm and 2.1 μm , as well as d_v/d_n to 2.21 and 1.28, respectively. It indicates a smaller droplet size and narrower distribution. As discussed in the section on Figure 4.4a, the increase of chain flexibility might be the main reason for this evolution. For pH values between 3.5 and 5.5, the chitosan-stabilized emulsions are considered as conventional owing to the fact that they are stabilized by linear chitosan chains.

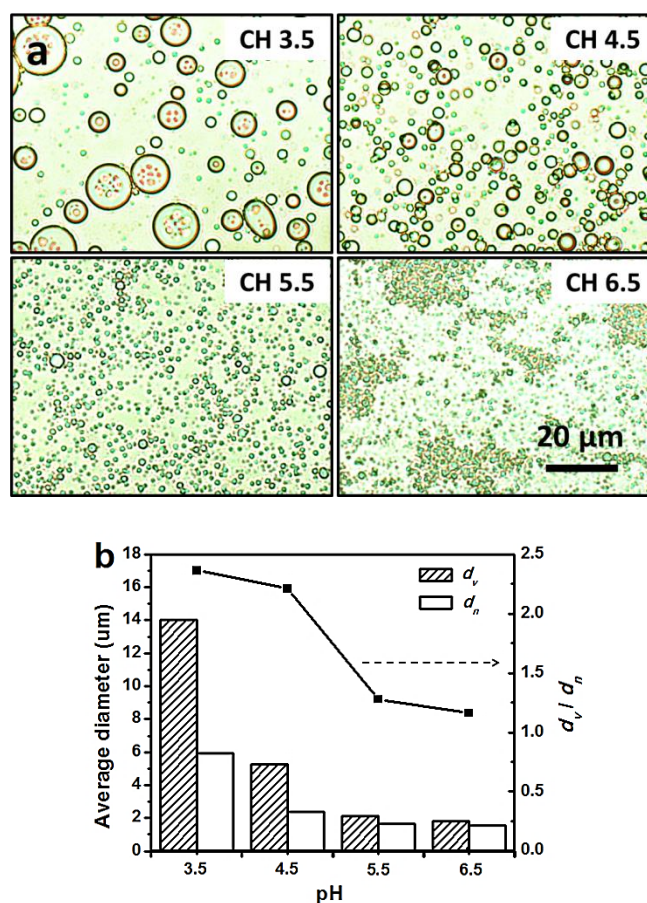


Figure 4.5: (a) Optical micrographs of chitosan-based emulsions prepared at different pH values (3.5-6.5), after 1 h of preparation. (b) Volume- and number- average diameter as well as size distribution of fresh chitosan-based emulsions droplets. The emulsions were prepared with 1 wt % chitosan and an oil volume fraction of 0.1, using HIU homogenization for 8 min.

Notably at pH 6.5, very fine emulsion droplets ($d_v = 1.7 \mu\text{m}$) and narrow distribution (dv / dn as low as 1.16) are generated, although droplet flocculation is also observed. The occurrence of flocculation is probably attributed to the lower ζ potential value (16.8 mV) at this pH, at which the emulsion droplets have more chance to interact with each other due to lower electrostatic repulsion. However, despite the very short distance between droplets, they seem not to coalesce (as shown later in the stability evaluation) because of the formation of a Pickering emulsion via irreversible absorption of chitosan nanoparticles at the oil/water interface.³⁸⁻³⁹ Last, it should be noted that the decrease of molecular weight and the disruption of chitosan agglomerates caused by HIU also contributes to the formation of the emulsions, since all of them were prepared using the HIU technique.

The long-term stability of chitosan-based emulsions was determined by the observation of creaming and calculation of creaming index (CI). Digital photographs of the O/W emulsions prepared with 1 wt % chitosan at different pH values and stored up to 5 months are shown in Figure 4.6a, and the corresponding calculated CI are shown as function of time in Figure 4.6b. In addition, the photograph of a control emulsion prepared with 1 % (v/v) AcOH (without chitosan) is shown in Figure 4.6c. The presence of chitosan greatly increases the emulsion stability, while the emulsion without chitosan is extremely unstable and the aqueous and oil phase separate the day following preparation. Specifically, at lower pH values, e.g., pH 3.5 and 4.5, the CI increases abruptly to a plateau value of 75% and 67%, respectively, within 40 days; at pH 5.5, the CI doesn't change during 40 days and increases progressively to 60% after 3 months, while for pH 6.5, the CI is virtually 0 for up to 80 days and only increases to 11% over 5 months of storage, demonstrating an impressive long-term stability. Hence our results show that the most stable chitosan-based emulsion is the one prepared at pH 6.5, which is a Pickering emulsion stabilized by particulate chitosan (Figure 4.2a, right bottom). In contrast to conventional surfactant-based emulsions, Pickering emulsions generally exhibit higher resistance to coalescence because of the effectively irreversible adsorption of solid particles.³⁹ Hence, in the case of pH 6.5, even though the flocculation of droplets can be observed in the freshly prepared emulsion (Figure 4.5a, pH 6.5), the stabilization by chitosan nanoparticles makes it stable against coalescence and subsequent creaming over time. From pH 3.5 to 5.5, the long-term stability increases with pH. As discussed in previous sections, the molecules conformation changes from an extended structure (more rigid) to a compact structure (more flexible) as pH increases. At pH 5.5, the hydrophobic

sites can penetrate into the oil phase more easily, whereas the hydrophilic parts located in the water phase can provide steric stabilization, which gives the corresponding emulsion a considerable long-term stability. In addition, the detailed study on the morphological evolution of the emulsions is also underway and the results will be reported in future work.

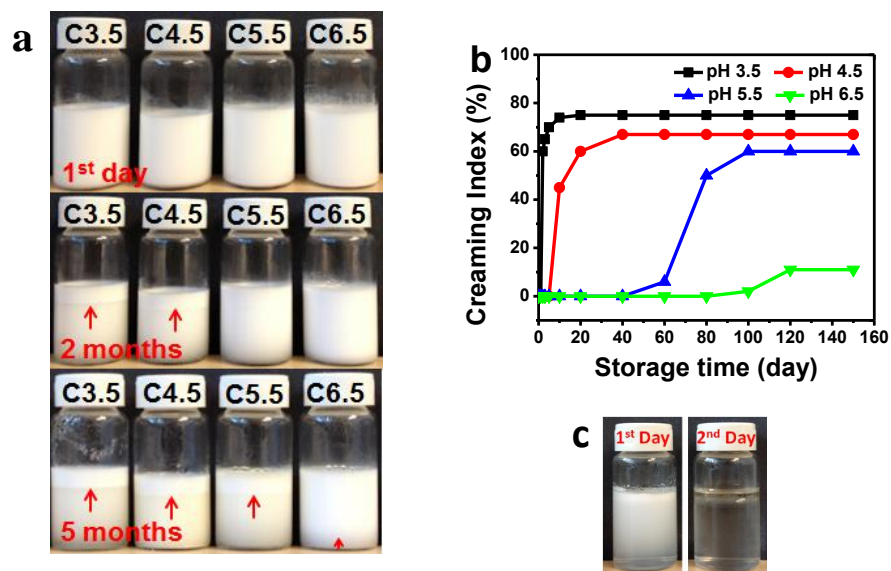


Figure 4.6: (a) Photographs and (b) creaming index of emulsions prepared with chitosan solution (1 wt %) at different pH values (3.5 to 6.5) and storage time (up to 5 months), with an oil volume fraction of 0.1. (c) Digital photographs of emulsion prepared with 1% (v/v) AcOH, with an oil volume fraction of 0.1.

It is worth noting that the production of chitosan-based emulsions is usually attributed to viscosity enhancement.⁴⁰⁻⁴¹ However, in our case, even though the viscosity decreases when pH increases to 5.5 (Figure 4.4b), the stability of emulsions nevertheless increases. To further figure out the effect of viscosity on the emulsifying properties, chitosan samples with different molecular weight but same DDA (90%) were used to prepare conventional emulsions at pH 4, and it showed that the chitosan with the lowest viscosity produced emulsions with the smallest droplet size, and accordingly, the longest stability (Supporting Information Figure 4.10). It implies that chitosan with lower molecular weight can benefit the formation of emulsions, and the viscosity enhancement of chitosan has a limiting effect on emulsion stabilization, compared to other factors, e.g., molecular weight and chain conformation.

As summarized in Figure 4.7 presented below, during the emulsion preparation the effect of increasing pH causes a chain conformation transition from extended to compact, while the role of HIU results in a disassembly of agglomerates and a decrease of molecular weight. The combined effects of pH and ultrasonication in this work are found beneficial to the improvement of emulsifying properties of chitosan. The long-term stability of the Pickering emulsion formed at pH 6.5 is remarkable due to the stabilization caused by chitosan nanoparticles, and that for the conventional emulsion formed at pH 5.5 is also considerable due to steric and electrostatic hindrance.

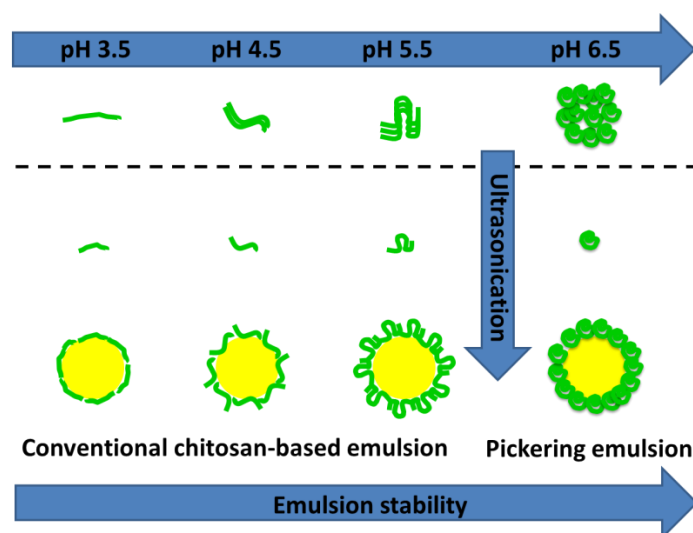


Figure 4.7: The formation of chitosan-based emulsions: the role of pH and ultrasonication.

4.5 Conclusion

In this work, the effect of pH and ultrasonication on the molecular characteristics of chitosan, including charge density, molecular weight and conformational structure was examined. In addition, their effect on the emulsification and stabilization properties of chitosan-based O/W emulsions was investigated. Our results showed that: chitosan can form two types of emulsions, namely, conventional emulsions and Pickering emulsions, with considerable long-term stability. The emulsifying properties of chitosan greatly depend on pH, which affects the charge density and chain conformation. High intensity ultrasonication is a powerful technique that has dual effects, homogenization and depolymerization, and favors the formation of chitosan-based emulsions. Our findings suggest that chitosan by itself has a great potential to be used as a pH-controlled emulsifier and stabilizer for the production of biodegradable, surfactant-free and even

edible O/W emulsions in food and non-food applications. This fundamental study based on chitosan also opens new perspectives for the use of other pH-controlled natural polymers in emulsion systems.

Acknowledgements

This research work has been funded by NSERC (Natural Sciences and Engineering Research Council of Canada). A scholarship for Ms. Wang provided by the China Scholarship Council (CSC) is also gratefully acknowledged. The authors also acknowledge Prof. Nick Virgilio (Polytechnique Montréal) for access to the optical contact angle measuring system, and Mr. Changsheng Wang (Polytechnique Montréal) for his help in AFM observation.

References

- (1) Kumar, M. A review of chitin and chitosan applications. *React. Funct. Polym.* **2000**, *46* (1), 1-27.
- (2) Rinaudo, M. Chitin and chitosan: Properties and applications. *Prog. Polym. Sci.* **2006**, *31* (7), 603-632.
- (3) Cho, J. Y.; Heuzey, M. C.; Begin, A.; Carreau, P. J. Physical gelation of chitosan in the presence of beta-glycerophosphate: The effect of temperature. *Biomacromolecules* **2005**, *6* (6), 3267-3275.
- (4) Kumar, M.; Muzzarelli, R. A. A.; Muzzarelli, C.; Sashiwa, H.; Domb, A. J. Chitosan chemistry and pharmaceutical perspectives. *Chem. Rev.* **2004**, *104* (12), 6017-6084.
- (5) Rabea, E. I.; Badawy, M. E. T.; Stevens, C. V.; Smagghe, G.; Steurbaut, W. Chitosan as antimicrobial agent: Applications and mode of action. *Biomacromolecules* **2003**, *4* (6), 1457-1465.
- (6) Riva, R.; Ragelle, H.; des Rieux, A.; Duhem, N.; Jerome, C.; Preat, V. Chitosan and Chitosan Derivatives in Drug Delivery and Tissue Engineering. *Chitosan for Biomaterials II* **2011**, *244*, 19-44.
- (7) Chen, R.-H.; Domard, A.; Muzzarelli, R. A. A.; Tokura, S.; Wang, D.-M. Advances in chitin/chitosan science and their applications. *Carbohydr. Polym.* **2011**, *84* (2), 695-695.

- (8) Laplante, S.; Turgeon, S. L.; Paquin, P. Emulsion stabilizing properties of various chitosans in the presence of whey protein isolate. *Carbohydr. Polym.* **2005**, *59* (4), 425-434.
- (9) Mun, S.; Decker, E. A.; McClements, D. J. Influence of droplet characteristics on the formation of oil-in-water emulsions stabilized by surfactant-chitosan layers. *Langmuir* **2005**, *21* (14), 6228-6234.
- (10) Klinkesorn, U. The Role of Chitosan in Emulsion Formation and Stabilization. *Food Rev. Int.* **2013**, *29* (4), 371-393.
- (11) Ogawa, S.; Decker, E. A.; McClements, D. J. Influence of environmental conditions on the stability of oil in water emulsions containing droplets stabilized by lecithin-chitosan membranes. *J. Agric. Food. Chem.* **2003**, *51* (18), 5522-5527.
- (12) Lomova, M. V.; Sukhorukov, G. B.; Antipina, M. N. Antioxidant Coating of Micronsize Droplets for Prevention of Lipid Peroxidation in Oil-in-Water Emulsion. *ACS Appl. Mat. Interfaces* **2010**, *2* (12), 3669-3676.
- (13) Jumaa, M.; Furkert, F. H.; Muller, B. W. A new lipid emulsion formulation with high antimicrobial efficacy using chitosan. *European Journal of Pharmaceutics and Biopharmaceutics* **2002**, *53* (1), 115-123.
- (14) Calvo, P.; RemunanLopez, C.; VilaJato, J. L.; Alonso, M. J. Development of positively charged colloidal drug carriers: Chitosan coated polyester nanocapsules and submicron-emulsions. *Colloid. Polym. Sci.* **1997**, *275* (1), 46-53.
- (15) Schulz, P. C.; Rodriguez, M. S.; Del Blanco, L. F.; Pistonesi, M.; Agullo, E. Emulsification properties of chitosan. *Colloid. Polym. Sci.* **1998**, *276* (12), 1159-1165.
- (16) Del Blanco, L. F.; Rodriguez, M. S.; Schulz, P. C.; Agullo, E. Influence of the deacetylation degree on chitosan emulsification properties. *Colloid. Polym. Sci.* **1999**, *277* (11), 1087-1092.
- (17) Payet, L.; Terentjev, E. M. Emulsification and stabilization mechanisms of o/w emulsions in the presence of chitosan. *Langmuir : the ACS journal of surfaces and colloids* **2008**, *24* (21), 12247-52.

- (18) Liu, H.; Wang, C.; Zou, S.; Wei, Z.; Tong, Z. Simple, Reversible Emulsion System Switched by pH on the Basis of Chitosan without Any Hydrophobic Modification. *Langmuir* **2012**, *28* (30), 11017-11024.
- (19) Liu, H.; Wei, Z.; Hu, M.; Deng, Y.; Tong, Z.; Wang, C. Fabrication of degradable polymer microspheres via pH-responsive chitosan-based Pickering emulsion photopolymerization. *Rsc Advances* **2014**, *4* (55), 29344-29351.
- (20) Wei, Z.; Wang, C.; Zou, S.; Liu, H.; Tong, Z. Chitosan nanoparticles as particular emulsifier for preparation of novel pH-responsive Pickering emulsions and PLGA microcapsules. *Polymer* **2012**, *53* (6), 1229-1235.
- (21) Chevalier, Y.; Bolzinger, M.-A. Emulsions stabilized with solid nanoparticles: Pickering emulsions. *Colloids and Surfaces a-Physicochemical and Engineering Aspects* **2013**, *439*, 23-34.
- (22) Huck-Iriart, C.; Alvarez-Cerimedo, M. S.; Candal, R. J.; Herrera, M. L. Structures and stability of lipid emulsions formulated with sodium caseinate. *Curr. Opin. Colloid Interface Sci.* **2011**, *16* (5), 412-420.
- (23) McClements, D. J. Edible nanoemulsions: fabrication, properties, and functional performance. *Soft Matter* **2011**, *7* (6), 2297-2316.
- (24) Robins, M. M. Emulsions - creaming phenomena. *Curr. Opin. Colloid Interface Sci.* **2000**, *5* (5-6), 265-272.
- (25) Piorkowski, D. T.; McClements, D. J. Beverage emulsions: Recent developments in formulation, production, and applications. *Food Hydrocolloids* **2014**, *42*, 5-41.
- (26) Gutierrez, J. M.; Gonzalez, C.; Maestro, A.; Sole, I.; Pey, C. M.; Nolla, J. Nano-emulsions: New applications and optimization of their preparation. *Curr. Opin. Colloid Interface Sci.* **2008**, *13* (4), 245-251.
- (27) Kelley, D.; McClements, D. J. Influence of sodium dodecyl sulfate on the thermal stability of bovine serum albumin stabilized oil-in-water emulsions. *Food Hydrocolloids* **2003**, *17* (1), 87-93.

- (28) Keowmaneechai, E.; McClements, D. J. Influence of EDTA and citrate on physicochemical properties of whey protein-stabilized oil-in-water emulsions containing CaCl_2 . *J. Agric. Food. Chem.* **2002**, *50* (24), 7145-7153.
- (29) Baxter, S.; Zivanovic, S.; Weiss, J. Molecular weight and degree of acetylation of high-intensity ultrasonicated chitosan. *Food Hydrocolloids* **2005**, *19* (5), 821-830.
- (30) Doi, M. E., S. F. Dynamic of concentrated polymer systems. Part 2. -Molecular motion under flow. *J. Chem. Soc., Faraday Trans. 2* **1978**, *74*, 1802-1818.
- (31) Yamaguchi, M.; Wakutsu, M.; Takahashi, Y.; Noda, I. Viscoelastic properties of polyelectrolyte solutions. 1. Zero-shear viscosity. *Macromolecules* **1992**, *25* (1), 470-474.
- (32) Wu, T.; Zivanovic, S.; Hayes, D. G.; Weiss, J. Efficient reduction of chitosan molecular weight by high-intensity ultrasound: Underlying mechanism and effect of process parameters. *J. Agric. Food. Chem.* **2008**, *56* (13), 5112-5119.
- (33) Colombo, E.; Cavalieri, F.; Ashokkumar, M. Role of Counterions in Controlling the Properties of Ultrasonically Generated Chitosan-Stabilized Oil-in-Water Emulsions. *ACS Appl. Mat. Interfaces* **2015**, *7* (23), 12972-12980.
- (34) Chen, R. H.; Lin, J. H.; Tsaih, T. Effect of urea on the conformation and chain flexibility of chitosan molecules with various degree of deacetylation. *J. Mar. Sci. Technol.* **1994**, *2* (1), 1-7.
- (35) Marrucci, G.; Bhargava, S.; Cooper, S. L. Models of shear-thickening behavior in physically cross-linked networks. *Macromolecules* **1993**, *26* (24), 6483-6488.
- (36) Xu, S. Q.; Damodaran, S. Kinetics of absorption of proteins at the air-water interface from a binary mixture. *Langmuir* **1994**, *10* (2), 472-480.
- (37) Nilsen-Nygaard, J.; Strand, S. P.; Varum, K. M.; Draget, K. I.; Nordgard, C. T. Chitosan: Gels and Interfacial Properties. *Polymers* **2015**, *7* (3), 552-579.
- (38) Binks, B. P.; Lumsdon, S. O. Influence of particle wettability on the type and stability of surfactant-free emulsions. *Langmuir* **2000**, *16* (23), 8622-8631.
- (39) Melle, S.; Lask, M.; Fuller, G. G. Pickering emulsions with controllable stability. *Langmuir* **2005**, *21* (6), 2158-2162.

(40) Speiciene, V.; Guilmineau, F.; Kulozik, U.; Leskauskaitė, D. The effect of chitosan on the properties of emulsions stabilized by whey proteins. *Food Chem.* **2007**, *102* (4), 1048-1054.

(41) Calero, N.; Munoz, J.; Cox, P. W.; Heuer, A.; Guerrero, A. Influence of chitosan concentration on the stability, microstructure and rheological properties of O/W emulsions formulated with high-oleic sunflower oil and potato protein. *Food Hydrocolloids* **2013**, *30* (1), 152-162.

4.6 Supporting information

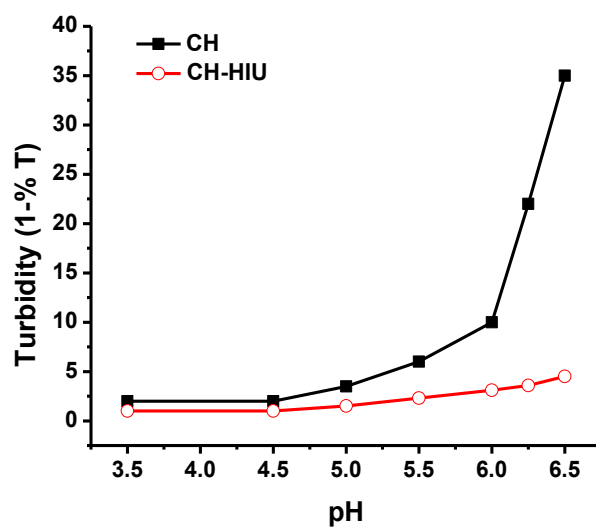


Figure 4.8: Turbidity profile of chitosan solutions (1 wt %) with and without HIU treatment and as a function of pH.

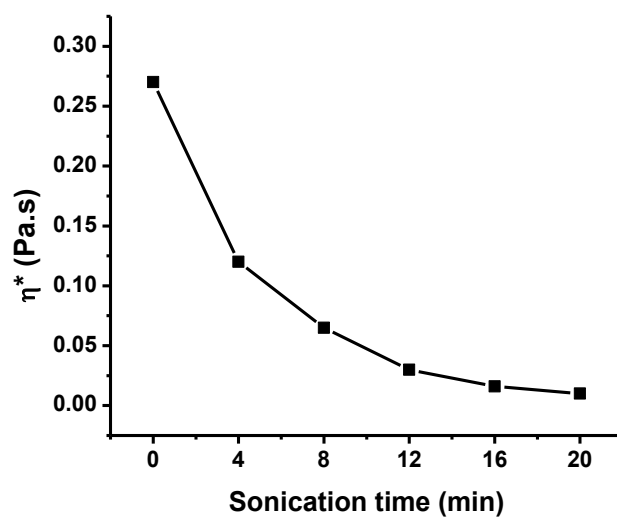


Figure 4.9: The effect of sonication time on the complex viscosity (1 rad/s) of a chitosan solution (DDA, 85%; dynamic viscosity, 60 mPa.s; concentration, 2 wt %, pH 3.9).

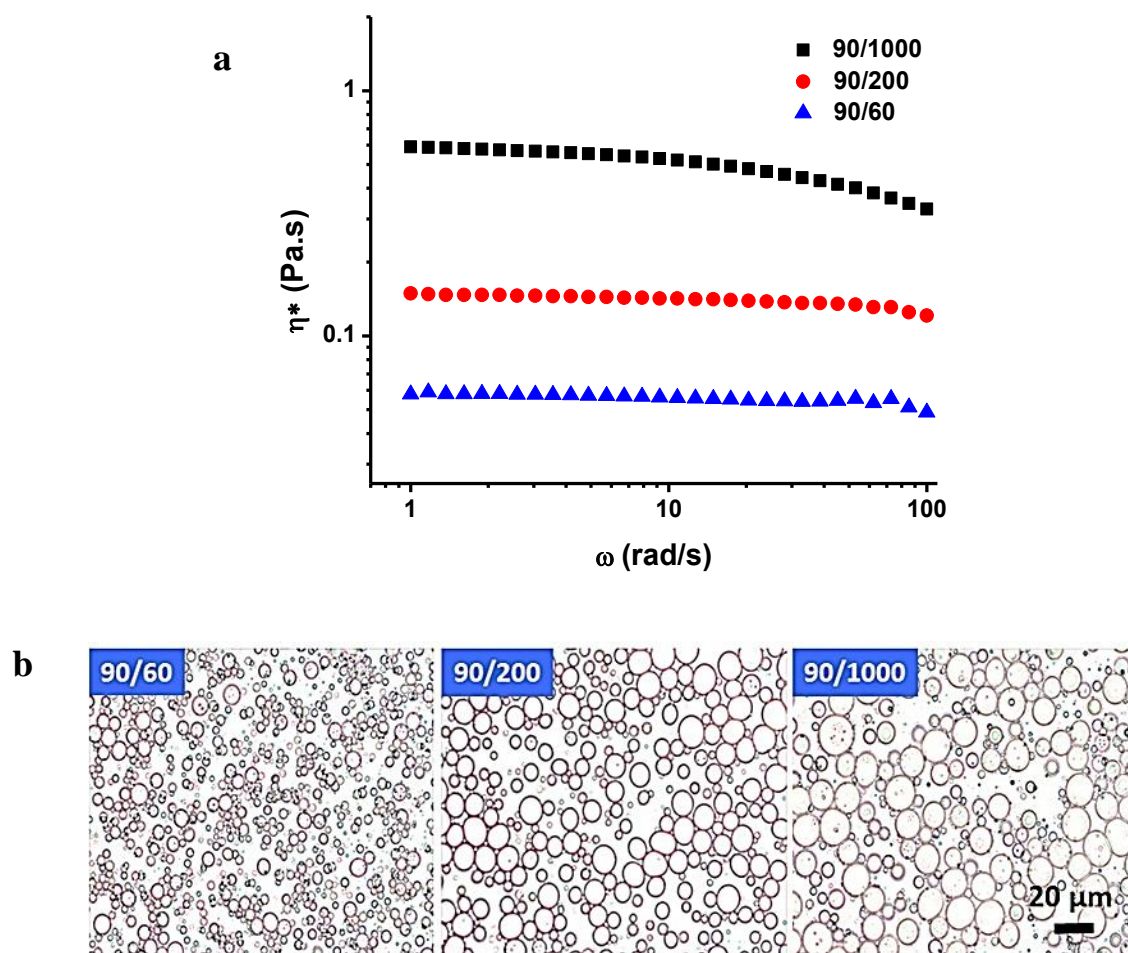


Figure 4.10: (a) Complex viscosity of chitosan solutions (1 wt %) at pH 4 for samples with same DDA (90%) but different molecular weights (dynamic viscosity varies from 60 to 1000 mPa.s).
 (b) Optical microscopy images of chitosan-based emulsions after 1 h of preparation, at an oil volume fraction of 0.2.

CHAPTER 5 ARTICLE 2: COMPLEXATION OF CHITOSAN AND GELATIN: FROM SOLUBLE COMPLEXES TO COLLOIDAL GEL

Xiao-Yan Wang, Chang-Sheng Wang & Marie-Claude Heuzey

Department of Chemical Engineering, CREPEC, Polytechnique Montreal, PO Box 6079, Station Centre-Ville, Montreal, QC Canada H3C 3A7

(This work was published in *International Journal of Polymeric Materials and Polymeric Biomaterials* on September 18, 2015)

5.1 Abstract

In this study, the formation of soluble and insoluble complexes between chitosan (CH) and gelatin type B (GB) was investigated as a function of pH (3.0-6.5), sodium chloride (NaCl) concentration (0-100 mM) and storage time (up to 40 days). The turbidity of the CH/GB complexes achieved a maximum value at pH 5.5 and increased with time. The increase of ionic strength first intensified the complex formation but then decreased it at higher salt content. After phase separation, the main component of the separated dense phase was water, from 95.5 to 97.8 wt %, depending on NaCl concentration. With increasing storage time, the insoluble phase changed from a liquid-like system to a thermoreversible colloidal gel, as supported by confocal laser scanning microscopy as well as rheological data. The formation of this colloidal gel is explained in terms of electrostatic complexation and hydrogen bonding.

5.2 Introduction

Protein/polysaccharide complex systems, mainly generated by electrostatic interactions between oppositely charged macromolecules, have received increasing interest in recent years [1-4]. Depending on the protein/polysaccharide molecular characteristics and processing parameters, electrically driven complex systems with various compositions and structures can be formed, including soluble and insoluble complexes, coacervates and gels. These systems can be used to

microencapsulate sensitive materials, to purify macromolecules or as delivery matrices, thus exhibiting a wide range of applications in biomaterials, cosmetics, pharmaceutical and medicine [5-10]. Protein/polysaccharide complex particles can be considered as colloidal entities. In order to reduce the system's free energy to reach thermodynamic equilibrium, soluble complexes tend to aggregate until the surface properties or size give rise to a phase separation, in which a concentrated colloidal phase coexists with a very dilute phase [11, 12]. The complexation process is mainly governed by pH, ionic strength, polymer ratio, polymer concentration and charge density. There is abundant scientific literature focusing on the interaction between anionic polysaccharides and proteins due to the wide pH window for complex formation [1, 13]. Recently, the electrostatic complexation between cationic polysaccharides and other polyelectrolytes has been attracting more attention due to the specific properties of cationic polymer-based materials. For example they exhibit a higher capacity to interact with negative biological membranes, thus enhancing the transport and transfer of drugs [14-16].

As the only naturally-derived cationic polysaccharide ($pK_a = 6.5$), chitosan, one of the most abundant polysaccharide on earth, has been employed in a wide range of applications owing to its good biodegradability, high biocompatibility, low toxicity, and outstanding antibacterial activity [17, 18]. In acidic aqueous solution, the amino groups on the chitosan chains are protonated, which enable it to interact with negatively charged proteins. However, due to the narrow pH range to form electrostatic interactions ($pI_{\text{protein}} < pH < pK_a_{\text{chitosan}}$), there are only a few studies investigating the electrostatic complexation between chitosan and proteins [16, 19, 20]. Gelatin, a linear polypeptide obtained from denatured collagen, is also a natural, non-toxic and biodegradable polymer with interesting properties [21]. As a polyampholyte, gelatin can interact with anionic polysaccharide below its isoelectric point (pI), and with cationic polysaccharide above its pI. Depending on the processing conditions, two types of gelatin can be produced, namely, acid-processed gelatin type A with a pI of 7 to 9, and alkaline-pretreated gelatin type B with a pI of 4.8 to 5.2. Both types of gelatin were investigated by other authors in the complexation with anionic polysaccharides, including mainly acacia gum, pectin and alginate [22-25]. To the best of our knowledge, very few papers have been published on chitosan/gelatin electrostatic complex systems, and most efforts have been devoted to optimizing the complexation conditions [16, 26-28]. Recently, it was reported that electrostatic interaction-induced chitosan/gelatin nanoparticles were able to encapsulate cocoa procyanidin and

significantly enhanced its stability and bioactivity [29]. However more detailed studies are required to understand the CH/GB complexation mechanisms and phase separation kinetics.

In this work, the complexation of chitosan and gelatin-B is systematically investigated as a function of pH, ionic strength and storage time. The properties of CH/GB complexes and the final colloidal gel are examined by measuring zeta-potential, turbidity, morphology and rheological properties. This work aims at elucidating the formation mechanisms and properties of CH/GB soluble and insoluble complexes under different conditions, monitoring their time evolution, and providing valuable information for the design of novel protein/polysaccharide complex systems with targeted properties.

5.3 Experimental

5.3.1 Materials

A commercial grade of chitosan (degree of deacetylation 85%, dynamic viscosity 60 mPa.s) was supplied in a powder form by BioLog Biotechnologie und Logistik GmbH (Landsberg, Germany). Gelatin-B with bloom strength of 75 and molecular weight in the range of 20-25 kDa, was purchased from Sigma-Aldrich Canada (Oakville, ON). Acetic acid (AcOH, 99.9%, Fisher Scientific, USA) was used to dissolve chitosan. Fluoresceine isothiocyanate (FITC) was purchased from Sigma-Aldrich Canada as a fluorescent marker. All other chemicals used in this work were of analytical grade.

5.3.2 Preparation of chitosan-gelatin soluble and insoluble complexes

Chitosan solutions were prepared by dissolving the powder in a 1% (v/v) acetic acid aqueous solution and stirring at a rate of 300 rpm, using a laboratory magnetic stirrer (PC-420 Corning Stirrer/Hot Plate, Corning Inc., MA, USA) at room temperature for 4 h. Gelatin solutions were prepared in distilled water at 40 °C with stirring (300 rpm) for 30 min. The CH/GB mixtures were obtained by mixing the two solutions at a volume ratio of 1:2 (CH:GB), at a stirring speed of 300 rpm and room temperature. The pH of the mixtures was adjusted from 3.5 to 6.5 using NaOH or HCl solutions at concentrations of 0.5 to 2 M, and for each pH adjustment, the higher concentration was used first to minimize the dilution effect. The ionic strength (from 0 to 100 mM) was varied by adding different amounts of sodium chloride (NaCl). The concentrations of

chitosan, gelatin and their mixtures were varied from 0.1 wt % to 2 wt % depending on the requirement for characterization. The CH/GB mixtures were also stored at room temperature for one week to allow phase separation. The separated phase at the bottom, namely the insoluble CH/GB complexes, was collected using centrifugation (Sorvall RC6 Plus Superspeed Centrifuge, Thermo Scientific, USA) at 5000 rpm for 15 min.

5.3.3 Zeta potential and particle size determination

The zeta potential and particle size of CH/GB mixtures at different pH and ionic strength were measured three individual times with a microelectrophoresis and dynamic light scattering (Nano-ZPS, Malvern Instruments, Worcestershire, UK). For each test, a very dilute sample solution (0.1 wt %) was filled into a disposable zeta-potential folded capillary cell (DTS1060). All the samples tested were freshly prepared. The instrument determined the electrophoretic mobility and the Smoluchowski model was then applied by the software for calculating the zeta-potential. For particle size measurement, the average radius (nm) was recorded.

5.3.4 Turbidity measurements

The turbidity profiles of CH/GB soluble complexes were examined from day 1 (freshly prepared samples) to day 3 (the samples were turbid but there were no phase separation), using spectrophotometric measurements in a UV-Vis Varian spectrophotometer, model Cary100 (Palo Alto, CA, USA), using a quartz cuvette with a 1 cm path length. The spectral measurements were taken in transmittance mode (% T) at 633 nm. The turbidity index (100 - % T at 633 nm) was plotted against pH and ionic strength for different storage times.

5.3.5 CLSM observation of soluble CH/GB complexes

The microstructure of CH/GB soluble complexes (pH 5.5) with different salt contents (from 0 to 100 mM) was investigated by CSLM (confocal laser scanning microscopy). The total biopolymer concentration was 1 wt %. Before preparing the CH/GB complexes, gelatin was firstly labeled by covalently linked fluorescent markers (fluoresceine isothiocyanate, FITC) with excitation:emission wavelength ratio of 485:530 nm. Labeling was achieved using the method established by Sanchez et al. with a small modification [30]: the pH of the gelatin dispersions was adjusted to 8.5 to favor the chemical reaction with the markers, and then 25 μ L of a 1 wt %

FITC dispersion in ethanol was added to 100 mL of the gelatin dispersion. The cross-linking reaction occurred under gentle stirring at room temperature for 90 min. Here a minimum amount of markers was used to reduce the presence of free markers, but sufficiently to provide labeling. This procedure allowed using the FITC–gelatin dispersions to form CH/GB complexes without any filtration or precipitation/drying treatments that could affect the molecular structure of the biopolymers. CLSM-images were recorded at room temperature with a Leica TCS SP5 confocal laser scanning microscope (Leica Microsystems Inc., Heidelberg, Germany), equipped with an inverted microscope (Model Leica DMI6000). The images were captured in the single photon mode with an Ar/Kr visible light laser and recorded with a 100× objective lens.

5.3.6 Water content determination

The water content of insoluble CH/GB complexes was determined by measuring the weight-loss as a function of temperature using a TA Instruments thermogravimetry analyzer TGA Q500 (TA Instruments, USA). The temperature was increased from 20 to 200 °C, at a heating rate of 5 °C/min, under a nitrogen atmosphere. The sample mass became constant above 150 °C, so the percentage of weight loss below 150 °C was used to infer the water content.

5.3.7 Rheological measurements

Dynamic rheological properties of CH/GB phase-separated complexes (namely, insoluble complexes) were characterized using a rotational rheometer (MCR 502, Anton Paar, Graz, Austria). Depending on the type of test, a coaxial double gap flow geometry (DG26.7) (inner cylinder with internal and external dimensions of 24.658 mm and 26.658 mm, and outer cylinder with internal and external dimensions of 23.82 mm and 27.602 mm) or a regular Couette geometry (CC17) (with cup and bob diameters of 18.08 and 16.66 mm, respectively) was used. First, a time sweep was carried out at 6.28 rad/s for 30 min, showing that the dense phase was stable within the test time span. Then a frequency sweep from 0.1 to 100 rad/s was performed in the linear viscoelastic regime at 25 °C. Temperature sweeps were also conducted for two heating and cooling cycles at a constant frequency (6.28 rad/s). Firstly, the temperature was increased from 25 to 60 °C at a heating rate of 2 °C/min, and then decreased to 5 °C with a cooling rate of 2 °C/min. The second cycle was carried out between 5 and 60 °C. During the tests, a low

viscosity silicon oil was used to cover the surface of the sample solutions to prevent evaporation of the solvent. The presence of the oil was shown not to impact the rheological measurements.

5.4 Results and discussion

5.4.1 Characterization of CH/GB soluble complexes

5.4.1.1 Zeta potential

Figure 5.1a shows the zeta potential of chitosan, gelatin and CH/GB mixtures at different pH values. As expected, the zeta-potential of gelatin-B is positive below its isoelectric point ($\text{pH} = 5$), while negative above that value. At pH 3, gelatin-B exhibits its highest zeta potential (20 mV), while it decreases to a value lower than -10 mV at pH 6.5. Chitosan is positively charged over the entire pH range investigated, confirming its cationic nature. The value of its zeta-potential also decreases with pH, from 70 mV at pH 3 to 15 mV at pH 6.5, where the solubility also drops significantly. After comparing the zeta-potential values of chitosan and gelatin-B at different pH, a same-charge range (from pH 3 to pH 5, Region A) and a narrow opposite-charge range (from pH 5 to pH 6.5, Region B) are identified. The zeta potential data for a CH/GB mixture ($\text{CH:GB} = 1:2$) are also shown in Figure 5.1a. At pH 3, the CH/GB mixture carries an intermediate net charge, between the low charge density gelatin and the high charge density chitosan; when the pH increases from 3 to 6.5, the zeta potential curve of the CH/GB mixture get gradually closer to the chitosan curve. It indicates that electrostatic interactions take place and some opposite charges are neutralized by this interaction when the pH moves towards Region B.

The zeta-potential of the CH/GB ($\text{CH:GB} = 1:2$) mixture with different salt concentrations and as a function of pH is shown in Figure 5.1b. The zeta-potential for all CH/GB samples is positive, and decreases gradually when the pH increases from 3 to 6.5. However, depending on the charge characteristics of chitosan and gelatin, the salt concentration effect is totally different. In the same charge range (pH 3-5, Region A), the salt screening effect is significant, resulting in a drop of the zeta potential, for instance at pH 3, from 45 mV to 15 mV. In the opposite charge region (pH 5-6.5, Region B), however, there is not much variation of the zeta-potential as the salt concentration increases from 0 to 100 mM. A similar phenomenon was observed in a recent work where chitosan and soy protein were used to form soluble complexes [31]. This is probably due

to the competitions between mobile ions and polyelectrolytes in the opposite charge zone, which leads to a decrease of the salt screening effect. Besides, the lower charge density of chitosan and gelatin molecules within this range (pH 5-6.5) is another possible reason.

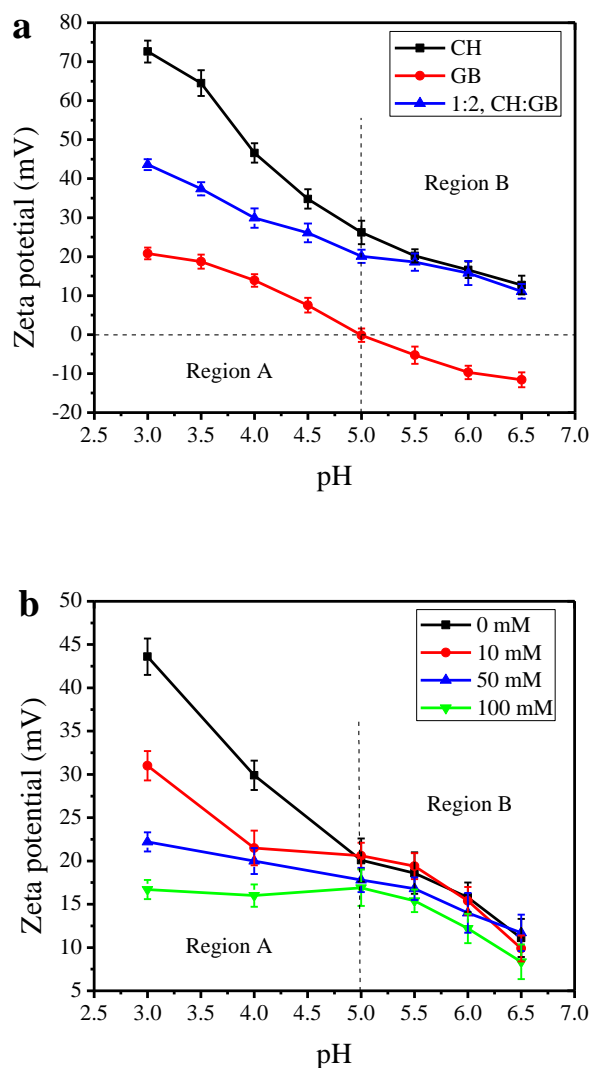


Figure 5.1: Zeta-potential of chitosan, gelatin and CH/GB complexes (0 mM NaCl) as a function of pH (a); CH/GB complexes at various pH and NaCl concentrations (b). Region A and Region B represent the same and opposite charge pH ranges, respectively, for chitosan and gelatin-B.

5.4.1.2 Turbidity, size and optical observation

The turbidity, arising mainly from the development and change in size of complex particles in the solution, is a very important indicator that can reflect the interaction between chitosan and

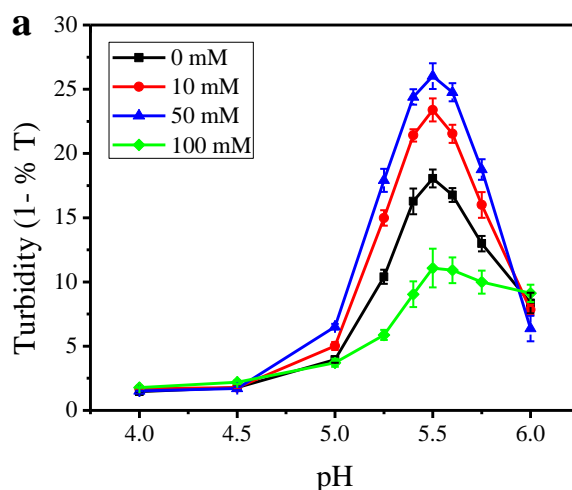
gelatin as well as the formation of complexes. Figure 5.2 shows the turbidity evolution of mixtures consisting of 1 wt % gelatin and 1 wt % chitosan at a volume ratio of 2:1. All the freshly prepared mixtures are transparent, but the turbidity increases significantly after 3 days (except for the sample at pH 4), indicating that the particle size of the complexes increases with time. The turbidity of the mixtures increases as pH is raised from 4 to 5.5, followed by a decrease with further increasing pH to 6.0, which suggests that chitosan and gelatin-B have the strongest interaction at pH 5.5. This result agrees with a previous study where the highest amount of complexes was obtained between pH 5 and 5.5 [26]. The formation of complexes is mainly due to electrostatic attraction, while pH-induced conformational change is another factor that could favor interactions, since both gelatin and chitosan were reported experiencing conformational changes with pH: gelatin from an ordered helix to a flexible pattern, and chitosan exhibiting a decreased persistence length as pH increases [32, 33]. It should also be noted that even at the same/opposite charge boundary (pH 5); a considerable amount of turbidity was still observed. Although the net charge of the gelatin molecules is zero at pH 5, as an amphoteric electrolyte, gelatin is able to interact with the positively charged chitosan molecules via electrostatic attraction forces, due to the presence of negatively charged groups, e.g. carboxylic groups. In fact, it has been reported by several researchers that complex formation can be observed even in a pH range where the polysaccharides and proteins have the same type of net charge [16, 34].



Figure 5.2: Photographs of CH/GB mixtures (total polymer concentration = 1 wt %, CH:GB = 1:2) at different pH and storage time.

Figure 5.3a shows the evolution of the turbidity index of CH/GB mixtures (total polymer concentration = 1 wt %, CH:GB = 1:2, storage time = 3 days) with different NaCl concentrations and as function of pH. In general higher NaCl concentration leads to higher turbidity, with the

maximum turbidity obtained at a concentration of 50 mM, and further increase of salt concentration to 100 mM decreases the turbidity significantly. A similar trend was also observed in the average size of the complex particles, displayed in Figure 5.3b. It indicates that salt facilitates the formation of CH/GB complexes at lower concentration, but hinders it at higher content. Similar salt-enhanced effect at lower salt concentration and salt-reduced effect at higher salt concentration was also observed in a previous work, where pectin and β -lactoglobulin were used to produce complexes [35]. The presence of salt can weaken the electrostatic attraction between the oppositely charged protein and polysaccharide, and meanwhile, it can also decrease the charge density of polymer chains and then reduce intra-molecular electrostatic repulsion, leading to a more flexible polymer chain, which is in favor of intermolecular interaction because of the lower steric hindrance [36]. Besides, the presence of salt may also decrease the hydrogen-bonded hydration water layer around polymer chains, which gives polymer chains more chance to interact with each other and even precipitate at high salt level [37]. For CH/GB complex system with lower salt concentrations (from 0 to 50 mM), although the electrostatic interaction is decreased by ion screening, the size of the complex particles still increases (Figure 5.3b) due to the conformational change and dehydration effect of the salt. However, the decrease of turbidity and particle size at 100 mM indicates that the impediment of electrostatic attraction between CH and GB is the dominant salt effect at this higher content, against complex formation.



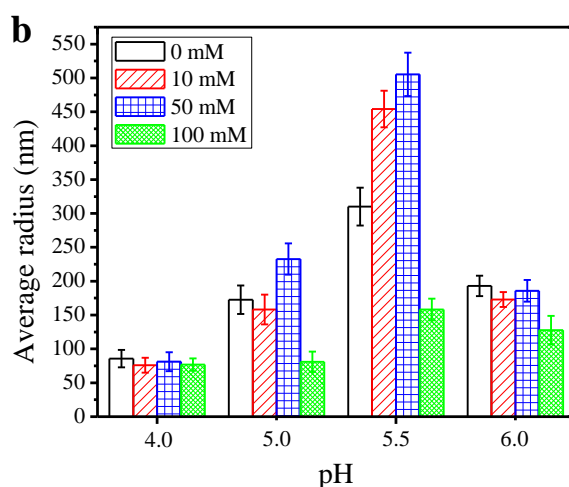


Figure 5.3: Turbidity profile (a) and average radius (b) of CH/GB complexes (total polymer concentration = 1 wt %, CH:GB = 1:2, storage time = 3 days) at various pH and NaCl concentration.

The evolution of CH/GB complexes formed at the optimum pH of 5.5 was investigated as a function of time. Figure 5.4 shows the photographs of samples (without centrifugation) after different storage times (day 3, day 7 and day 40, respectively). At the beginning, the turbidity of soluble complexes increases with time, suggesting that larger complex particles are gradually formed. Then, as the size or interaction of complex particles increases, the complexes become insoluble and phase separation eventually occurs. Interestingly, after phase separation, the internal structure of the insoluble phase gradually changes with time, since a gel-like structure is observed for the sample stored for 40 days. The schematic diagram representing this process is also shown in Figure 5.4, from a microscopic viewpoint. It is assumed that the gel ultimately obtained is colloidal in nature, i.e. its network structure is formed by connecting particle flocs or aggregates. Some evidences that support this assumption are presented in the next section on CLSM observations. Aiming to characterize this evolution quantitatively, further investigation on the separated dense phase was also carried out by rheological measurements and results are reported in Section 5.4.2.2.

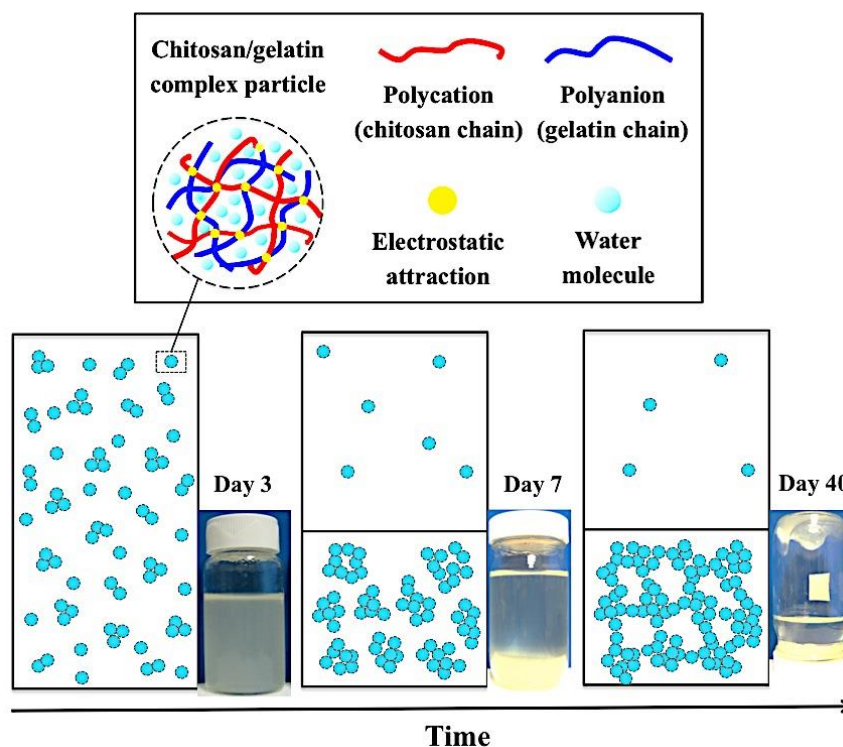


Figure 5.4: Schematic diagram and photographs of time evolution of CH/GB complexes (total polymer concentration = 1 wt %, CH:GB = 1:2, pH = 5.5).

5.4.1.3 CLSM observations

CLSM was used to examine the morphology of soluble CH/GB complexes in aqueous state (pH 5.5) at different NaCl concentrations (0, 10, 50 and 100 mM) and after storage for 3 days. From the CLSM micrographs shown in Figure 5.5, where labeled gelatin appears in green, particle flocs and clusters are already formed on day 3, as agglomeration between particles can be observed. Meanwhile, it gives a direct proof that the gel formed after 40 days of storage is a particulate colloidal gel, since the flocculated complex particles shown in the CLSM micrographs are elemental units for the network structure formation. The size of agglomerates also varies with salt content, and the strongest interactions between particles are found in Panel C (50 mM NaCl). The presence of gelatin agglomerates (small green spots) in Panel D (100 mM NaCl) also indicates that gelatin participates less in the CH/GB complex formation, because of the weaker electrostatic interactions at this salt content. Based on the information obtained from the turbidity data and CLSM observations, we can propose the time evolution of CH/GB complexes, as shown in the schematic diagram of Figure 5.4. First, soluble complexes are formed (e.g., Day 3 in Figure

5.4), then they tend to interact with each other to further reduce the free energy of the system until their size or charge properties lead to insolubilization and bulk phase separation (e.g., Day 7 in Figure 5.4).

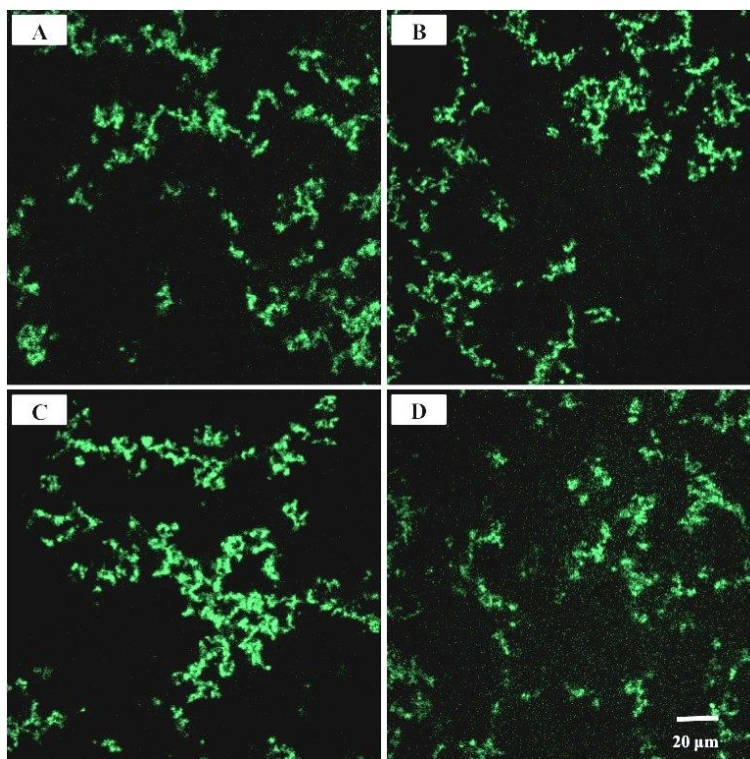


Figure 5.5: CLSM graph of CH/GB complexes (total polymer concentration = 1 wt %, CH:GB = 1:2, pH = 5.5, storage time = 3 days) with various NaCl concentration (A, 0 mM; B, 10 mM; C, 50 mM; D, 100 mM).

5.4.2 Characterization of insoluble CH/GB complexes

5.4.2.1 Water content

Figure 5.6 shows the water content of CH/GB insoluble complexes after different storage times (day 7 and day 40). It can be seen that the water content of all insoluble complexes is very high on day 7 (the day the insoluble complexes were separated using centrifugation), ranging from 95.5 to 97.8 wt %. It is worth mentioning that the water content of the CH/GB insoluble complexes is higher than that of globular protein/polysaccharide complex systems (about 80 to 90%) [2]. We speculate that this is due to the linear structure of gelatin molecules that allows the formation of a molecular network structure with linear chitosan chains. More water may be

trapped inside the complex particles (as shown in the schematic diagram of Figure 5.4), since flexible linear proteins (i.e. gelatin or casein) are able to form a maximum number of contacts with oppositely charged polysaccharides, as compared to globular proteins [32, 38]. The high-water-content feature of the insoluble complexes makes it also potentially attractive in the scope of drug and cell delivery, since it can compare with organism's body parts that usually contain 70-90% water and the diffusion efficiency is always higher due to the inner formation of a richly porous 3D network [39].

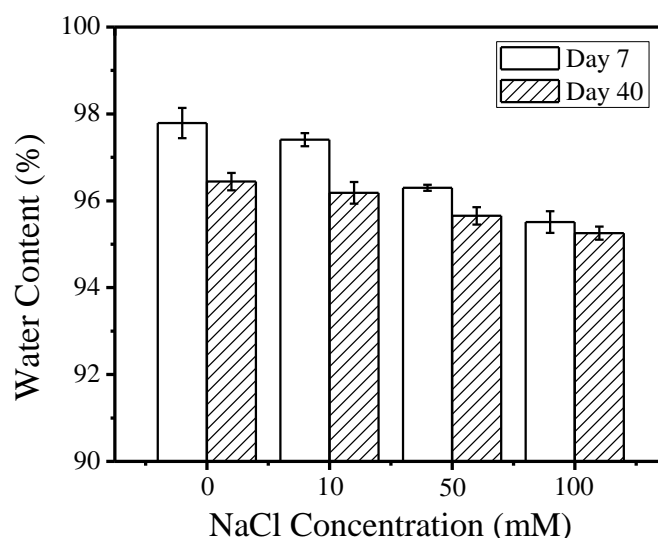


Figure 5.6: Water content of CH/GB insoluble complexes (CH:GB = 1:2, pH 5.5) at various NaCl concentration and for two storage times (day 7 and day 40).

The addition of salt has a prominent effect on the complexes' composition, resulting in a decrease of the water content by about 2% as the NaCl concentration increases from 0 to 100 mM, and consequently the polymer mass content is almost doubled (from 2.3 to 4.5 wt %). Considering that a larger particle size is assumed to accelerate the formation of insoluble complexes, the insoluble complexes formed at higher salt concentration (50 mM) tend to be more concentrated. For insoluble complexes with 100 mM NaCl, the higher mass content (lower water content) may be due to the dehydration effect at higher salt concentration. When salt is added in aqueous solution, the ions may compete for water molecules with the polymer chains that are surrounded by a layer of hydration water [37]. The decrease of hydration water may increase the interaction between polymer molecules, therefore, in a CH/GB complex system at higher salt

content, chitosan and gelatin may form more compact particles with less trapped water inside. A previous report has shown similar results, where a high water content complex system with protein (β -lactoglobulin) and polysaccharide (pectin) was formed by the addition of NaCl at less than 0.21M [40]. After the centrifuged CH/GB dense phase was stored at room temperature for another 33 days (40 days total), all the insoluble complex samples showed a syneresis effect supported by the decrease of water content of the complexes (Figure 5.6). It suggests that a more compact structure is building up, resulting in a release of the trapped water molecules. The degree of shrinkage is dependent on NaCl content. Less shrinkage is observed at higher salt concentration, since the water content difference between day 7 and day 40 decreases gradually (from 1.35% to 0.25%), as salt concentration increases from 0 to 100 mM NaCl, respectively. This finding agrees with the experimental results of Laneuville et al., who found that a lower syneresis electrostatic gel could be obtained with xanthan gum and BSA in the presence of a small amount of NaCl [41].

5.4.2.2 Time evolution of viscoelasticity

Figure 5.7 shows the complex viscosity and moduli (storage modulus G' and loss modulus G'') of insoluble CH/GB complexes (pH 5.5, without NaCl) as functions of angular frequency and after different storage times. Considering the syneresis effect shown in Figure 5.6, namely the increase of mass content from day 7 (2.21 wt %) to day 40 (3.56 wt %), the complex viscosity and moduli data are divided by the polymer mass content, as to compare the viscoelastic behavior in similar conditions. Increasing of storage time significantly increases the complex viscosity, up to ten times from 7 days to 40 days (Figure 5.7a). More specifically, the change in complex viscosity from day 7 to day 20 is larger than that from day 20 to day 40, suggesting that the self-assembled structure is formed faster at the beginning, and that it may be stabilized after a long period of storage. All the samples exhibit a typical shear-thinning behavior within the shear rate range examined, as the complex viscosity decreases with increasing frequency as displayed in Figure 5.7a. As storage time increases, the slope gets steeper and the power law index (n) becomes smaller (day 7, $n = 0.74$; day 20, $n = 0.28$; day 40, $n = 0.18$), hence getting closer to a solid-like behavior. On day 7, G' is lower than G'' on the entire frequency range, which indicates a liquid-like behavior of the insoluble CH/GB complexes. It is however interesting to note that G' does not exhibit the typical terminal slope of 2 and instead shows a slight plateau, indicative of a precursor network. After 20 days of storage, both G' and G'' increase, but G' rises much faster

and becomes higher than G'' , indicating the formation of a network between the complex particles. As storage time increases to 40 days, the evolution trend for G' and G'' continues and the difference between the two is more significant, which suggests an enhanced gel strength and elasticity of the CH/GB complexes. It has been shown in other complex gel systems that electrostatic interactions are the main driving force for gel structure formation [2, 42]. Other factors that may affect this phenomenon are hydrogen bonding and hydrophobic effect between polymer molecules or complex particles [12]. In the following sections, the effect of salt and temperature on the evolution of viscoelasticity for the phase-separated complexes is discussed, aiming at identifying the predominant driving force in the formation of the CH/GB colloidal gel.

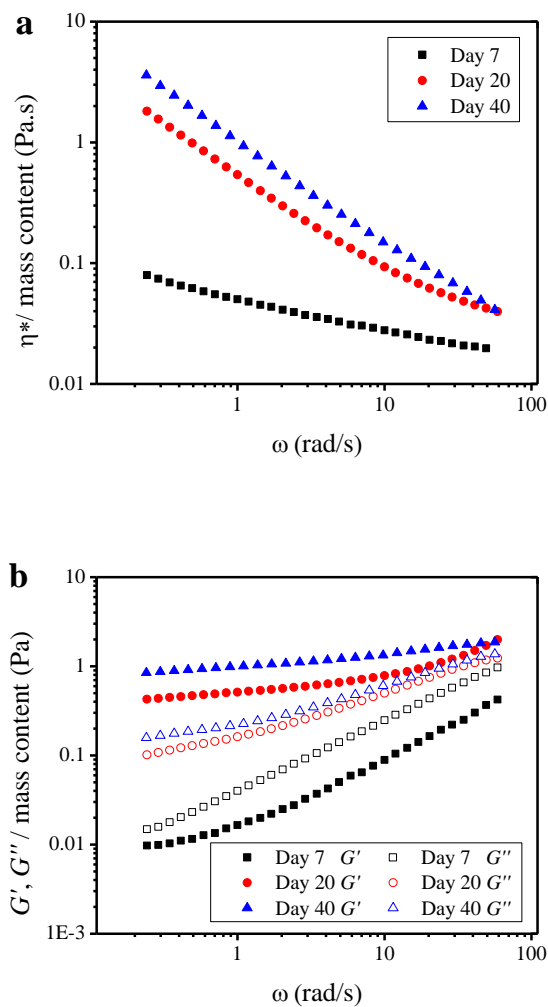


Figure 5.7: Time evolution of complex viscosity (a) and moduli (G' and G'') (b) for insoluble CH/GB complexes formed at pH 5.5 without salt.

5.4.2.3 Effect of salt on viscoelasticity of insoluble CH/GB complexes

The presence of salt affects the charge properties and conformational structure of protein and polysaccharide, as well as their interactions and complex particle agglomeration, thus should have an impact on the rheological properties of insoluble complexes [3, 40, 42]. The time evolution for the viscoelasticity of complexes in the presence of salt was quite similar to that of the original complex (without salt, Figure 5.7), and for easy comparison, only the values of G' and G'' at a frequency of 1 rad/s are plotted in Figure 5.8, as functions of storage time and salt concentration. The moduli data were again divided by the polymer mass content to allow comparison in similar conditions. Initially (day 7), all the samples show lower G' comparing to G'' , suggesting that the liquid-like structure of the CH/GB soluble complexes was not affected by the addition of salt. On day 40, there is a large increase of both G' and G'' , and most importantly, G' becomes larger than G'' , indicating the formation of a network structure, or gel, for all the insoluble complex samples. Interestingly, the value of both G' and G'' depends on the concentration of NaCl: a higher NaCl concentration leads to higher G' and G'' values. Different from the formation of soluble complexes, where the maximum interaction is found for the sample containing a medium salt concentration (50 mM) and further increase of the salt content to 100 mM decreases the size of soluble complexes (Figure 5.3a and Figure 5.3b in Section 5.3.1.2), the increase of salt content from 0 to 100 mM favors the formation of the network structure in insoluble complexes. Considering that the electrostatic interaction is relatively lower at higher salt content, we suppose that apart from electrostatic interaction, other non-electrostatic physical interactions (e.g. hydrogen bonding, hydrophobic effect) may participate in the network formation of CH/GB insoluble complexes. Therefore, the effect of temperature on the viscoelastic properties of the CH/GB insoluble complexes is examined in the next section in order to shed light on possible additional driving forces such as hydrogen bonding and hydrophobic interactions in the gel formation.

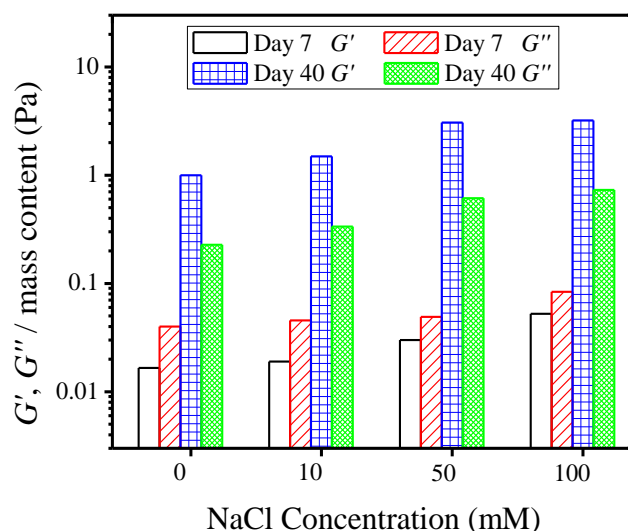


Figure 5.8: Effect of salt concentration and storage time on storage and loss moduli ($\omega = 1$ rad/s) of insoluble CH/GB complexes formed at pH 5.5 (reproducibility was within 5% for all conditions).

5.4.2.4 Temperature sweep of gel-like complexes

It has been reported that non-covalent interactions can be affected by relatively small temperature changes [43]. Specifically, increasing temperature can weaken ionic bonding, hydrogen bonding and van der Waals forces, which are formed with the release of heat, but can stabilize hydrophobic interactions that are accompanying heat adsorption. Successive heating and cooling cycles were applied in order to investigate the thermoreversibility of the CH/GB complex gel (pH 5.5, 50 mM NaCl, day 40). As shown in Figure 5.9, during the first heating cycle there is a sharp decrease of both moduli where G' decreases faster than G'' , and becomes even lower after the crossover point at 42 °C (gel-sol transition), indicating the structuration of a gel mainly maintained by hydrogen bonding and electrostatic interactions. Further increase in temperature has little effect on G' and G'' , suggesting a rearrangement of the network structure driven by hydrophobic effect. In the first cooling cycle, both G' and G'' increase slowly in the high temperature region (25 °C < T < 60 °C), and a crossover between G' and G'' is observed around 10 °C (sol-gel transition). In the low temperature region (5 °C < T < 25 °C), the rapid rise of G' indicates that the gel-like structure starts to form again as hydrogen bonding and electrostatic interactions become stronger at lower temperature. In the second heating cycle, G' keeps

increasing between 5 and 12 °C, which indicates a hysteresis phenomenon for the network formation at low temperature. Similar to the first cycle, a drop of G' and G'' occurs again when $T > 20$ °C, followed by a crossover of G' and G'' at 30 °C, happening at a lower gel-sol transition temperature than in the first heating ramp, which may be due to the different starting point of the heating cycle or a weaker network. The second cooling cycle results in a very similar pattern that in the first one, suggesting that the formation and dissociation of the CH/GB network is almost fully thermoreversible.

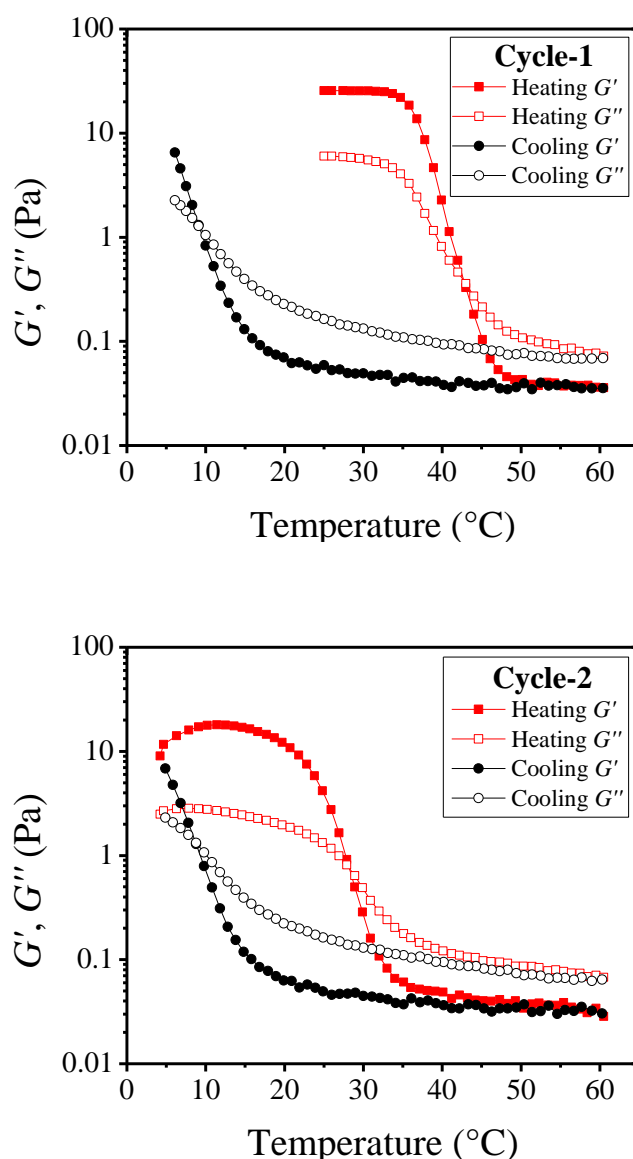


Figure 5.9: Temperature sweep (two cycles) of insoluble CH/GB complexes formed at pH 5.5 in the presence of 50 mM NaCl (storage time = 40 days)

5.5 Conclusions

This study demonstrated that soluble and gel-like insoluble complexes (colloidal gel) could be formed in the pH region with opposite charge (pH 5–pH 6.5) for chitosan and gelatin type B, depending on the storage time. The addition of salt significantly affected the interactions between chitosan and gelatin, and thus influenced the size of soluble complexes, the water content and network structure of insoluble complexes. The formation of CH/GB complexes was mainly driven by electrostatic attraction and favored by lower steric hindrance. The agglomeration of soluble complexes resulted in a liquid-liquid phase separation, and as storage time increased, a network structure mainly maintained by electrostatic interactions and hydrogen bonding was gradually formed in the dense phase, leading to a high-water-content thermoreversible colloidal gel. The insoluble CH/GB complexes and the corresponding colloidal gel developed here may find interesting uses in the scope of delivery of sensitive bioactive molecules or nutrients with tailored properties.

Acknowledgements

The authors acknowledge Prof. Nick Virgilio (Polytechnique Montréal) and Prof. Julian Zhu (Université de Montréal) for their advice and help with some of the experiments.

Funding

The authors thank the financial support from NSERC (Natural Sciences and Engineering Research Council of Canada). A scholarship for Ms. Wang provided by the China Scholarship Council (CSC) is also acknowledged.

References

1. de Kruif C. G.; Weinbreck F.; de Vries R. *Curr. Opin. Colloid Interface Sci.* **2004**, 9(5), 340.
2. Schmitt C., Turgeon S. L. *Adv. Colloid Interface Sci.* **2011**, 167(1-2), 63.
3. Turgeon S. L.; Schmitt C.; Sanchez C. *Curr. Opin. Colloid Interface Sci.* **2007**, 12(4-5), 166.
4. Schmitt C.; Sanchez C.; Desobry-Banon S.; Hardy J. *Crit. Rev. Food Sci. Nutr.* **1998**, 38(8), 689.

5. Benichou A.; Aserin A.; Garti N. *J. Dispersion Sci. Technol.* **2002**, 23(1-3), 93.
6. Braudo E. E.; Plashchina I. G.; Schwenke K. D. *Nahrung-Food.* **2001**, 45(6), 382.
7. Dickinson E. *Soft Matter.* **2008**, 4(5), 932.
8. Evans M.; Ratcliffe I.; Williams P. A. *Curr. Opin. Colloid Interface Sci.* **2013**, 18(4), 272.
9. Ooi V. E. C.; Liu F. *Curr. Med. Chem.* **2000**, 7(7), 715.
10. Bouyer E.; Mekhloufi G.; Rosilio V.; Grossiord J. L.; Agnely F. *Int. J. Pharm.* **2012**, 436(1-2), 359.
11. Tolstoguzov V. *Int. Rev. Cytol.* **2000**, 192, 1923.
12. Turgeon S. L.; Beaulieu M.; Schmitt C.; Sanchez C. *Curr. Opin. Colloid Interface Sci.* **2003**, 8(4-5), 401.
13. Perez A. A.; Carrara C. R.; Carrera Sanchez C.; Rodriguez Patino J. M.; Santiago L. G. *Food Chem.* **2009**, 116(1), 104.
14. Luo Y., Wang Q. *Int. J. Biol. Macromol.* **2014**, 64353.
15. Lee A.-C.; Hong Y.-H. *Food Res. Intl.* **2009**, 42(5-6), 733.
16. Gupta A. N.; Bohidar H. B.; Aswal V. K. *J. Phys. Chem. B.* **2007**, 111(34), 10137.
17. Prabakaran M. *J. Biomater. Appl.* **2008**, 23(1), 5.
18. Vinsova J.; Vavrikova E. *Curr. Pharm. Design.* **2011**, 17(32), 3596.
19. Elmer C.; Karaca A. C.; Low N. H.; Nickerson M. T. *Food Res. Int.* **2011**, 44(5), 1441.
20. Guzey D.; McClements D. J. *Food Hydrocolloids.* **2006**, 20(1), 124.
21. Karim A. A.; Bhat R. *Food Hydrocolloids.* **2009**, 23(3), 563.
22. Antonov Y. A.; Zubova O. M. *Int. J. Biol. Macromol.* **2001**, 29(2), 67.
23. Piacentini E.; Giorno L.; Dragosavac M. M.; Vladislavljevic G. T.; Holdich R. G. *Food Res. Int.* **2013**, 53(1), 362.
24. Saravanan M.; Rao K. P. *Carbohydr. Polym.* **2010**, 80(3), 808.
25. Gilsenan P. M.; Richardson R. K.; Morris E. R. *Food Hydrocolloids.* **2003**, 17(6), 723.
26. RemunanLopez C.; Bodmeier R. *Int. J. Pharm.* **1996**, 135(1-2), 63.
27. Silva M. C.; Andrade C. T. *Polimeros: Ciencia E Tecnologia.* **2009**, 19(2), 133.
28. Kang M. K.; Dai J.; Kim J. C. *J. Ind. Eng. Chem.* **2012**, 18(1), 355.
29. Zou T.; Percival S. S.; Cheng Q.; Li Z.; Rowe C. A.; Gu L. *Eur. J. Pharm. Biopharm.* **2012**, 82(1), 36.

30. Sanchez C.; Mekhloufi G.; Schmitt C.; Renard D.; Robert P.; Lehr C. M.; Lamprecht A.; Hardy J. *Langmuir*. **2002**, 18(26), 10323.
31. Yuan Y.; Wan Z.-L.; Yin S.-W.; Teng Z.; Yang X.-Q.; Qi J.-R.; Wang X.-Y. *Food Hydrocolloids*. **2013**, 31(1), 85.
32. Lv Y.; Zhang X.; Zhang H.; Abbas S.; Karangwa E. *Food Hydrocolloids*. **2013**, 30(1), 323.
33. Tsaih M. L.; Chen R. H. *J. Appl. Polym. Sci.* **1999**, 73(10), 2041.
34. Koupantsis T.; Kiosseoglou V. *Food Hydrocolloids*. **2009**, 23(4), 1156.
35. Wang X.; Lee J.; Wang Y.-W.; Huang Q. *Biomacromolecules*. **2007**, 8(3), 992.
36. Cho J. Y.; Heuzey M. C.; Begin A.; Carreau P. J. *J. Food Eng.* . **2006**, 74(4), 500.
37. Amorim L. V.; Barbosa M. I. R.; Lira H. d. L.; Ferreira H. C. *Mater. Res.* **2007**, 10(1), 53.
38. Doublier J. L.; Garnier C.; Renard D.; Sanchez C. *Curr. Opin. Colloid Interface Sci.* **2000**, 5(3-4), 202.
39. Huang Y.; Zhang M.; Ruan W. *J. Mater. Chem. A*. **2014**, 2(27), 10508.
40. Wang X. Y.; Lee J. Y.; Wang Y. W.; Huang Q. R. *Biomacromolecules*. **2007**, 8(3), 992.
41. Laneuville S. I.; Turgeon S. L.; Sanchez C.; Paquin P. *Langmuir*. **2006**, 22(17), 7351.
42. Ru Q. M.; Wang Y. W.; Lee J.; Ding Y. T.; Huang Q. R. *Carbohydr. Polym.* **2012**, 88(3), 838.
43. Cho J.; Heuzey M.-C.; Bégin A.; Carreau P. J. *Biomacromolecules*. **2005**, 6(6), 3267.

CHAPTER 6 ARTICLE 3: PICKERING EMULSION GELS BASED ON INSOLUBLE CHITOSAN/GELATIN ELECTROSTATIC COMPLEXES

Xiao-Yan Wang and Marie-Claude Heuzey

Department of Chemical Engineering, CREPEC, Polytechnique Montreal, PO Box 6079, Station
Centre-Ville, Montreal, QC Canada H3C 3A7

(This work was submitted to *RSC Advances* on April 21, 2016)

6.1 Abstract

Food-grade colloidal particles or complexes made from natural polymers via noncovalent interactions can be good candidates for applications in food and beverage industries. In this work, insoluble chitosan/gelatin-B (CH/GB) complex particles were used for the first time as effective Pickering emulsifiers to make long-term stable oil-in-water emulsions and emulsion gels by one-step homogenization. The CH/GB complexes were only formed in the oppositely charged pH region via electrostatic complexation of CH and GB and the pH showed a remarkable effect on the surface activity of CH/GB mixed systems. The presence of CH/GB insoluble complexes significantly decreased the surface tension of the oil/water interface, therefore benefited the formation of smaller emulsion droplet size and effectively hindered droplet coalescence as supported by the increase of emulsion long-term stability. Increasing oil volume fraction significantly accelerated the formation of a droplet network structure, resulting in a more solid-like thermoreversible emulsion gel with tunable viscoelastic properties. Our results suggest that CH/GB insoluble complex particles are promising particulate emulsifiers for the preparation of surfactant-free Pickering emulsions as well as emulsion gels.

6.2 Introduction

Pickering emulsions are emulsions stabilized by solid particles instead of surfactants, either water-in-oil (W/O), oil-in-water (O/W), or even multiple emulsions, with very high resistance to coalescence.¹⁻² Recently, the development of bio-sourced particulate Pickering emulsifiers has received increasing attention, since most of the particles used in the fundamental studies of Pickering emulsions are synthetic or inorganic particles (e.g., silica, TiO₂ particles), which greatly limit their applications in food, cosmetic, and pharmaceutical industries.³⁻⁴ However, finding an effective bio-based Pickering emulsifier is challenging because it should have intermediate wettability and meanwhile insolubility in both the water and oil phases.⁵⁻⁶ In the past decades, only a few biocompatible materials, including chitin nanocrystal particles,⁷ starch granules,⁸ cellulose particles⁹ and water-insoluble zein,¹⁰ have been shown employable as effective Pickering emulsifiers. Therefore, to meet the variable requests for specific applications, the development of more bio-based and even edible Pickering emulsifiers is desirable.

Here, we introduce chitosan/gelatin-B (CH/GB) complex particles as a novel class of Pickering emulsifiers. Both chitosan and gelatin are polyelectrolytes (chitosan is a polycation and gelatin is a polyampholyte), and they are biocompatible, biodegradable, edible polymers and also abundantly and commercially available.¹¹⁻¹² Specifically, chitosan is the only naturally occurring cationic polysaccharide, obtained from the alkaline deacetylation of chitin, while gelatin is a linear protein, derived from collagen either by acid hydrolysis (type A, pI = pH 7-9) or alkaline treatment (type B, pI = pH 4.8-5.2). We have previously shown that the complexation of CH and GB is a kinetic process, and CH/GB complexes can evolve from soluble to insoluble complexes, to eventually form a colloidal gel.¹³ In the present work, we mainly focus on the temporal evolution of insoluble CH/GB complexes, and the use of these particles as Pickering emulsifiers.

The electrostatic-driven complexation between proteins and polysaccharides has been investigated extensively.¹⁴⁻¹⁶ Mainly depending on the molecular charge density and conformation, three different structures can be formed based on the electrostatic attraction between proteins and polysaccharides, i.e., soluble/insoluble complexes,¹⁷⁻¹⁸ gels¹⁹ and coacervates.²⁰ It is still not completely understood which mechanisms favor the formation of these different structures, but a general trend emerges where proteins or polysaccharides having high charge density and/or stiff structure preferably form complexes, whereas the reverse, i.e.,

moderate charge density and flexible conformation, favor the formation of coacervate.¹⁴ Therefore, the final structures are unique properties of each protein/polysaccharide couple, and by selecting different proteins and polysaccharides, different distinctive structures can be obtained. In addition, there are several studies using protein-polysaccharide complexes directly to form emulsions, or fabricating emulsions by having polysaccharide molecules absorbed on protein-coated oil droplets to form an interfacial complex layer.²¹⁻²⁴ However, up to now and to our knowledge, whether it is possible to use protein-polysaccharide complexes as effective Pickering emulsifiers is still unknown.

As compared with existing particulate stabilizers, CH/GB particles acting as Pickering emulsifiers would have the following advantages: (i) they have positive charges, which results in cationic droplets that make emulsions less prone to destabilization by multivalent cations (e.g., Ca^{2+}),²⁵ and give a high antimicrobial efficacy;²⁶ (ii) compared to synthetic or inorganic particles (e.g., silica, TiO_2), they are soft and hence can deform and occupy large areas at the interface, which in turn can enhance the emulsion stability; (iii) they are made from nutritional and functional food ingredients; (iv) they can form networks, and as a consequence, a gel-like emulsion structure will lead to extraordinary stability against coalescence.¹³ In this work, we investigate the role of CH/GB insoluble complex particles as Pickering emulsion stabilizers. In addition, the influence of parameters such as pH and oil fraction on the emulsion stability is examined, while the viscoelastic properties of the resulting Pickering emulsions are characterized.

6.3 Experimental

Materials. Gelatin type B (GB) with bloom strength of 75 and molecular weight in the range of 20-25 kDa, was purchased from Sigma-Aldrich Canada (Oakville, ON). Commercial chitosan (CH) with DDA of 85%, dynamic viscosity of 60 mPa·s, and weight-average molecular weight of 173 kDa was supplied in powder form by BioLog Biotechnologie und Logistik GmbH (Landsberg, Germany). A fluorescent marker, fluoresceine isothiocyanate (FITC) was purchased from Sigma-Aldrich Canada. Acetic acid (99.9% AcOH) from Fisher Scientific (USA) was used to dissolve chitosan. Corn oil was purchased from a local supermarket in Montreal (Canada). All other chemicals used in this work were of analytical grade from Sigma-Aldrich.

Preparation of CH/GB insoluble complexes. CH and GB solutions were first prepared separately: CH was dissolved in a 1% (v/v) acetic acid solution and stirred with a magnetic stirrer (PC-420 Corning Stirrer/Hot Plate, Corning Inc., MA, USA) at 300 rpm for 4 h, and then stored overnight at room temperature to allow complete hydration and dissolution. GB was dissolved in deionized water at 40 °C and stirred (300 rpm) for 30 min. CH/GB mixtures were prepared by mixing CH and GB solutions at a volume ratio of 1:2 (CH:GB) and stirred (300 rpm) for 30 min at room temperature. The pH of the mixtures was adjusted from 3.5 to 6.5 using NaOH or HCl solutions at concentrations of 0.5 to 5 M (higher concentration was used first to minimize the dilution effect for each pH adjustment), and then the CH/GB mixtures were stored at room temperature up to 5 days to allow the formation of insoluble complexes. The concentrations of CH, GB and CH/GB aqueous solutions were varied from 0.1 to 1 wt % depending on the requirement for characterization.

Preparation of CH/GB emulsions. CH/GB mixtures at a total polymer concentration of 1 wt % were used to prepare CH/GB-stabilized oil/water emulsions, at different pH (3.5 to 6.5). Specifically, CH/GB aqueous solutions were mixed with corn oil at an oil volume fraction (ϕ) from 0.1 to 0.4, and then homogenized using a high intensity ultrasonic processor (UIP1000hd (20 kHz, 1000 W), Hielscher Ultrasonics GmbH, Teltow, Germany) with 90% amplitude for 8 min. During the homogenization, an ice bath was used to control temperature and avoid overheating. For comparison purposes, oil/water emulsions were also prepared with either CH or GB aqueous solutions. All the emulsions were stored at room temperature for further observation and characterization.

Characterization of CH/GB complexes. Zeta (ζ) potential and particle size of three individual samples of the same solutions were measured using a dynamic light scattering instrument (Nano-ZPS, Malvern Instruments, Worcestershire, UK). The turbidity evolution was monitored using a UV-Vis Varian spectrophotometer (Cary100, Palo Alto, CA, USA) in transmittance mode (%T) at 633 nm, by plotting the turbidity index (100 - %T at 633 nm) against pH. The microstructure of CH/GB insoluble complexes was observed using confocal laser scanning microscopy (CSLM) (Model Leica TCS SP5, Leica Microsystems Inc., Heidelberg, Germany), equipped with an inverted microscope (Model Leica DMI6000). Before CLSM observation, labeling was conducted using the method established by Sanchez *et al.*²⁷ GB was firstly labeled by covalently linking a minimum amount of fluorescent markers (fluoresceine

isothiocyanate, FITC) at pH 8.5 for 90 min, and then FITC-GB solutions were mixed with CH solutions at pH 5.5 to form CH/GB complexes. The interfacial surface tension of CH/GB mixtures and their solvents were determined using an optical contact angle measuring system (OCA-20, DataPhysics Instruments GmbH, Germany) by analyzing the pendant drop shape using the Young-Laplace equation. The data of interfacial tension were then used to calculate surface pressure (π), which is equal to $\gamma_s - \gamma_c$, where γ_c and γ_s are the surface tensions of CH/GB mixtures and the corresponding solvent (at a comparable test time), respectively.

Characterization of CH/GB emulsions The microstructure of freshly prepared CH/GB emulsions was observed with a Zeiss Axioskop 40 optical microscope (Carl Zeiss Microscopy GmbH, Jena, Germany). The average emulsion droplet size in terms of volume-average diameter (d_v) and number-average diameter (d_n) was calculated from microscopy images using a digitizing table from Wacom and SigmaScan v.5 software. The calculation was performed by randomly selecting three images from two parallel experiments and choosing at least 500 droplets. The long-term emulsion stability was assessed by visual observation and calculation of the creaming index (CI), which is reported as $(H_s/H_t) \times 100$, where H_t is the total height of the emulsion and H_s is the height of the serum layer (the sum of the transparent and/or the turbid layers at the bottom of the container). Viscoelastic properties of CH/GB emulsions were characterized using a rotational rheometer (MCR 502, Anton Paar, Graz, Austria) under small amplitude oscillatory shear (SAOS) mode. A regular Couette geometry (with cup and bob diameters of 18.08 and 16.66 mm, respectively) was used. A time sweep was first conducted at 1 rad/s for 20 min, showing that the CH/GB emulsions were stable within the test time range. Then a frequency sweep was carried out from 1 to 100 rad/s at 25 °C, and several temperature sweeps were also performed at a constant frequency (1 rad/s). Specifically, the system temperature was first increased from 25 to 60 °C at a heating rate of 2 °C/min, and then decreased to 5 °C with a cooling rate of 2 °C/min, and then two further heating and cooling cycles were carried out between 5 and 60 °C. During the temperature sweep tests, the surface of the emulsion samples was covered with a low viscosity silicon oil to prevent evaporation of the solvent, and the presence of the oil was shown not to impact the rheological measurements. All the tests were performed within the linear viscoelastic range. All measurements were performed at least in duplicates at room temperature, unless otherwise specified.

6.4 Results and discussion

Evolution of CH/GB Complexes. The complexation of proteins and polysaccharides is a kinetic process.²⁸ To clarify the evolution mechanism from solubility to insolubility, the physical properties of CH/GB complexes, including zeta (ζ) potential, turbidity and microstructure were characterized as a function of time. Figure 6.1A reports the ζ potential of CH, GB and CH/GB aqueous solutions at different storage times (from day 1 to day 5), and as a function of pH. CH has positive charges in the test pH range and its ζ potential decreases as pH increases, due to the deprotonation of amino groups. On the other hand, the net charge of GB is positive at pH 3.5 and 4.5, but negative at 5.5 and 6.5 (the isoelectric point of gelatin-B is around pH 5¹³). After mixing CH and GB solutions at a ratio of 1 to 2, the ζ potential of the CH/GB mixtures gradually decreases as pH increases from 3.5 to 6.5, and an interesting observation is that the charge density of CH/GB gets gradually closer to that of CH at higher pH values (e.g., pH 6.5). If there would be no interaction between CH and GB, the ζ potential of the CH/GB mixture ($\zeta_{\text{CH/GB}}$) would just be a simple mixing rule with respect to the ratio of CH and GB (1:2), using the equation:

$$\zeta_{\text{CH/GB}} = 1/3*\zeta_{\text{CH}} + 2/3*\zeta_{\text{GB}} \quad (4)$$

where ζ_{CH} and ζ_{GB} are respectively the ζ potentials of CH and GB at a corresponding pH. The calculated result is compared in Figure 6.1B with the actual values of ζ_{CH} and $\zeta_{\text{CH/GB}}$. We can see that the latter evolves gradually away from the calculated $\zeta_{\text{CH/GB}}$ but closer to ζ_{CH} , as pH increases to 6.5. Previous studies have shown that oppositely charged polyelectrolytes can form complex particles with a neutralized core and a shell made of the excess component in the case of non-stoichiometric ratios.²⁸⁻²⁹ In the CH/GB system, there is almost no electrostatic interaction between CH and GB at pH 3.5; at pH 4.5, very weak complexation occurs between CH and the negatively charged patches of the GB molecules; however, at pH 5.5 and 6.5, the electrostatic attraction force between CH and GB is enough to form a neutralized core with a shell containing excess CH, which would explain why $\zeta_{\text{CH/GB}}$ is almost the same as ζ_{CH} in the opposite charge region. Figure 6.1 A also shows that an increase in storage time does not change the ζ potential of CH/GB in the similar charge region (pH 3.5 and 4.5), but slightly decreases it in the opposite charge region (pH 5.5 and 6.5). It indicates that electrostatic interactions may not be the only driving force in the growth of the CH/GB complexes, although play a very important role in the

formation of primary particles. As seen for other polyelectrolyte complex systems,^{15, 28} the evolution of CH/GB complexes should be an intricate interplay of electrostatic, van der Waals, hydrogen bonding, and hydrophobic interactions.

In addition, the difference between complexes particles formed at pH 5.5 and 6.5 also need to be considered. First of all, it should be noted that the molecular weight of CH (173 kDa) used in this work is about 8 times that of GB (20-25 kDa), and thus when CH and GB interact with each other, CH may act as a framework in the structuration of the CH/GB complex particles. Another point is that the conformation of CH greatly depends on pH, and the extended molecular structure can gradually turn to be more compact as pH increases, mainly due to the deprotonation of amino groups.^{13, 30} Therefore, the structure of the corresponding CH/GB complexes should be denser at pH 6.5, while looser at pH 5.5.

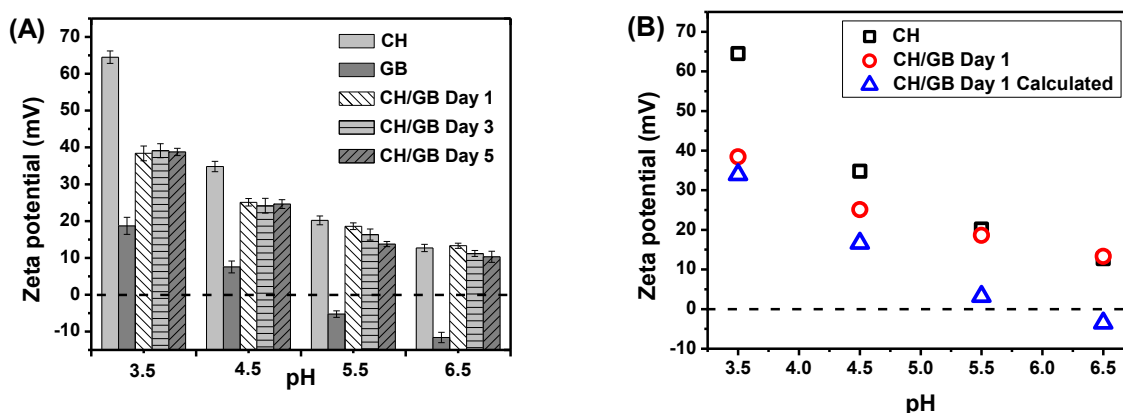


Figure 6.1: (A) Zeta potential of CH solutions (0.1 wt %), GB solutions (0.1 wt %) and CH/GB mixtures (0.1 wt %, CH:GB = 1:2) at different storage times, as a function of pH; (B) Comparison of ζ_{CH} , $\zeta_{CH/GB}$, and calculated $\zeta_{CH/GB}$ for freshly prepared samples.

The temporal evolution of CH/GB complexes was monitored by measuring turbidity, microstructure and hydrodynamic diameter. And meanwhile, considering that the CH/GB-stabilized emulsions were prepared using high intensity ultrasonic (HIU) homogenization, the effect of HIU on the CH/GB particle size was also examined. As shown in Figure 6.2A, increasing storage time up to 5 days significantly changes the turbidity curves plotted against pH: in the opposite charge range, turbidity indexes steadily increase with time and the maximum is located at pH 5.5, which is in accordance with visual observations shown in Figure 6.9

(Supporting information). It implies that the size of CH/GB complexes is increasing with time and CH/GB complexes evolve from soluble to insoluble. Figure 6.2B shows the CLSM image of CH/GB insoluble complexes at pH 5.5 and 3 days of age, where green particles represent CH/GB complexes. It can be observed that CH/GB complex particles with size less than 1 μm coexist with their flocs, and it is believed that the growth of these flocs might be the main reason for the turbidity increase. The measurement of the hydrodynamic diameter clearly maps out the evolution of CH/GB complexes as functions of pH, time and HIU treatment (Figure 6.2C). For freshly prepared CH/GB mixtures, an increase of pH from 3.5 to 6.5 results in an increase of hydrodynamic diameter (volume average diameter, d_v increases from 6.2 to 212.1 μm), indicating the formation of CH/GB complexes at higher pH (e.g., pH 5.5 and 6.5). After 3 days of storage, no significant change is observed for pH 3.5 and 4.5, but a remarkable increase of the hydrodynamic diameter can be seen for pH 5.5 and 6.5 from Figure 6.2C, e.g., d_v increases from 33.9 to 459.3 μm for pH 5.5, suggesting the growth of CH/GB flocculates with time. Interestingly, after treating the insoluble CH/GB complexes formed at pH 5.5 and 6.5 (3 days of age) with HIU, d_v decreases significantly, e.g., it drops from 459.3 and 877.2 to 39.5 and 60.8 nm for pH 5.5 and 6.5, respectively, after 8 min of HIU treatment. The hydrodynamic diameter data agrees well with the visual observation of HIU-treated CH/GB complexes, which becomes transparent after HIU treatment (Figure 6.10, Supporting information). Then, the driving force for the flocculation of CH/GB complexes needs to be clarified. Based on the analysis of Figure 6.1, it is already known that CH/GB complex particles are colloidal, with a ζ potential lower than 20 mV. Generally, a ζ potential larger than 30 mV is necessary for a stable electrostatic stabilized dispersion, otherwise, flocculation may take place. The origin for particles flocculation was summarized from a theoretical point of view in a recent work, which describes that same-charge complex particles tend to interact with each other to form larger secondary particles, once short-range attractions (e.g., van der Waals, hydrophobic effect) overcome long-range electrostatic repulsion.²⁸

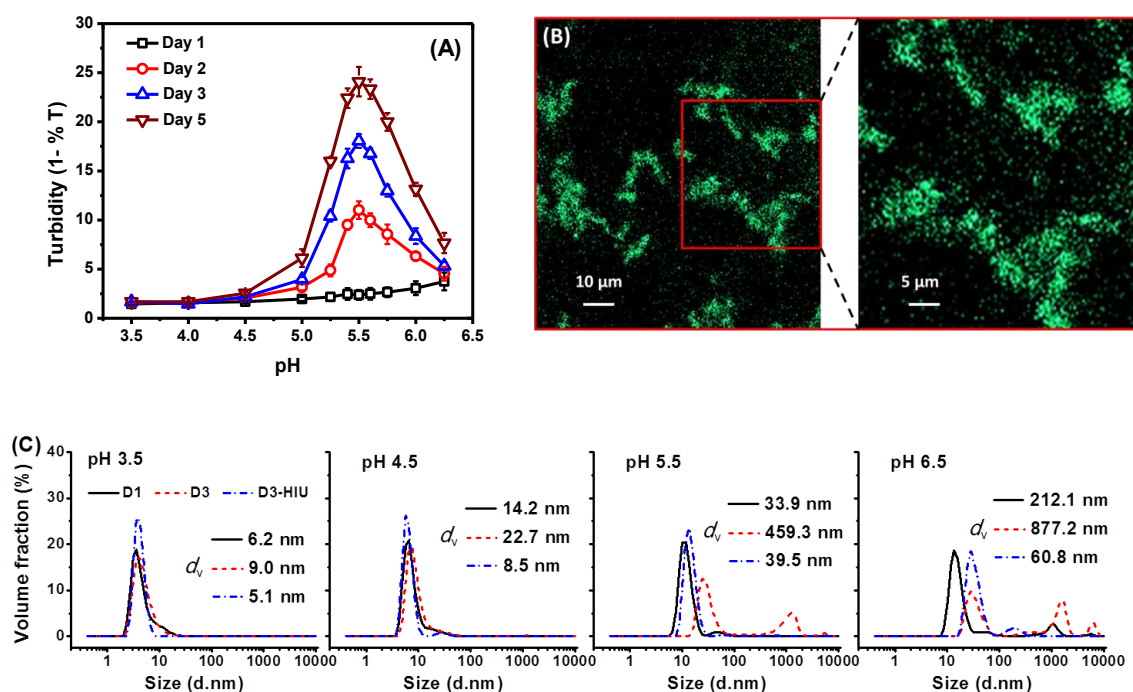


Figure 6.2: (A) Time evolution of turbidity for CH/GB mixtures (1 wt %, CH:GB = 1:2) as a function of pH; (B) CLSM images of CH/GB complexes (1 wt %, CH:GB = 1:2, pH 5.5, 3 days of age); (C) hydrodynamic diameter of CH/GB complexes as functions of pH, storage time and HIU treatment. D1, D3 indicates freshly prepared CH/GB complexes and CH/GB with three days of age, and D3-HIU means CH/GB complexes stored for 3 days and then treated with HIU for 8 min.

Interfacial Adsorption Behavior of Insoluble CH/GB Complexes. The interfacial adsorption kinetics of insoluble CH/GB complexes (3 days of age) was characterized, and the role of pH (3.5 to 5.5) was examined in the formation dynamics of the films at the oil/water interface. Surface pressure (π) is plotted against $t^{1/2}$ (up to 2.5 h) in Figure 6.3, and in the initial diffusion-controlled adsorption process, the slope of the plot represents the diffusion rate constant (k_{diff}). The values of k_{diff} and π at the beginning (0 s; π_0) and end (9000 s; π_{9000}) of adsorption are summarized in Table 6.1. All the curves show an increase in surface pressure (π), especially in the first 400 s, however, there is a significant difference between the testing pH values: the higher the pH, the higher the π value, indicating better surface activities. At pH 3.5, the suspension is made of soluble mixed biopolymers, since there is almost no interaction between CH and GB.

Thus, CH and GB molecules tend to absorb independently on the oil/water interface. Compared to the π value of CH alone at a comparable time,³¹ π is higher because of the presence of GB molecules. At pH 4.5, based on the analysis of zeta potential results, soluble complexes of CH and GB are formed, and as a consequence, they absorb on the oil/water interface and thus decrease the interfacial tension. As pH increases to 5.5, the adsorption of insoluble CH/GB complexes greatly increases the π value as compared to CH at the same pH (e.g., at the end of the adsorption test, π is only 5.95 mN·m⁻¹ for CH alone,³¹ while it rises to 9.06 mN·m⁻¹ for CH/GB complexes in this work). It indicates that the complexation of CH and GB results in CH/GB particles with higher surface activities, due to the combination of functional groups in CH and GB. By comparing k_{diff} , π_0 and π_{9000} in Table 6.1, the improvement of surface activities induced by increasing pH can be seen quantitatively: e.g., pH increasing from 3.5 to 5.5 makes k_{diff} increase from 0.16 to 0.26 mN·m⁻¹·s^{-0.5}, which implies a faster adsorption of molecules or colloidal particles at the oil/water interface; both π_0 and π_{9000} increased from 0.22 to 2.03 mN·m⁻¹, and from 3.99 to 9.06 mN·m⁻¹, respectively.

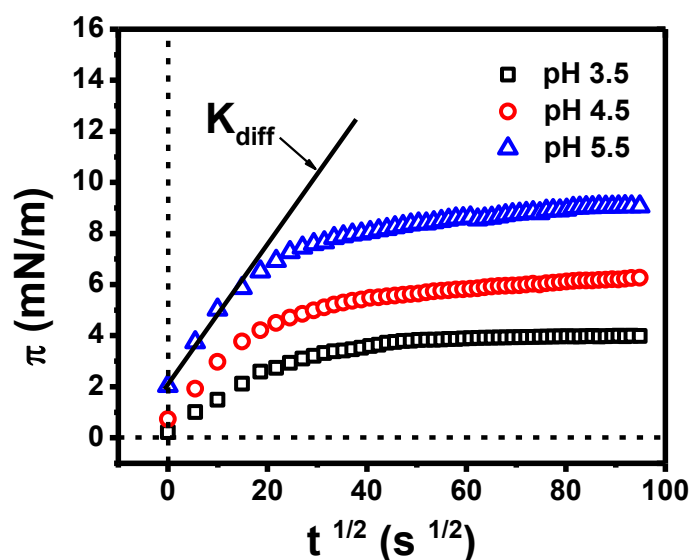


Figure 6.3: Time evolution of surface pressure for the adsorption of CH/GB complexes (1 wt %, CH:GB = 1:2, 3 days of age) at an oil/water interface for different pH values.

Table 6.1: Diffusion rate constants (k_{diff}) and surface pressure at the beginning (0 s; π_0) and end (9000 s; π_{9000}) of adsorption for CH/GB complexes (1 wt %, CH:GB = 1:2, 3 days of age) at an oil/water interface.

pH	k_{diff} ($\text{mN}\cdot\text{m}^{-1}\cdot\text{s}^{-0.5}$) (LR)	π_0 ($\text{mN}\cdot\text{m}^{-1}$)	π_{9000} ($\text{mN}\cdot\text{m}^{-1}$)
3.5	0.16 (0.997)	0.22	3.99
4.5	0.21 (0.995)	0.73	6.27
5.5	0.26 (0.984)	2.03	9.06

LR = linear regression coefficient (in parenthesis)

Emulsifying Capacity and Emulsion Stability. Figure 6.4A shows the optical microscopy images of fresh emulsions prepared with CH/GB mixtures at various pH values, and the volume- and number- average droplet sizes are summarized in Figure 6.4B. In accordance with the interfacial adsorption behavior shown in Figure 6.3, the emulsion capacity is totally different for CH/GB mixtures with different pH values: the formation of CH/GB complexes, either soluble (pH 4.5) or insoluble (pH 5.5 and 6.5), can benefit the formation of an emulsion with a better distribution; while at pH 3.5, the adsorption of CH and GB molecules also contributes to the formation of a fine emulsion droplet, but large aggregations can be observed, which directly leads to an unstable emulsion system. It has been shown in our previous work that the emulsifying properties of CH alone increases with pH,³¹ however, as indicated in Figure 6.11 (Supporting Information), the emulsifying properties of GB are higher at lower pH (e.g., pH 3.5 and 4.5). The reason for droplet aggregation at pH 3.5 is still unclear and more work would be required to clarify it. However, in this work we are more concerned about the evolution of emulsifying capacity from pH 4.5 and 6.5. By comparing the volume- and number- average diameter (d_v and d_n) as well as size distribution (d_v/d_n) of CH/GB-based emulsion droplets (Figure 6.4B), it can be concluded that the emulsion capacity of CH/GB complexes can be improved by increasing pH, since a smaller droplet size (d_v drops to $2.1\ \mu\text{m}$) and a better size distribution (d_v/d_n as low as 1.1) are obtained at the highest pH value. According to the ζ potential results displayed in Figure 6.1A, it is reasonable to conclude that CH/GB complexes can be more compact as pH increases,

due to the conformational contraction of the CH molecules. And it will be easier for CH/GB complexes with more compact structure to adsorb at the oil/water interface because of lower steric hindrance, and also to form a firmer coating layer around oil droplets. In addition, a slight flocculation can be observed at pH 6.5, which is probably due to the lower ζ potential value (11.2 mV) at this pH, at which the emulsion droplets tend to interact with each other because of the lower electrostatic repulsion.

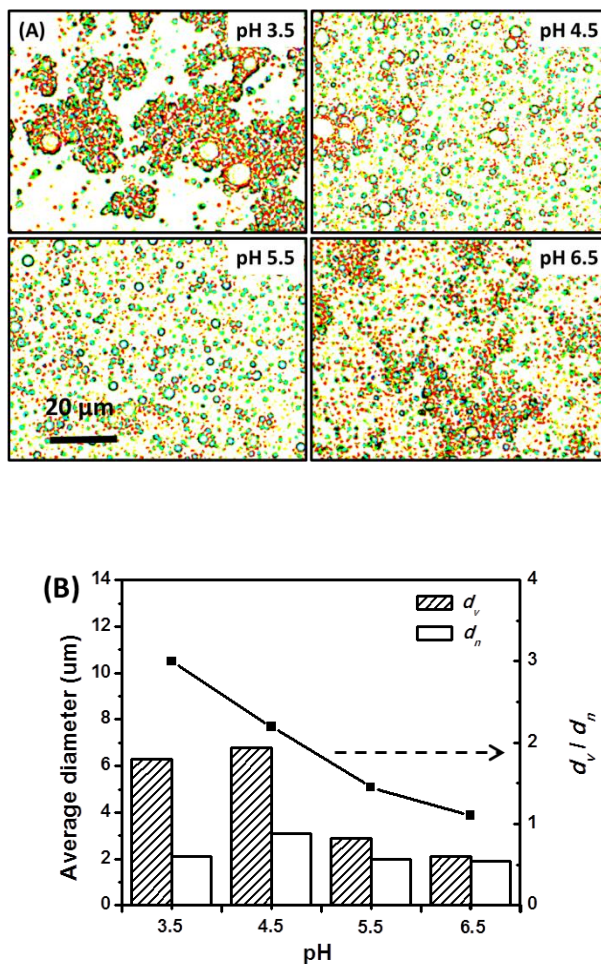


Figure 6.4: (A) Optical microscopy images of fresh emulsions prepared with CH/GB mixtures at different pH values (3.5-6.5). (B) Volume- and number-average diameter as well as size distribution of fresh CH/GB-based emulsion droplets. The concentration of CH/GB mixtures is 1 wt %, and the oil volume fraction is 0.1.

The freshly prepared CH/GB-based emulsions were kept at room temperature for one year and the stability was determined by visual observation of creaming and calculation of creaming

index (CI), which reveals information about the extent of droplet agglomeration or coalescence in an emulsion.³² Figure 6.5A shows photographs of CH/GB-based O/W emulsion vials at different pH and storage time, and the calculated CI as function of time is summarized in Figure 6.5B. As indicated from optical microscopy, the emulsion prepared with CH/GB mixture at pH 3.5 is extremely unstable, and there is a large amount of serum layer even for the fresh one; while for the other three pH values, the emulsions are homogeneous at least within the first 10 days. Then, with an increase of storage time up to 20 days, the CI gradually increases to 62% for the CH/GB emulsion prepared at pH 4.5; and after one month, CI for pH 5.5 and 6.5 rises to 7% and 3%, respectively. Afterwards the CI was continuously recorded for up to 5 months but there was no further increase. Moreover, based on visual observations, there was no obvious change for all the pH values except that the surface of the emulsion turned to be yellowish after 8 months (data not shown), which might be due to the oxidation of the oil. Compared to CH-based emulsions³¹ and GB-based emulsions (Figure 6.12, Supporting Information), the pH-induced evolution of CI for CH/GB-stabilized emulsions is similar with that of CH, but the value of CI at a comparable pH is lower than CH-stabilized emulsions, especially at higher pH (e.g., at pH 5.5, the highest CI for CH/GB emulsions is just 7% in this work but it goes up to 60% for CH emulsions).³¹ It suggests that the bonding of GB with CH molecules confers a higher surface activity to the CH/GB complexes and also a denser structure, thus favoring the formation of a stronger protecting layer around oil droplets and consequently a stable emulsion. Another point to note is that the long-term stability of the emulsion prepared at pH 6.5 is better than that at pH 5.5, possibly because of the denser structure of CH/GB at pH 6.5, as mentioned in the section on zeta potential. In Figure 6.5A, the vials of emulsions prepared at different pH values and with 2 months of age are also displayed in a bottom-up position. It is interesting to point out that a gel-like emulsion is formed at pH 5.5 and 6.5 with an increase of storage time. Normally, emulsion droplets tend to flocculate as attractive forces are larger than repulsion forces between droplets, and as a consequence, the gelation of emulsion droplets may occur once the flocculation rate is higher than the creaming rate in the system.³³ In our previous work, it had been shown that CH/GB complex particles (formed at pH 5.5) tend to form a network structure after storage at room temperature for 20 days, and the elasticity of CH/GB gel continues to increase with time.¹³ Once these particles adsorb on the surface of oil droplets, they can benefit the formation of a network structure via particle-particle interactions combined to droplet-droplet contacts, thus resulting in a uniform

emulsion gel. Furthermore, the formation of a gel-like structure among emulsion droplets can impart remarkable stability against coalescence and creaming of the emulsions. At last, it should be noted that the homogenization technique (HIU) used in this work is also an effective way to break insoluble CH/GB complexes into nanoscale particles (Figure 6.2C), which can facilitate the adsorption of CH/GB particles at the oil/water interface.

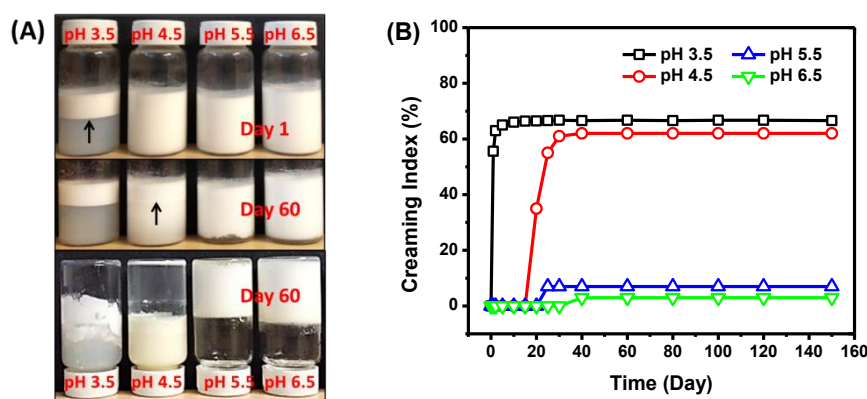


Figure 6.5: (A) Photographs of vials and (B) creaming index of emulsions prepared with CH/GB mixtures at different pH (3.5 to 6.5) and storage time (up to 5 months), with an oil volume fraction of 0.1.

Rheological Properties of Emulsions Stabilized with CH/GB Complexes. Depending on oil volume fraction (ϕ), the rheological properties of emulsions generally vary from Newtonian for non-flocculated and dilute emulsions, to shear-thinning for concentrated and highly flocculated emulsions. To further examine the effect of oil volume fraction and pH on the microstructural properties of CH/GB emulsions, the rheological properties were investigated. As shown in Figure 6.6, the moduli (storage modulus G' and loss modulus G'') of CH/GB emulsions greatly depend on pH and oil volume fraction. Specifically, for all pH values, an increase of ϕ leads to an increase of both G' and G'' , and G' is higher than G'' when ϕ reaches 0.4. As demonstrated in Knudsen's work, the possible reason should be attributed to the droplet packing effect, namely, the oil droplets are close enough to interact with others in concentrated emulsions, and consequently, a network structure may build up among oil droplets.³⁴ At a comparable ϕ , an increase of pH from 3.5 to 6.5 significantly increases the modulus, indicating a stronger inter-droplet interaction at higher pH, which is consistent with optical microscopy observations (Figure 6.4A). Interestingly, at pH 5.5 and 6.5, with the increase of ϕ , G' turns to be higher than G'' for

the whole test frequency range, implying the existence of an elastic gel-like emulsion. The difference in the moduli dependence on ϕ between low pH (pH 4.5) and high pH (pH 5.5 and 6.5) emulsions is mainly due to the difference in CH/GB particle interactions in the system. As shown in Figure 6.2C, where the hydrodynamic diameter of CH/GB complexes is affected by pH and storage time, the pH-dependent particle-particle interactions is well illustrated. It is clear that the CH/GB particles formed at higher pH values have stronger attractive interactions than the lower pH ones, thus leading to more agglomerated particles, as supported by the data of hydrodynamic diameter. For CH/GB complexes formed at pH 5.5 and 6.5 the hydrodynamic diameter increases significantly with time (e.g., from 33.89 to 459.25 nm for pH 5.5), while it just changes slightly for pH 4.5 (from 14.18 to 22.74 nm). Therefore, stronger inter-droplet interactions can be the result of CH/GB inter-particle interactions, especially when the CH/GB particles with higher attractive interactions are used to stabilize oil droplets.

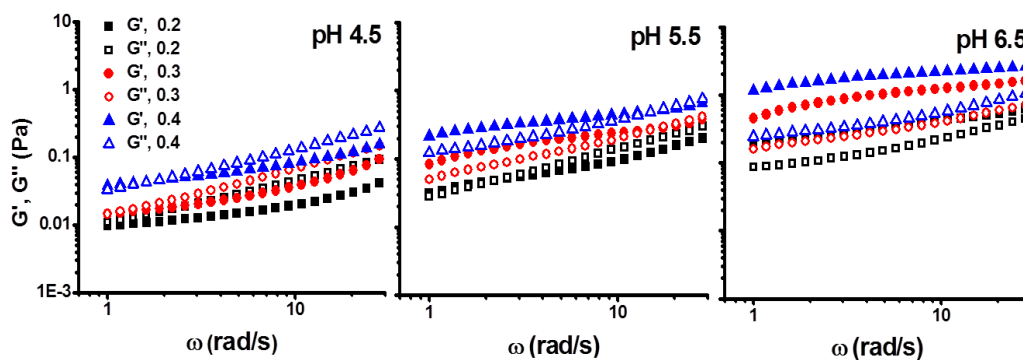


Figure 6.6: Moduli (G' and G'') of fresh emulsions prepared with CH/GB complexes at different pHs (4.5 to 6.5) and oil volume fractions (0.2 to 0.4).

It has been reported that a relatively small temperature change can affect non-covalent interactions. Specifically, the bonding formed with the release of heat, like ionic bonding, hydrogen bonding and van der Waals forces, can be weakened by increasing temperature, while hydrophobic interactions which are accompanied by heat absorption can be facilitated upon increasing temperature.³⁵ Aiming to further identify the driving force for the formation of the droplet network structure, three successive heating and cooling cycles were carried out for CH/GB emulsions at pH 5.5 and 6.5 ($\phi = 0.4$). At pH 5.5, as shown in Figure 6.7A, an increase of temperature from 25 to 60 °C in the first cycle decreases both G' and G'' , but the three-dimensional network formed by the flocculated droplets is still maintained. Then, a decrease of

temperature from 60 to 5 °C continuously increases both G' and G'' , and the increase rate of G' is larger than for G'' , which indicates that a stronger network structure dominated by hydrogen bonding is formed at lower temperature. In the second and third heating and cooling cycles, a quite similar rheological behavior can be observed. Interestingly, at pH 6.5 (Figure 6.7B), the rheological response to temperature is different with that at pH 5.5. In the first temperature sweep cycle, the heating process increases both G' and G'' , while the cooling process shows a negligible effect on modulus. In the second and third cycles, the curves are almost the same. By comparing Figure 6.7A and Figure 6.7B, it can be concluded that the emulsion gel formed at pH 5.5 and 6.5 are both thermoreversible within the test temperature range. However their different responses to temperature suggest that hydrophobic interactions contribute more in the formation of the emulsion gel in the case of pH 6.5, which could be attributed to the differences in the structural properties of CH/GB particles formed at pH 5.5 and 6.5, respectively.

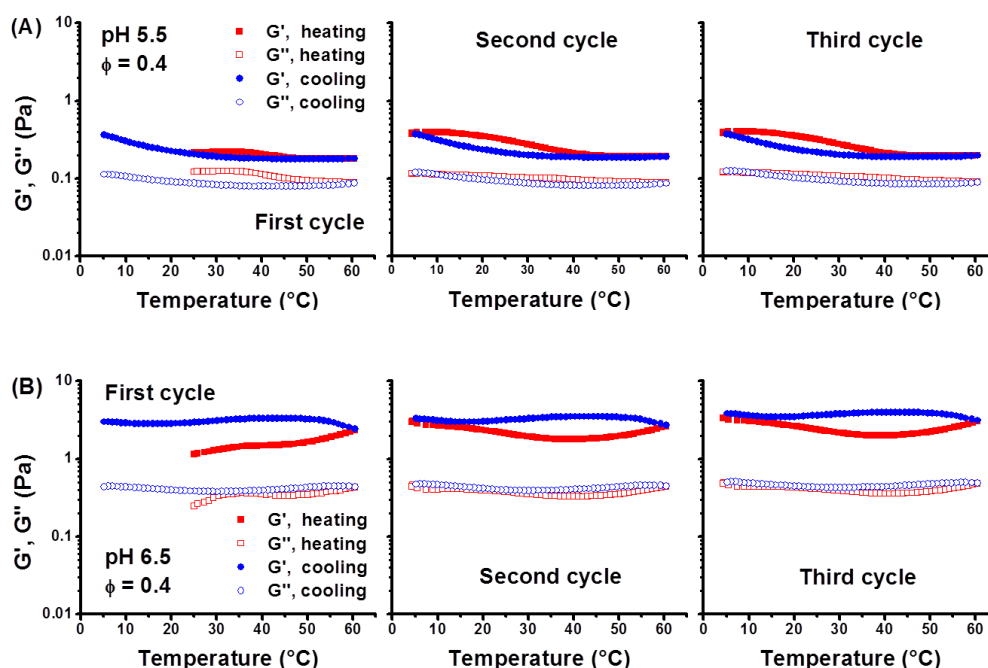


Figure 6.7: Temperature sweep (three cycles) of fresh CH/GB-based emulsions prepared at pH 5.5 (A) and 6.5 (B), at an oil volume fraction (ϕ) of 0.4.

Figure 6.8 presents the schematic mechanism of the formation of CH/GB-based Pickering emulsions at pH values of 5.5 and 6.5, which can be used to illustrate the difference in the corresponding emulsions. The insoluble CH/GB complexes formed at pH 5.5 and 6.5 are both able to form a protective coating layer around oil droplet, and thus form a Pickering emulsion

with considerable long-term stability. However, the pH-induced difference in the properties of CH/GB particles (e.g., charge density and conformational structure) directly determines the emulsification and stabilization performance. First, the lower charge density of CH/GB complexes prepared at pH 6.5 (ζ potential is 16.4 and 11.2 mV for pH 5.5 and 6.5, respectively) gives the CH/GB particles more opportunity to interact with each other, therefore, the emulsion stabilized with CH/GB particles at pH 6.5 shows more droplet flocculation (Figure 6.4A). Furthermore, the higher extent of droplet flocculation can somehow facilitate the formation of the gel-like structure within the emulsions and greatly improve the long-term stability. Furthermore, with respect to conformational structure, CH is more extended at pH 5.5, and thus the structure of CH/GB particle is looser than that of pH 6.5, where the structure of CH/GB particle is denser because CH chains tend to contract and agglomerate to form a more compact particle. When these compact particles adsorb on the surface of oil droplets, they provide a stronger protection against coalescence and creaming, and this is another important reason why emulsions prepared at pH 6.5 have better long-term stability.

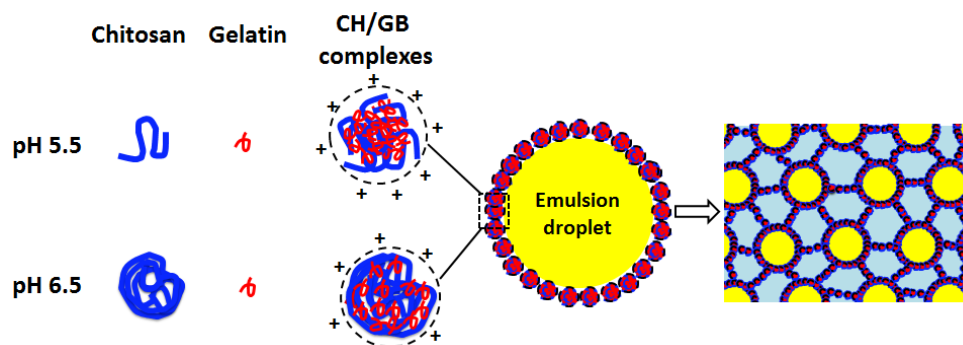


Figure 6.8: The formation of Pickering emulsion gels stabilized with CH/GB insoluble complexes.

6.5 Conclusion

In this study, the effects of pH and storage time on the properties of CH/GB complexes, including charge density, hydrodynamic size, microstructure and interfacial tension were investigated. The emulsification and stabilization properties of the CH/GB complex particles were also examined in oil/water systems. It was found that the formation and properties of CH/GB complexes greatly depend on pH and storage time: insoluble CH/GB complexes were only formed in the oppositely charged pH range ($5 < \text{pH} < 6.5$), and the size of insoluble CH/GB

particles increased with time. The emulsions stabilized with insoluble CH/GB complexes showed a smaller droplet size and a better long-term stability when compared soluble complexes, due to the stronger protecting barrier at the oil/water interface. For CH/GB complexes prepared at pH 5.5 and 6.5, the difference in charge density and conformational structure also resulted in corresponding emulsions with different creaming rates, and flocculation and gelling properties. Our results suggest that CH/GB insoluble complexes can be used as effective pH-controlled Pickering emulsifiers and stabilizers, for the production of surfactant-free and bio-based O/W emulsions for food and non-food applications. This work might also inspire further developments in exploiting biocompatible Pickering emulsifiers based on the electrostatic complexation of proteins and polysaccharides.

Acknowledgements

This research work has been funded by NSERC (Natural Sciences and Engineering Research Council of Canada). A scholarship for Ms. Wang provided by the China Scholarship Council (CSC) is also gratefully acknowledged.

Notes and References

- (1) Hunter, T. N.; Pugh, R. J.; Franks, G. V.; Jameson, G. J., The role of particles in stabilising foams and emulsions. *Advances in Colloid and Interface Science* **2008**, *137* (2), 57-81.
- (2) Chevalier, Y.; Bolzinger, M.-A., Emulsions stabilized with solid nanoparticles: Pickering emulsions. *Colloids and Surfaces a-Physicochemical and Engineering Aspects* **2013**, *439*, 23-34.
- (3) Dickinson, E., Food emulsions and foams: Stabilization by particles. *Current Opinion in Colloid & Interface Science* **2010**, *15* (1-2), 40-49.
- (4) Zhu, Y.; Jiang, J.; Liu, K.; Cui, Z.; Binks, B. P., Switchable Pickering Emulsions Stabilized by Silica Nanoparticles Hydrophobized in Situ with a Conventional Cationic Surfactant. *Langmuir* **2015**, *31* (11), 3301-3307.
- (5) Melle, S.; Lask, M.; Fuller, G. G., Pickering emulsions with controllable stability. *Langmuir* **2005**, *21* (6), 2158-2162.

- (6) Binks, B. P.; Clint, J. H., Solid wettability from surface energy components: Relevance to pickering emulsions. *Langmuir* **2002**, *18* (4), 1270-1273.
- (7) Tzoumaki, M. V.; Moschakis, T.; Kiosseoglou, V.; Biliaderis, C. G., Oil-in-water emulsions stabilized by chitin nanocrystal particles. *Food Hydrocolloids* **2011**, *25* (6), 1521-1529.
- (8) Yusoff, A.; Murray, B. S., Modified starch granules as particle-stabilizers of oil-in-water emulsions. *Food Hydrocolloids* **2011**, *25* (1), 42-55.
- (9) Kalashnikova, I.; Bizot, H.; Cathala, B.; Capron, I., New Pickering Emulsions Stabilized by Bacterial Cellulose Nanocrystals. *Langmuir* **2011**, *27* (12), 7471-7479.
- (10) de Folter, J. W. J.; van Ruijven, M. W. M.; Velikov, K. P., Oil-in-water Pickering emulsions stabilized by colloidal particles from the water-insoluble protein zein. *Soft Matter* **2012**, *8* (25), 6807-6815.
- (11) Rinaudo, M., Chitin and chitosan: Properties and applications. *Progress in Polymer Science* **2006**, *31* (7), 603-632.
- (12) Karim, A. A.; Bhat, R., Fish gelatin: properties, challenges, and prospects as an alternative to mammalian gelatins. *Food Hydrocolloids* **2009**, *23* (3), 563-576.
- (13) Wang, X.-Y.; Wang, C.-S.; Heuzey, M.-C., Complexation of chitosan and gelatin: From soluble complexes to colloidal gel. *International Journal of Polymeric Materials and Polymeric Biomaterials* **2016**, *65* (2), 96-104.
- (14) Turgeon, S. L.; Beaulieu, M.; Schmitt, C.; Sanchez, C., Protein-polysaccharide interactions: phase-ordering kinetics, thermodynamic and structural aspects. *Current Opinion in Colloid & Interface Science* **2003**, *8* (4-5), 401-414.
- (15) Turgeon, S. L.; Schmitt, C.; Sanchez, C., Protein-polysaccharide complexes and coacervates. *Current Opinion in Colloid & Interface Science* **2007**, *12* (4-5), 166-178.
- (16) Cooper, C. L.; Dubin, P. L.; Kayitmazer, A. B.; Turksen, S., Polyelectrolyte-protein complexes. *Current Opinion in Colloid & Interface Science* **2005**, *10* (1-2), 52-78.

- (17) Fioramonti, S. A.; Perez, A. A.; Elena Aringoli, E.; Rubiolo, A. C.; Santiago, L. G., Design and characterization of soluble biopolymer complexes produced by electrostatic self-assembly of a whey protein isolate and sodium alginate. *Food Hydrocolloids* **2014**, *35*, 129-136.
- (18) Rocha, C. M. R.; Souza, H. K. S.; Magalhaes, N. F.; Andrade, C. T.; Goncalves, M. P., Rheological and structural characterization of agar/whey proteins insoluble complexes. *Carbohydrate Polymers* **2014**, *110*, 345-353.
- (19) Ding, X.; Yao, P., Soy Protein/Soy Polysaccharide Complex Nanogels: Folic Acid Loading, Protection, and Controlled Delivery. *Langmuir* **2013**, *29* (27), 8636-8644.
- (20) de Kruif, C. G.; Weinbreck, F.; de Vries, R., Complex coacervation of proteins and anionic polysaccharides. *Current Opinion in Colloid & Interface Science* **2004**, *9* (5), 340-349.
- (21) Evans, M.; Ratcliffe, I.; Williams, P. A., Emulsion stabilisation using polysaccharide-protein complexes. *Current Opinion in Colloid & Interface Science* **2013**, *18* (4), 272-282.
- (22) Benichou, A.; Aserin, A.; Garti, N., Protein-polysaccharide interactions for stabilization of food emulsions. *Journal of Dispersion Science and Technology* **2002**, *23* (1-3), 93-123.
- (23) Dickinson, E., Interfacial structure and stability of food emulsions as affected by protein-polysaccharide interactions. *Soft Matter* **2008**, *4* (5), 932-942.
- (24) Yin, B.; Deng, W.; Xu, K.; Huang, L.; Yao, P., Stable nano-sized emulsions produced from soy protein and soy polysaccharide complexes. *Journal of Colloid and Interface Science* **2012**, *380*, 51-59.
- (25) Ogawa, S.; Decker, E. A.; McClements, D. J., Production and characterization of O/W emulsions containing cationic droplets stabilized by lecithin-chitosan membranes. *J. Agric. Food. Chem.* **2003**, *51* (9), 2806-2812.
- (26) Jumaa, M.; Furkert, F. H.; Muller, B. W., A new lipid emulsion formulation with high antimicrobial efficacy using chitosan. *European Journal of Pharmaceutics and Biopharmaceutics* **2002**, *53* (1), 115-123.
- (27) Sanchez, C.; Mekhloufi, G.; Schmitt, C.; Renard, D.; Robert, P.; Lehr, C. M.; Lamprecht, A.; Hardy, J., Self-assembly of beta-lactoglobulin and acacia gum in aqueous solvent: Structure and phase-ordering kinetics. *Langmuir* **2002**, *18* (26), 10323-10333.

- (28) Zhang, Y.; Yildirim, E.; Antila, H. S.; Valenzuela, L. D.; Sammalkorpi, M.; Lutkenhaus, J. L., The influence of ionic strength and mixing ratio on the colloidal stability of PDAC/PSS polyelectrolyte complexes. *Soft Matter* **2015**, *11* (37), 7392-7401.
- (29) Dautzenberg, H.; Karibyants, N., Polyelectrolyte complex formation in highly aggregating systems. Effect of salt: response to subsequent addition of NaCl. *Macromolecular Chemistry and Physics* **1999**, *200* (1), 118-125.
- (30) Colombo, E.; Cavalieri, F.; Ashokkumar, M., Role of Counterions in Controlling the Properties of Ultrasonically Generated Chitosan-Stabilized Oil-in-Water Emulsions. *Acs Applied Materials & Interfaces* **2015**, *7* (23), 12972-12980.
- (31) Wang, X.-Y.; Heuzey, M.-C., Chitosan-Based Conventional and Pickering Emulsions with Long-Term Stability. *Langmuir* **2016**.
- (32) Keowmaneechai, E.; McClements, D. J., Influence of EDTA and citrate on physicochemical properties of whey protein-stabilized oil-in-water emulsions containing CaCl₂. *Journal of Agricultural and Food Chemistry* **2002**, *50* (24), 7145-7153.
- (33) van Aken, G. A.; Blijdenstein, T. B. J.; Hotrum, N. E., Colloidal destabilisation mechanisms in protein-stabilised emulsions. *Current Opinion in Colloid & Interface Science* **2003**, *8* (4-5), 371-379.
- (34) Knudsen, J. C.; Ogendal, L. H.; Skibsted, L. H., Droplet surface properties and rheology of concentrated oil in water emulsions stabilized by heat-modified beta-lactoglobulin B. *Langmuir* **2008**, *24* (6), 2603-2610.
- (35) Cho, J. Y.; Heuzey, M. C.; Begin, A.; Carreau, P. J., Physical gelation of chitosan in the presence of beta-glycerophosphate: The effect of temperature. *Biomacromolecules* **2005**, *6* (6), 3267-3275.

6.6 Supporting information

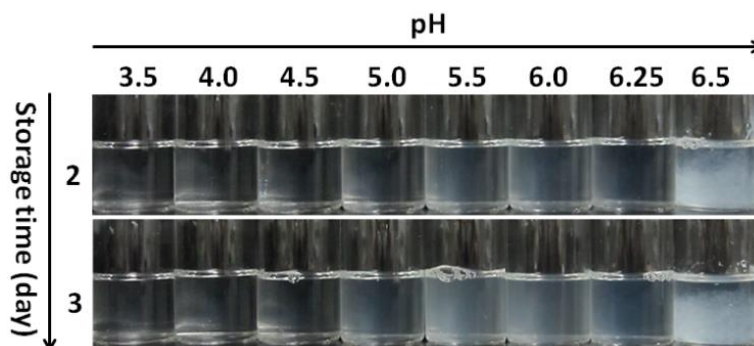


Figure 6.9: Visual observation of CH/GB complexes (1 wt %, CH:GB = 1:2) at various pH values (3.5 to 6.5) and storage times (day 2 and day 3). All the samples are transparent on day 1 except for pH 6.5.

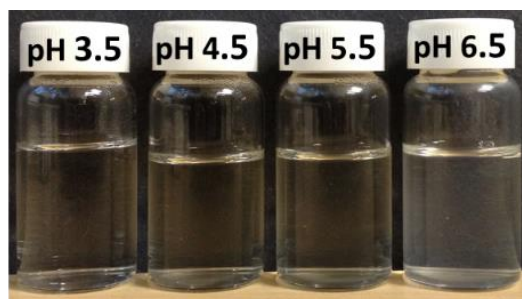


Figure 6.10: Visual observation of high intensity ultrasonication-treated CH/GB complexes (1 wt %, CH:GB = 1:2, storage time: 3 days) at various pH values (3.5 to 6.5).

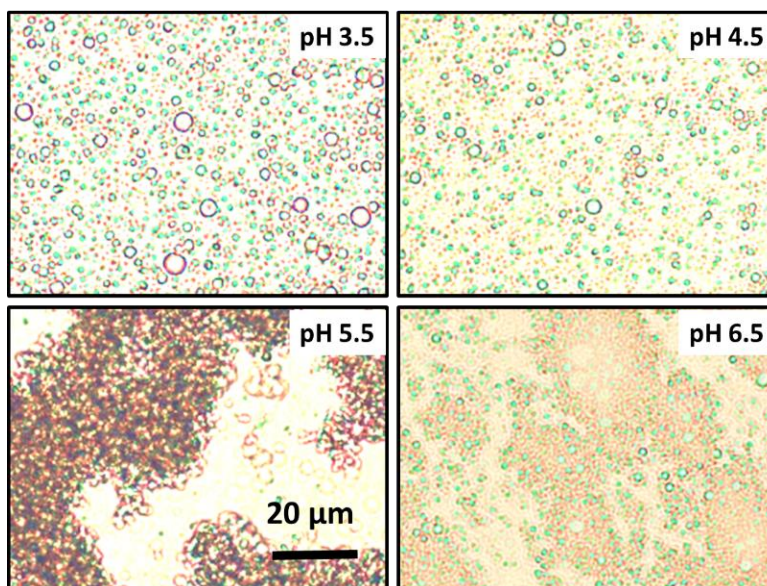


Figure 6.11: Optical microscopy images of fresh emulsions prepared with GB at different pH values (3.5-6.5).

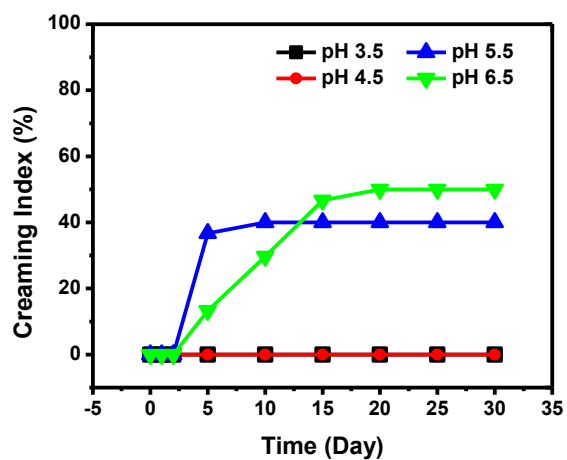


Figure 6.12: Creaming index of GB-based emulsions (oil volume fraction = 0.1) prepared at different pH (3.5 to 6.5) and storage time (up to 1 month).

CHAPTER 7 GENERAL DISCUSSION

Using biopolymers from natural resources to stabilize emulsions is an interesting topic from both a theoretical and practical point of view. In this work, chitosan and chitosan/gelatin complexes were used to prepare both conventional and Pickering emulsions. Based on the literature review, chitosan itself is not a satisfactory emulsifier compared to the commonly used polymeric emulsifiers such as proteins and adsorbing polysaccharides. Even though, according to the literature, the emulsifying properties can be increased by altering the pH of chitosan solutions, and a pH-responsive Pickering emulsion can even be formed as pH reaches the pK_a of chitosan, the droplet size, distribution as well as the long-term stability are still not as good as expected, and thus need to be improved as undertaken in the current work.

In this work, the use of high intensity ultrasonic (HIU) homogenization greatly decreased the droplet size and increased the long-term stability of emulsions stabilized by chitosan. During the emulsification process, the dual effect of HIU, namely, the decrease of chitosan molecular weight and the disassembly of chitosan agglomerates were found to be beneficial factors for the improvement of emulsion stability. Besides, the role of pH on the emulsifying properties of chitosan complexes was investigated comprehensively, which helps to draw a clearer map of the pH-controlled emulsifying properties of chitosan. In addition to pH value, other parameters such as DDA and Mw of chitosan, ionic strength and polymer concentration may also affect emulsifying properties, and thus should be examined in the future.

The electrostatic combination of gelatin molecules on chitosan chains made the corresponding complexes more surface-active than chitosan alone and effectively increased the emulsion's long-term stability. Gelatin type B was used to form complexes with chitosan because of its suitable pI which enables the formation of complexes, its specific linear structure and thermoreversible gelling properties. Besides, similar to chitosan, gelatin is also an abundant bio-based polymer and its relatively low price as compared to most of globular proteins is another reason why it could be of great potential for a large-scale industrial application. In this work, gelatin-B with bloom strength of only 75 was used to form complexes with chitosan; however, it could be interesting to explore the feasibility for other bloom strengths. During the complexation of chitosan and gelatin-B, fixed chitosan/gelatin ratio, polymer concentration and temperature were used, however, the complexation and temporal evolution of all the protein/polysaccharide

systems are very sensitive to these parameters, and thus need to be investigated further. Another issue that needs to be addressed in the future is the determination of stoichiometric ratios for chitosan and gelatin using isothermal titration calorimetry (ITC), which would be helpful for the quantitative analysis and understanding of chitosan/gelatin complexation.

The findings of this work provide valuable information. From a theoretical point of view, the investigations on the role of pH and ultrasonication on the emulsifying properties of chitosan have shed light on the relationships between chitosan molecular characteristics and its emulsifying properties, as well as the evolution of chitosan molecular structure during the emulsifying process. The research on the temporal complexation of chitosan and gelatin may also give some insights on the time-induced structural evolution of other protein/polysaccharide complex systems. Meanwhile, it also opens new perspectives for the use of other pH-controlled natural polymers in emulsion systems. From a practical point of view, the long-term stable emulsions stabilized using chitosan and its complexes with gelatin has revealed good candidates as green pH-controlled emulsifiers and stabilizers, and may find applications in the production of biodegradable and surfactant-free O/W emulsions in food and non-food applications with reasonable price.

During the performance of this project, several challenges had to be overcome. The first one was about pH adjustment. Chitosan is very sensitive to the addition of sodium hydroxide that is commonly used to adjust the pH value. Sodium hydroxide solution should be added in the chitosan solution drop by drop, at a very slow speed, otherwise there were some large aggregates appearing. In addition, the dilution effect caused by the addition of sodium hydroxide solution should also be considered, and to minimize the dilution effect, sodium hydroxide solution with different concentrations should be prepared. For example, in this work, sodium hydroxide solutions from 0.5 to 5 M were prepared and the higher concentration was used first to minimize the dilution effect.

Several techniques were used in this work for morphology observations, and the selection of a suitable technique turned to be of key importance for the achievement of reliable results. For example, SEM was first used to observe the pH-induced transition of chitosan molecular aggregation as well as the morphology of chitosan/gelatin complexes; however, the results were not as good as expected because of the dehydration effect. Compared to SEM, cryo-SEM would

be a better choice since the observation may be done in the liquid state. However, considering that there was no such equipment available to us, AFM was used instead to observe the molecular transition of chitosan induced by pH. Fortunately, except for aggregations, we could even see how the molecular chains of chitosan were affected by pH, which provided us with a visualized proof for the explanation of the pH-induced changes on chitosan's conformation and emulsifying properties. During the AFM observations, the concentration of chitosan solution should be well controlled, a higher concentration led to the overlap of chitosan chains, while a lower concentration also made the observation difficult. To better observe the morphology of chitosan/gelatin complexes, CLSM was finally used and better results were obtained. By covalently bonding a fluorescent dye on gelatin molecules, the agglomeration of primary complex particles could be observed clearly. Regarding the observation of emulsion droplet morphology, there are two commonly used techniques, namely, CLSM and optical microscopy. Although CLSM is able to provide images with better quality, the need for the addition of a fluorescent dye makes it less practical compared to optical microscopy, which is also a more cost-effective option. When using an optical microscope to perform the observation, the sample preparation greatly determines the image quality, thus should be paid extra attention. Only a tiny drop of emulsion was needed for the observation using optical microscopy, otherwise there were overlaps of emulsion droplets, which made the observation difficult.

At last, a special attention should be put on the emulsification process. It is well known that the usage of high intensity ultrasonication can increase the solution's temperature and thus may affect the properties of the materials. Therefore, an ice-bath is a necessary setup during the homogenization, which will help to control temperature and avoid overheating.

Despite the challenges met in this study, important information has been unveiled on the interactions between the only bio-sourced cationic polysaccharide, chitosan, with a linear protein gelatin, and it may open new perspectives for the use of these biopolymers in food and non-food emulsion systems.

CHAPTER 8 CONCLUSION AND RECOMMENDATIONS

8.1 Conclusion

In this thesis, long-term stable oil/water emulsions were developed using chitosan alone or chitosan/gelatin electrostatic complexes with the assistance of ultrasonication. The role of pH and ultrasonication on the emulsifying properties was investigated comprehensively. Our findings suggest that chitosan and CH/GB insoluble complexes have a great potential to be used as a pH-controlled emulsifier and stabilizer for the production of biodegradable and surfactant-free O/W emulsions in food and non-food applications. The following conclusions are drawn from this work:

Chitosan can form both conventional and Pickering emulsions with considerable long-term stability. PH value greatly influenced the emulsifying properties of chitosan since it affected its charge density and chain conformation. Increasing pH from 3.5 to 5.5 made the conformation of chitosan chains transferring from an extended state to a more flexible structure, and thus led to the formation of conventional emulsions with decreasing droplet size and increasing emulsion stability. As pH reached 6.5, the presence of chitosan nanoparticles resulted in a Pickering emulsion with the smallest droplet size ($d_v = 1.7 \mu\text{m}$) and longest stability (up to 5 months). The dual effects of high intensity ultrasonication (i.e., homogenization and depolymerisation) also contributed to the formation of stable chitosan-based emulsions.

The electrostatic complexation between chitosan and gelatin type B mainly happened in the pH region with opposite charge (pH 5-pH 6.5). Depending on pH and storage time, the complexes evolved from soluble to insoluble and finally to a colloidal gel. The addition of salt significantly affected the interactions between chitosan and gelatin, and thus influenced the size of complexes, the water content and the network structure of the corresponding gel. The insoluble CH/GB complexes and the corresponding colloidal gel developed in this work may find interesting uses in the scope of delivery of sensitive bioactive molecules or nutrients with tailored properties.

Compared to soluble complexes, the emulsions stabilized with insoluble CH/GB complexes showed a smaller droplet size and a better long-term stability due to the stronger protecting

barriers at the oil/water interface. The difference in charge density and conformational structure of complexes formed at pH 5.5 and 6.5 makes the corresponding emulsions also different in creaming rate, flocculation and gelling properties.

The main contribution of this work is the fundamental and practical information it provides on using chitosan and chitosan/gelatin complexes to fabricate long-term stable surfactant-free conventional and Pickering emulsions, resulting in more alternatives for the encapsulation of lipophilic nutrients.

8.2 Recommendations

The following aspects are recommended for further exploration in future work:

- 1) The effect of DDA and molecular weight of chitosan should be investigated for the formation of chitosan-based emulsions, which will help draw a clearer map on the emulsifying properties of chitosan.
- 2) The effect of parameters such as chitosan/gelatin ratio, polymer concentration and temperature on the complexation of chitosan and gelatin should also be examined.
- 3) The isothermal titration test should be performed again, using isothermal titration calorimetry (ITC) to detect the stoichiometric ratios of chitosan and gelatin, which will be greatly helpful for the understanding of chitosan/gelatin complexation.
- 4) The emulsification can be conducted using other homogenization techniques such as high shear mixers, high pressure homogenizers and membrane homogenizers, for comparison with ultrasonic homogenizers.
- 5) The emulsion stability as affected by environmental stresses such as pH, ionic strength and heating should be considered.
- 6) Lipophilic nutrients such as ω -3 fatty acids and oil-soluble vitamins can be added in the oil phase before emulsification, and the encapsulation efficiency should be examined.

BIBLIOGRAPHY

1. McClements, D.J. and Y. Li, *Structured emulsion-based delivery systems: Controlling the digestion and release of lipophilic food components*. Advances in Colloid and Interface Science, 2010. **159**(2): p. 213-228.
2. Dima, S., C. Dima, and G. Iordachescu, *Encapsulation of Functional Lipophilic Food and Drug Biocomponents*. Food Engineering Reviews, 2015. **7**(4): p. 417-438.
3. Augustin, M.A. and Y. Hemar, *Nano- and micro-structured assemblies for encapsulation of food ingredients*. Chemical Society Reviews, 2009. **38**(4): p. 902-912.
4. Gibbs, B.F., et al., *Encapsulation in the food industry: a review*. International Journal of Food Sciences and Nutrition, 1999. **50**(3): p. 213-224.
5. McClements, D.J., *Emulsion Design to Improve the Delivery of Functional Lipophilic Components*, in *Annual Review of Food Science and Technology, Vol 1*, M.P. Doyle and T.R. Klaenhammer, Editors. 2010. p. 241-269.
6. Kakran, M. and M.N. Antipina, *Emulsion-based techniques for encapsulation in biomedicine, food and personal care*. Current Opinion in Pharmacology, 2014. **18**: p. 47-55.
7. Matalanis, A., O.G. Jones, and D.J. McClements, *Structured biopolymer-based delivery systems for encapsulation, protection, and release of lipophilic compounds*. Food Hydrocolloids, 2011. **25**(8): p. 1865-1880.
8. Bouyer, E., et al., *Proteins, polysaccharides, and their complexes used as stabilizers for emulsions: Alternatives to synthetic surfactants in the pharmaceutical field?* International Journal of Pharmaceutics, 2012. **436**(1-2): p. 359-378.
9. Tolstoguzov, V.B., *Functional properties of food proteins and role of protein-polysaccharide interaction*. Food Hydrocolloids, 1991. **4**(6): p. 429-468.
10. Benichou, A., A. Aserin, and N. Garti, *Protein-polysaccharide interactions for stabilization of food emulsions*. Journal of Dispersion Science and Technology, 2002. **23**(1-3): p. 93-123.

11. Dickinson, E., *Interfacial structure and stability of food emulsions as affected by protein-polysaccharide interactions*. Soft Matter, 2008. **4**(5): p. 932-942.
12. Shchukina, E.M. and D.G. Shchukin, *LbL coated microcapsules for delivering lipid-based drugs*. Advanced Drug Delivery Reviews, 2011. **63**(9): p. 837-846.
13. Su, J.H., J. Flanagan, and H. Singh, *Improving encapsulation efficiency and stability of water-in-oil-in-water emulsions using a modified gum arabic (Acacia (sen) SUPER GUM (TM))*. Food Hydrocolloids, 2008. **22**(1): p. 112-120.
14. Taylor, T.M., et al., *Liposomal nanocapsules in food science and agriculture*. Critical Reviews in Food Science and Nutrition, 2005. **45**(7-8): p. 587-605.
15. Matos, M., et al., *Preparation and encapsulation properties of double Pickering emulsions stabilized by quinoa starch granules*. Colloids and Surfaces a-Physicochemical and Engineering Aspects, 2013. **423**: p. 147-153.
16. Wong, S.F., J.S. Lim, and S.S. Dol, *Crude oil emulsion: A review on formation, classification and stability of water-in-oil emulsions*. Journal of Petroleum Science and Engineering, 2015. **135**: p. 498-504.
17. He, L., et al., *Interfacial sciences in unconventional petroleum production: from fundamentals to applications*. Chemical Society Reviews, 2015. **44**(15): p. 5446-5494.
18. McClements, D.J. and J. Rao, *Food-Grade Nanoemulsions: Formulation, Fabrication, Properties, Performance, Biological Fate, and Potential Toxicity*. Critical Reviews in Food Science and Nutrition, 2011. **51**(4): p. 285-330.
19. McClements, D.J., *Nanoemulsions versus microemulsions: terminology, differences, and similarities*. Soft Matter, 2012. **8**(6): p. 1719-1729.
20. Fathi, M., M.R. Mozafari, and M. Mohebbi, *Nanoencapsulation of food ingredients using lipid based delivery systems*. Trends in Food Science & Technology, 2012. **23**(1): p. 13-27.
21. Solans, C., et al., *Nano-emulsions*. Current Opinion in Colloid & Interface Science, 2005. **10**(3-4): p. 102-110.

22. Tadros, T., *Principles of emulsion stabilization with special reference to polymeric surfactants*. Journal of Cosmetic Science, 2006. **57**(2): p. 153-169.
23. Sakai, T., *Surfactant-free emulsions*. Current Opinion in Colloid & Interface Science, 2008. **13**(4): p. 228-235.
24. Chevalier, Y. and M.-A. Bolzinger, *Emulsions stabilized with solid nanoparticles: Pickering emulsions*. Colloids and Surfaces A: Physicochemical and Engineering Aspects, 2013. **439**: p. 23-34.
25. Aveyard, R., B.P. Binks, and J.H. Clint, *Emulsions stabilised solely by colloidal particles*. Advances in Colloid and Interface Science, 2003. **100**: p. 503-546.
26. Binks, B.P., *Particles as surfactants - similarities and differences*. Current Opinion in Colloid & Interface Science, 2002. **7**(1-2): p. 21-41.
27. Schrade, A., K. Landfester, and U. Ziener, *Pickering-type stabilized nanoparticles by heterophase polymerization*. Chemical Society Reviews, 2013. **42**(16): p. 6823-6839.
28. Binks, B.P. and S.O. Lumsdon, *Influence of particle wettability on the type and stability of surfactant-free emulsions*. Langmuir, 2000. **16**(23): p. 8622-8631.
29. Tsabet, È. and L. Fradette, *Effect of Processing Parameters on the Production of Pickering Emulsions*. Industrial & Engineering Chemistry Research, 2015. **54**(7): p. 2227-2236.
30. Piorkowski, D.T. and D.J. McClements, *Beverage emulsions: Recent developments in formulation, production, and applications*. Food Hydrocolloids, 2014. **42**: p. 5-41.
31. McClements, D.J., E.A. Decker, and J. Weiss, *Emulsion-based delivery systems for lipophilic bioactive components*. Journal of Food Science, 2007. **72**(8): p. R109-R124.
32. Kralova, I. and J. Sjoblom, *Surfactants Used in Food Industry: A Review*. Journal of Dispersion Science and Technology, 2009. **30**(9): p. 1363-1383.
33. Dickinson, E., *Food emulsions and foams: Stabilization by particles*. Current Opinion in Colloid & Interface Science, 2010. **15**(1-2): p. 40-49.

34. Zhu, Y., et al., *Switchable Pickering Emulsions Stabilized by Silica Nanoparticles Hydrophobized in Situ with a Conventional Cationic Surfactant*. Langmuir, 2015. **31**(11): p. 3301-3307.
35. Melle, S., M. Lask, and G.G. Fuller, *Pickering emulsions with controllable stability*. Langmuir, 2005. **21**(6): p. 2158-2162.
36. Binks, B.P. and J.H. Clint, *Solid wettability from surface energy components: Relevance to pickering emulsions*. Langmuir, 2002. **18**(4): p. 1270-1273.
37. Tzoumaki, M.V., et al., *Oil-in-water emulsions stabilized by chitin nanocrystal particles*. Food Hydrocolloids, 2011. **25**(6): p. 1521-1529.
38. Yusoff, A. and B.S. Murray, *Modified starch granules as particle-stabilizers of oil-in-water emulsions*. Food Hydrocolloids, 2011. **25**(1): p. 42-55.
39. Kalashnikova, I., et al., *New Pickering Emulsions Stabilized by Bacterial Cellulose Nanocrystals*. Langmuir, 2011. **27**(12): p. 7471-7479.
40. de Folter, J.W.J., M.W.M. van Ruijven, and K.P. Velikov, *Oil-in-water Pickering emulsions stabilized by colloidal particles from the water-insoluble protein zein*. Soft Matter, 2012. **8**(25): p. 6807-6815.
41. Sole, I., et al., *Optimization of nano-emulsion preparation by low-energy methods in an ionic surfactant system*. Langmuir, 2006. **22**(20): p. 8326-8332.
42. Sole, I., et al., *Nano-emulsions preparation by low energy methods in an ionic surfactant system*. Colloids and Surfaces a-Physicochemical and Engineering Aspects, 2006. **288**(1-3): p. 138-143.
43. Walstra, P., *PRINCIPLES OF EMULSION FORMATION*. Chemical Engineering Science, 1993. **48**(2): p. 333-349.
44. Liu, F. and C.-H. Tang, *Emulsifying Properties of Soy Protein Nanoparticles: Influence of the Protein Concentration and/or Emulsification Process*. Journal of Agricultural and Food Chemistry, 2014. **62**(12): p. 2644-2654.
45. Dickinson, E., *Hydrocolloids as emulsifiers and emulsion stabilizers*. Food Hydrocolloids, 2009. **23**(6): p. 1473-1482.

46. Damodaran, S., *Protein stabilization of emulsions and foams*. Journal of Food Science, 2005. **70**(3): p. R54-R66.
47. Paunov, V.N., et al., *Emulsions stabilised by food colloid particles: Role of particle adsorption and wettability at the liquid interface*. Journal of Colloid and Interface Science, 2007. **312**(2): p. 381-389.
48. Schmidts, T., et al., *Multiple W/O/W emulsions-Using the required HLB for emulsifier evaluation*. Colloids and Surfaces a-Physicochemical and Engineering Aspects, 2010. **372**(1-3): p. 48-54.
49. Babak, V.G., et al., *Impact of bulk and surface properties of some biocompatible hydrophobic polymers on the stability of methylene chloride-in-water mini-emulsions used to prepare nanoparticles by emulsification-solvent evaporation*. Colloids and Surfaces B-Biointerfaces, 2007. **59**(2): p. 194-207.
50. Hou, Z.Q., et al., *Effect of chitosan molecular weight on the stability and rheological properties of beta-carotene emulsions stabilized by soybean soluble polysaccharides*. Food Hydrocolloids, 2012. **26**(1): p. 205-211.
51. Taherian, A.R., et al., *Ability of whey protein isolate and/or fish gelatin to inhibit physical separation and lipid oxidation in fish oil-in-water beverage emulsion*. Food Hydrocolloids, 2011. **25**(5): p. 868-878.
52. Guezey, D. and D.J. McClements, *Influence of environmental stresses on OAV emulsions stabilized by beta-lactoglobulin-pectin and beta-lactoglobulin-pectin-chitosan membranes produced by the electrostatic layer-by-layer deposition technique*. Food Biophysics, 2006. **1**(1): p. 30-40.
53. Ogawa, S., E.A. Decker, and D.J. McClements, *Production and characterization of O/W emulsions containing droplets stabilized by lecithin-chitosan-pectin multilayered membranes*. Journal of Agricultural and Food Chemistry, 2004. **52**(11): p. 3595-3600.
54. Gharsallaoui, A., et al., *Utilisation of pectin coating to enhance spray-dry stability of pea protein-stabilised oil-in-water emulsions*. Food Chemistry, 2010. **122**(2): p. 447-454.

55. Li, Y., et al., *Controlling the functional performance of emulsion-based delivery systems using multi-component biopolymer coatings*. European Journal of Pharmaceutics and Biopharmaceutics, 2010. **76**(1): p. 38-47.
56. Laplante, S., S.L. Turgeon, and P. Paquin, *Effect of pH, ionic strength, and composition on emulsion stabilising properties of chitosan in a model system containing whey protein isolate*. Food Hydrocolloids, 2005. **19**(4): p. 721-729.
57. Tcholakova, S., et al., *Effects of electrolyte concentration and pH on the coalescence stability of beta-lactoglobulin emulsions: Experiment and interpretation*. Langmuir, 2005. **21**(11): p. 4842-4855.
58. Tadros, T.F., *FUNDAMENTAL PRINCIPLES OF EMULSION RHEOLOGY AND THEIR APPLICATIONS*. Colloids and Surfaces a-Physicochemical and Engineering Aspects, 1994. **91**: p. 39-55.
59. Matsumura, Y., *Supramolecular structure and functional properties of food macromolecules*. Journal of the Japanese Society for Food Science and Technology-Nippon Shokuhin Kagaku Kogaku Kaishi, 1999. **46**(11): p. 685-691.
60. Jones, O.G. and D.J. McClements, *Functional Biopolymer Particles: Design, Fabrication, and Applications*. Comprehensive Reviews in Food Science and Food Safety, 2010. **9**(4): p. 374-397.
61. Leman, J. and J.E. Kinsella, *SURFACE-ACTIVITY, FILM FORMATION, AND EMULSIFYING PROPERTIES OF MILK-PROTEINS*. Critical Reviews in Food Science and Nutrition, 1989. **28**(2): p. 115-138.
62. Dickinson, E., *Adsorbed protein layers at fluid interfaces: interactions, structure and surface rheology*. Colloids and Surfaces B-Biointerfaces, 1999. **15**(2): p. 161-176.
63. El-Salam, M.H.A., S. El-Shibiny, and A. Salem, *Factors Affecting the Functional Properties of Whey Protein Products: A Review*. Food Reviews International, 2009. **25**(3): p. 251-270.
64. Paraskevopoulou, A., D. Boskou, and V. Kiosseoglou, *Stabilization of olive oil-lemon juice emulsion with polysaccharides*. Food Chemistry, 2005. **90**(4): p. 627-634.

65. Dickinson, E., *Hydrocolloids at interfaces and the influence on the properties of dispersed systems*. Food Hydrocolloids, 2003. **17**(1): p. 25-39.
66. Schmitt, C., et al., *Structure and technofunctional properties of protein-polysaccharide complexes: A review*. Critical Reviews in Food Science and Nutrition, 1998. **38**(8): p. 689-753.
67. Schmitt, C. and S.L. Turgeon, *Protein/polysaccharide complexes and coacervates in food systems*. Advances in Colloid and Interface Science, 2011. **167**(1-2): p. 63-70.
68. Liu, S.H., N.H. Low, and M.T. Nickerson, *Effect of pH, Salt, and Biopolymer Ratio on the Formation of Pea Protein Isolate-Gum Arabic Complexes*. Journal of Agricultural and Food Chemistry, 2009. **57**(4): p. 1521-1526.
69. Gupta, A.N., H.B. Bohidar, and V.K. Aswal, *Surface patch binding induced intermolecular complexation and phase separation in aqueous solutions of similarly charged gelatin-chitosan molecules*. Journal of Physical Chemistry B, 2007. **111**(34): p. 10137-10145.
70. Cho, J.Y., et al., *Physical gelation of chitosan in the presence of beta-glycerophosphate: The effect of temperature*. Biomacromolecules, 2005. **6**(6): p. 3267-3275.
71. Antonov, Y.A., A.P. Dmitrochenko, and A.L. Leontiev, *Interactions and compatibility of 11 S globulin from Vicia Faba seeds and sodium salt of carboxymethylcellulose in an aqueous medium*. International Journal of Biological Macromolecules, 2006. **38**(1): p. 18-24.
72. Antonov, Y.A. and B.A. Wolf, *Calorimetric and structural investigation of the interaction between bovine serum albumin and high molecular weight dextran in water*. Biomacromolecules, 2005. **6**(6): p. 2980-2989.
73. Weinbreck, F., et al., *Complexation of whey proteins with carrageenan*. Journal of Agricultural and Food Chemistry, 2004. **52**(11): p. 3550-3555.
74. de Kruif, C.G., F. Weinbreck, and R. de Vries, *Complex coacervation of proteins and anionic polysaccharides*. Current Opinion in Colloid & Interface Science, 2004. **9**(5): p. 340-349.

75. Turgeon, S.L., et al., *Protein-polysaccharide interactions: phase-ordering kinetics, thermodynamic and structural aspects*. Current Opinion in Colloid & Interface Science, 2003. **8**(4-5): p. 401-414.
76. Weinbreck, F., et al., *Complex coacervation of whey proteins and gum arabic*. Biomacromolecules, 2003. **4**(2): p. 293-303.
77. Park, J.M., et al., *EFFECTS OF PROTEIN CHARGE HETEROGENEITY IN PROTEIN-POLYELECTROLYTE COMPLEXATION*. Macromolecules, 1992. **25**(1): p. 290-295.
78. Laneuville, S.I., et al., *Gelation of native beta-lactoglobulin induced by electrostatic attractive interaction with xanthan gum*. Langmuir, 2006. **22**(17): p. 7351-7357.
79. Zhang, Y.P., et al., *The influence of ionic strength and mixing ratio on the colloidal stability of PDAC/PSS polyelectrolyte complexes*. Soft Matter, 2015. **11**(37): p. 7392-7401.
80. Jin, K.M. and Y.H. Kim, *Injectable, thermo-reversible and complex coacervate combination gels for protein drug delivery*. Journal of Controlled Release, 2008. **127**(3): p. 249-256.
81. Wang, L.H., E. Khor, and L.Y. Lim, *Chitosan-alginate-CaCl₂ system for membrane coat application*. Journal of Pharmaceutical Sciences, 2001. **90**(8): p. 1134-1142.
82. Laplante, S., S.L. Turgeon, and P. Paquin, *Emulsion-stabilizing properties of chitosan in the presence of whey protein isolate: Effect of the mixture ratio, ionic strength and pH*. Carbohydrate Polymers, 2006. **65**(4): p. 479-487.
83. Lutz, R., et al., *Double emulsions stabilized by a charged complex of modified pectin and whey protein isolate*. Colloids and Surfaces B-Biointerfaces, 2009. **72**(1): p. 121-127.
84. Surh, J., et al., *Influence of environmental stresses on stability of OM emulsions containing cationic droplets stabilized by SDS-fish gelatin membranes*. Journal of Agricultural and Food Chemistry, 2005. **53**(10): p. 4236-4244.
85. Benichou, A., A. Aserin, and N. Garti, *W/O/W double emulsions stabilized with WPI-polysaccharide complexes*. Colloids and Surfaces a-Physicochemical and Engineering Aspects, 2007. **294**(1-3): p. 20-32.

86. Pongsawatmanit, R., T. Harnsilawat, and D.J. McClements, *Influence of alginate, pH and ultrasound treatment on palm oil-in-water emulsions stabilized by beta-lactoglobulin*. Colloids and Surfaces a-Physicochemical and Engineering Aspects, 2006. **287**(1-3): p. 59-67.
87. Bouyer, E., et al., *Stabilization mechanism of oil-in-water emulsions by beta-lactoglobulin and gum arabic*. Journal of Colloid and Interface Science, 2011. **354**(2): p. 467-477.
88. Brugnerotto, J., et al., *Overview on structural characterization of chitosan molecules in relation with their behavior in solution*. Macromolecular Symposia, 2001. **168**: p. 1-20.
89. Klinkesorn, U., *The Role of Chitosan in Emulsion Formation and Stabilization*. Food Reviews International, 2013. **29**(4): p. 371-393.
90. Rinaudo, M., *Chitin and chitosan: Properties and applications*. Progress in Polymer Science, 2006. **31**(7): p. 603-632.
91. Kumar, M., et al., *Chitosan chemistry and pharmaceutical perspectives*. Chemical Reviews, 2004. **104**(12): p. 6017-6084.
92. Chenite, A., et al., *Rheological characterisation of thermogelling chitosan/glycerol-phosphate solutions*. Carbohydrate Polymers, 2001. **46**(1): p. 39-47.
93. Chen, R.H., W.C. Lin, and J.H. Lin, *EFFECTS OF PH, IONIC-STRENGTH, AND TYPE OF ANION ON THE RHEOLOGICAL PROPERTIES OF CHITOSAN SOLUTIONS*. Acta Polymerica, 1994. **45**(1): p. 41-46.
94. Kasaai, M.R., J. Arul, and C. Charlet, *Intrinsic viscosity-molecular weight relationship for chitosan*. Journal of Polymer Science Part B-Polymer Physics, 2000. **38**(19): p. 2591-2598.
95. Rabea, E.I., et al., *Chitosan as antimicrobial agent: Applications and mode of action*. Biomacromolecules, 2003. **4**(6): p. 1457-1465.
96. Riva, R., et al., *Chitosan and Chitosan Derivatives in Drug Delivery and Tissue Engineering*. Chitosan for Biomaterials II, 2011. **244**: p. 19-44.

97. Chen, R.-H., et al., *Advances in chitin/chitosan science and their applications*. Carbohydrate Polymers, 2011. **84**(2): p. 695-695.
98. Baldrick, P., *The safety of chitosan as a pharmaceutical excipient*. Regulatory Toxicology and Pharmacology, 2010. **56**(3): p. 290-299.
99. Agullo, E., et al., *Present and future role of chitin and chitosan in food*. Macromolecular Bioscience, 2003. **3**(10): p. 521-530.
100. Mei, L.Y., E.A. Decker, and D.J. McClements, *Evidence of iron association with emulsion droplets and its impact on lipid oxidation*. Journal of Agricultural and Food Chemistry, 1998. **46**(12): p. 5072-5077.
101. Silvestre, M.P.C., et al., *Ability of surfactant headgroup size to alter lipid and antioxidant oxidation in oil-in-water emulsions*. Journal of Agricultural and Food Chemistry, 2000. **48**(6): p. 2057-2061.
102. Faldt, P., B. Bergenstahl, and P.M. Claesson, *STABILIZATION BY CHITOSAN OF SOYBEAN OIL-EMULSIONS COATED WITH PHOSPHOLIPID AND GLYCOCHOLIC ACID*. Colloids and Surfaces a-Physicochemical and Engineering Aspects, 1993. **71**(2): p. 187-195.
103. Kulmyrzaev, A., M.P.C. Silvestre, and D.J. McClements, *Rheology and stability of whey protein stabilized emulsions with high CaCl₂ concentrations*. Food Research International, 2000. **33**(1): p. 21-25.
104. Li, X. and W. Xia, *Effects of concentration, degree of deacetylation and molecular weight on emulsifying properties of chitosan*. International Journal of Biological Macromolecules, 2011. **48**(5): p. 768-772.
105. Rodriguez, M.S., L.A. Albertengo, and E. Agullo, *Emulsification capacity of chitosan*. Carbohydrate Polymers, 2002. **48**(3): p. 271-276.
106. Schulz, P.C., et al., *Emulsification properties of chitosan*. Colloid and Polymer Science, 1998. **276**(12): p. 1159-1165.
107. Del Blanco, L.F., et al., *Influence of the deacetylation degree on chitosan emulsification properties*. Colloid and Polymer Science, 1999. **277**(11): p. 1087-1092.

108. Payet, L. and E.M. Terentjev, *Emulsification and stabilization mechanisms of o/w emulsions in the presence of chitosan*. Langmuir : the ACS journal of surfaces and colloids, 2008. **24**(21): p. 12247-52.
109. Liu, H., et al., *Simple, Reversible Emulsion System Switched by pH on the Basis of Chitosan without Any Hydrophobic Modification*. Langmuir, 2012. **28**(30): p. 11017-11024.
110. Liu, H., et al., *Fabrication of degradable polymer microspheres via pH-responsive chitosan-based Pickering emulsion photopolymerization*. Rsc Advances, 2014. **4**(55): p. 29344-29351.
111. Wei, Z., et al., *Chitosan nanoparticles as particular emulsifier for preparation of novel pH-responsive Pickering emulsions and PLGA microcapsules*. Polymer, 2012. **53**(6): p. 1229-1235.
112. Ho, K.W., et al., *Comparison of self-aggregated chitosan particles prepared with and without ultrasonication pretreatment as Pickering emulsifier*. Food Hydrocolloids, 2016. **52**: p. 827-837.
113. Baziwane, D. and Q.A. He, *Gelatin: The Paramount food additive*. Food Reviews International, 2003. **19**(4): p. 423-435.
114. Gomez-Guillen, M.C., et al., *Fish gelatin: a renewable material for developing active biodegradable films*. Trends in Food Science & Technology, 2009. **20**(1): p. 3-16.
115. Liu, D., et al., *Collagen and Gelatin*, in *Annual Review of Food Science and Technology*, Vol 6, M.P. Doyle and T.R. Klaenhammer, Editors. 2015. p. 527-557.
116. Duconseille, A., et al., *Gelatin structure and composition linked to hard capsule dissolution: A review*. Food Hydrocolloids, 2015. **43**: p. 360-376.
117. Karim, A.A. and R. Bhat, *Fish gelatin: properties, challenges, and prospects as an alternative to mammalian gelatins*. Food Hydrocolloids, 2009. **23**(3): p. 563-576.
118. Lobo, L., *Coalescence during emulsification - 3. Effect of gelatin on rupture and coalescence*. Journal of Colloid and Interface Science, 2002. **254**(1): p. 165-174.

119. Dickinson, E. and G. Lopez, *Comparison of the emulsifying properties of fish gelatin and commercial milk proteins*. Journal of Food Science, 2001. **66**(1): p. 118-123.
120. Aewsiri, T., et al., *Surface activity and molecular characteristics of cuttlefish skin gelatin modified by oxidized linoleic acid*. International Journal of Biological Macromolecules, 2011. **48**(4): p. 650-660.
121. Aewsiri, T., et al., *Chemical compositions and functional properties of gelatin from pre-cooked tuna fin*. International Journal of Food Science and Technology, 2008. **43**(4): p. 685-693.